



UNIVERSITÀ DI PARMA

UNIVERSITA' DEGLI STUDI DI PARMA

DOTTORATO DI RICERCA IN
SCIENZE MEDICHE

XXXI CICLO

Novel Therapeutic Approaches for the Treatment of Solid Tumors

Coordinatore:

Chiar.mo Prof. Carlo Ferrari

Tutore:

Chiar.mo Prof. Pier Giorgio Petronini

Dottorando: Andrea Ravelli

Anni 2015/2018

Table of contents

List of abbreviations	1
Chapter 1	3
Thesis outline	5
Chapter contents	5
References	7
Chapter 2	9
Breast cancer: epidemiology and molecular subtypes	11
Targeting the cell-cycle machinery in BC	11
Anti CDK4/6 in ER-positive BC	12
Anti CDK4/6 in HER2 positive BC	14
Other CDK4/6 inhibitors	17
References	20
Chapter 3	24
Preliminary data and rationale of the study	26
Materials and methods	27
Cell culturing	27
Drug treatment	27
Evaluation of cell proliferation, cell death, and cell cycle	27
Western blotting	29
Quantitative real-time PCR	29
Glucose uptake and consumption	29
Statistical analysis	29
Results	30
Effects of palbociclib on cell proliferation and cell cycle distribution in TNBC cells	30
Effects of palbociclib in combination with PI3K/mTOR inhibitors	33
Effect of palbociclib and PI3K/mTOR inhibition on glucose energy metabolism	40
Conclusion	42
Acknowledgements	45
References	46
Chapter 4	49
Introduction	51
The role of the immune system in the context of cancer	51
Immunoediting and TIL	52
Early immunotherapy and immune checkpoint inhibition	54
CTLA-4	54
PD-1/PD-L1	55
Immune checkpoint inhibition: critical aspects	55
Adoptive Cell Therapies (ACTs)	56
Cancer vaccines	57
References	59
Chapter 5	63
Introduction	65
TIL therapy: the melanoma experience	65

TIL as prognostic factor	66
TIL therapy: main advantages	67
TIL therapy: critical aspects	68
TIL therapy: how is it performed?	71
References	74
Chapter 6	78
Introduction	80
Lung cancer statistics and histological subtypes	80
Immunotherapies for lung cancer	82
Lung cancer: the next candidate for TIL therapy?	83
Outline of the project	84
The ICON study: patient population	85
Task 1: TIL immunophenotyping in fresh tumor tissues	87
Introduction	87
Materials and methods	87
Staining and flow cytometry evaluation	87
Results	89
Task 2: immunosignatures detection	95
Introduction	95
Materials and methods	95
Unsupervised hierarchical clustering	95
Results	96
Task 3: isolation and expansion of TIL from NSCLC	98
Introduction	98
Materials and methods	98
Isolation and expansion of TIL <i>ex vivo</i>	98
Results	99
Task 4: autologous neoantigen recognition	102
Introduction	102
Materials and methods	103
<i>In silico</i> prediction and peptide synthesis	103
Evaluation of autologous reactivity	104
Results	106
Conclusion	109
Acknowledgements	110
References	111

List of Abbreviations

ACT	Adoptive T Cell Therapy
AKT	Protein Kinase B
ALK	Anaplastic Lymphoma Kinase
APC(s)	Antigen-Presenting Cell(s)
BC	Breast Cancer
CAR	Chimeric Antigen Receptor
CD	Cluster Differentiation
CDK	Cyclin-Dependent Kinase
CR	Complete Remission
CT(s)	Cancer/Testis Antigen(s)
CTLA-4	Cytotoxic T-Lymphocyte Antigen 4
CV	Crystal Violet
DC(s)	Dendritic Cell(s)
DMSO	Dimethyl Sulfoxide
EGFR	Epidermal Growth Factor Receptor
ER	Estrogen Receptor
ESMO	European Society for Medical Oncology
FBS	Fetal Bovine Serum
FDA	Food and Drug Administration
HD	High Dose
HER2	Human Epidermal growth factor Receptor 2
HIF-1 α	Hypoxia-Induced Factor-1 α
HLA	Human Leukocyte Antigen
IFN- γ	Interferon- γ
IL	Interleukin
MDSC(s)	Myeloid-Derived Suppressor Cell(s)
MHC	Major Histocompatibility Complex
mTOR	Mammalian Target Of Rapamycin
NK(s)	Natural Killer cell(s)
NSCLC	Non-Small Cell Lung Carcinoma
ORR	Objective Response Rate
OS	Overall Survival
pCR	Pathological Complete Response
PCR	Polymerase Chain Reaction
PD-1	Programmed Death-1
PD-L1	Programmed Death - Ligand 1
PFS	Progression Free Survival
PgR	Progesteron Receptor
PI3K	Phosphoinositide 3 Kinase
Rb	Retinoblastoma
REP	Rapid Expansion Protocol
SCLC	Small-Cell Lung Carcinoma
TA(s)	Tumor Antigen(s)
TAA(s)	Tumor-Associated Antigen(s)
TBI	Total Body Irradiation
TCR	T Cell Receptor
TGF- β	Transforming Growth Factor- β
TIL	Tumor-Infiltrating Lymphocyte(s)
TME	Tumor Microenvironment
TNBC	Triple-Negative Breast Cancer
Treg(s)	CD4+ T-regulatory Lymphocyte(s)

Chapter 1

Thesis outline

Thesis outline

The present PhD thesis can be divided into two main sections as it aims to cover two of the latest therapeutic frontiers for the treatment of solid tumors:

- Cell cycle inhibition for the treatment of Triple-Negative Breast Carcinoma (TNBC);
- Adoptive T Cell Therapy (ACT) based on the utilization of autologous *ex vivo*-expanded Tumor-Infiltrating Lymphocytes (TIL) - more simply referred to as TIL therapy - for the treatment of Non-Small Cell Lung Cancer (NSCLC).

In particular, the results presented in this thesis intend to be representative of a highly-translational work, reflecting the current need to fill the gap between preclinical studies and the clinical setting.

Chapter contents

In **Chapter 2**, the current therapeutic options targeting the cell cycle machinery for the treatment of breast cancer are summarized, following a review article which has been published in 2017. The author of this thesis contributed to writing the paper as second name [1].

In **Chapter 3**, the results of an experimental study are presented. The preclinical work described in this chapter aimed to evaluate the anti-tumor activity of CDK4/6 inhibitor palbociclib on a panel of TNBC cell lines. Among the described results, one particular evidence highlights the combination of palbociclib with PI3K/mTOR inhibitors as a novel effective therapeutic approach for the treatment of TNBC, a type of cancer which nowadays still dramatically needs new therapeutic options.

The studies described in the first part of this thesis have been performed at the Experimental Oncology Laboratory - Department of Medicine and Surgery (Laboratorio di Oncologia Sperimentale, Dipartimento di Medicina e Chirurgia), University of Parma, Italy, in collaboration with Cremona Cancer Center. The described results are representative of a published article in which the PhD student has authorship as second name [2].

In **Chapter 4**, an introduction about immunoediting and immune-related therapeutic approaches for the treatment of solid tumors is presented. This chapter intends to properly introduce a highly-intriguing hot topic of research of current times, represented by immunotherapy based on immune regulatory checkpoint inhibition and immunotherapies based on the infusion of autologous T lymphocytes (adoptive cell therapies). The author of this thesis contributed to the topic by publishing a review article in 2015-2016 as first name [3].

In **Chapter 5**, the attention will be focused on TIL therapy, a therapeutic approach today known for the impressive clinical results obtained in the setting of metastatic melanoma. The same topic has been object of a recently-published review article in which the author of this thesis has contributed as first name [4].

In **Chapter 6**, the results of a section of the ICON (ImmunogenomiC profiling of early stage NNSCLC) study ongoing at the MD Anderson Cancer Center in Houston, Texas, USA are presented. Briefly, the study aimed to test whether TIL therapy may be a feasible approach also for the treatment of NSCLC. The results highlight an applicability of TIL therapy also for this type of solid tumor, and document a series of findings translationally supporting this rationale. The results described in this Chapter have been generated by a visiting exchange period of about 18 months at the Melanoma Medical Oncology Department – Division of Cancer Medicine, The University of Texas MD Anderson Cancer Center in Houston, Texas, USA (Principal Investigator: Chantale Bernatchez). The data was obtained through a collaborative initiative with the Thoracic Medical Oncology department (Principal Investigator: Don Gibbons) funded by the MD Anderson Cancer Moonshot initiative.

With regards to this section, two abstracts and a poster presentation have been published in 2017-2018. The author of the present thesis contributed to the development of the aforementioned material as fourth name with regards to one abstract, and as second name with regards to one abstract and a poster presentation. On behalf of the results described in Chapter 6, a manuscript is being prepared and will be soon submitted to an international journal.

References

1. Corona, S.P., et al., *CDK4/6 inhibitors in HER2-positive breast cancer*. Crit Rev Oncol Hematol, 2017. **112**: p. 208-214.
2. Cretella, D., et al., *The anti-tumor efficacy of CDK4/6 inhibition is enhanced by the combination with PI3K/AKT/mTOR inhibitors through impairment of glucose metabolism in TNBC cells*. J Exp Clin Cancer Res, 2018. **37**(1): p. 72.
3. Ravelli, A., et al., *Immune-related strategies driving immunotherapy in breast cancer treatment: a real clinical opportunity*. Expert Rev Anticancer Ther, 2015. **15**(6): p. 689-702.
4. Ravelli, A., et al., *Tumor-infiltrating lymphocytes and breast cancer: Beyond the prognostic and predictive utility*. Tumour Biol, 2017. **39**(4): p. 1010428317695023.

Chapter 2

CDK4/6 inhibition for the treatment of breast cancer

Breast cancer: epidemiology and molecular subtypes

Notwithstanding the development of several novel therapeutic approaches and next-generation diagnostic tools during the last decades, Breast Cancer (BC) still represents the second leading cause of cancer-related death among women worldwide [1]. BC molecular subtypes are categorized according to the expression of three different receptors: hormonal receptors, including Estrogen Receptor (ER) and/or Progesterone Receptor (PgR) (both representing ~75% of cases), and Human Epidermal growth factor Receptor 2 (HER2) (which is overexpressed/amplified in ~20% of cases, half of which also show positivity for hormone receptors). Malignancies characterized by a total lack of such receptors are routinely referred to as TNBC, representing ~5%–10% of total diagnoses [2]. Moreover, it is possible to further divide BC into several other molecular classes based on data provided by molecular gene expression profiling using high-throughput analysis: luminal A, luminal B, HER2-enriched, basal-like, claudin-low, and normal-like subtypes [3].

The majority of TNBCs are basal-like and typically share high aggressiveness and poor prognosis. Due to the total lack of pharmacological targets, current therapeutic approaches for TNBC are based on chemotherapy, pointing out the dramatic need for the identification of new treatment options.

Targeting the cell-cycle machinery in BC

De-regulation of the cell cycle machinery was recognised by Hanahan et al as one of the hallmarks of cancer leading to uncontrolled proliferation of tumor cells [4, 5]. This behaviour, which is highly typical of malignancies, drove the discovery of cyclins and Cyclin-Dependent Kinases (CDKs), proteins able to finely regulate the cell cycle through the different phases (G_0 , G_1 , S, M, G_2) [6]. The discovery of these molecules, firstly characterized in yeasts (1970s) and then in humans, granted the Nobel prize award for Medicine in 2001 and attracted a huge interest over the scientific community during the following years [7, 8].

Considering the case of malignant cells, aberrations of the cyclin D/CDK/pRb pathway have been shown to arise in 90% of solid tumors; considering BC, such pathway is found to be disrupted in 50–70% of cases [9-11]. The most frequent molecular alteration is represented

by the overexpression of Cyclin D1, observed in around 50–60% of BCs - particularly in luminal B and HER2 positive histotypes [10, 12]. On the other hand, loss of expression of retinoblastoma (Rb) protein occurs in 20–30% of BCs, mainly in TNBC molecular subtype. Moreover, loss of p16 is documented in about 50% of invasive BCs; p16 is a cyclin-dependent kinase inhibitor which abrogates the binding site of cyclin D1 on CDK4/6. Loss of functional p16 triggers a de-regulation of CDK4/6 activity, leading to persistent Rb protein phosphorylation and increased cell proliferation [13].

The TNBC molecular subtype has been documented to often be associated with p16 loss, as compared with other BC histotypes [14]. In addition, the lack of p16 expression has been correlated with the development of cancer stem cell-like features, leading to an increased rate of failure to respond to chemotherapy-based therapies [15]. Also, the inactivation of the Rb gene, due to both mutation or homozygous loss, has been documented with regards to all BC subtypes, with increased frequency in TNBC (7–20%) [16, 17].

Anti CDK4/6 in ER-positive BC

Targeting the cell cycle machinery for the treatment of BC poses its scientific rationale in the fact that cyclin D1 is a downstream effector of the estrogen stimulation pathway.

The first generation of CDK4/6 inhibitors was characterized by a high rate of drug-induced side effects due to the lack of selectivity for the target (pan-CDK inhibitors), generating disappointing results in clinical trials [18-20]. Flavopiridol, the most extensively studied compound of this type of drugs, gave rise to scarce anti-tumor activity as a single agent and a moderate activity in association with chemotherapy [20]. In addition, the compliance of patients for these drugs was very low due to the intravenous route of administration also requiring an accurate timing. However, the next generation of CDK inhibitors demonstrated a much higher selectivity, as they were specifically designed for targeting CDK4 and CDK6. Moreover, the oral route of administration further rendered these new drugs more compliant [21-23]. Palbociclib (PD 0332991) represents the most important compound of next-generation CDK4/6 inhibitors and the most advanced in clinical development.

In preclinical studies, palbociclib showed activity in xenografts from a range of cancer-derived cell lines (colon, breast, glioblastoma and prostate amongst them) [21]. In BC, the

Chapter 2

best results in terms of anti-tumor activity were later demonstrated in luminal-type BC cell lines, mainly ER and HER2 positive BC [23]. Nonetheless, tumors lacking endogenous Rb protein have been shown to be resistant to palbociclib-based treatment, resulting in an increase of tumor-cell proliferation when the drug was administered [21, 24]. This finding is in line with the observation that tumors lacking functional Rb protein are resistant to tamoxifen, and therefore confirms the convergence of the estrogen and cyclin D/Rb pathways [25].

A first-in-human phase I study of palbociclib in patients with Rb positive solid tumors and lymphomas demonstrated an highly-positive safety/toxicity profile for the compound, with myelosuppression and in particular neutropenia being the main dose-limiting toxicities [26, 27]. However, the observed neutropenia was totally reversible, diversely from the neutropenia typically induced by cytotoxic drugs [28]. In a phase II clinical trial enrolling patients with Rb positive BC, palbociclib showed only minimal activity as a single agent, retrieving a 7% rate of partial responses and a 14% rate of stable disease lasting for more than 6 months [29]. These “partial” results highlighted the potential administration of palbociclib in combination with other targeted drugs for synergistic anti-tumor activity, and the findings highlighted preclinically suggested that a combination with hormone-therapies may be a feasible approach. Thus, a multicentre, randomized phase I/II clinical trial (PALOMA-1) evaluated the combination of palbociclib with letrozole (a non-steroidal aromatase inhibitor approved for treatment of advanced and metastatic ER positive tumors in post-menopausal women) in comparison to letrozole single-agent for the treatment of advanced BCs in post-menopausal women, showing very promising anti-cancer activity. Of note, the study did not document serious interactions between the two drugs [30]. Subsequently, a phase 2 study demonstrated that the association of palbociclib with letrozole possesses increased anti-tumor efficacy as compared to letrozole alone as confirmed by the augmentation of Progression Free Survival (PFS) from 7.5 months to 26.1 months (HR 0.37, $p < 0.001$) [31]. This combined treatment resulted in very high tolerability and documented the following expected toxicities: neutropenia, leukopenia, fatigue and anaemia. Of note, febrile neutropenia did not arise in any patient [31]. The described impressive results led to the approval of palbociclib by the Food and Drug Administration (FDA) in February of 2015 for the treatment of patients with advanced or metastatic ER positive, HER2 negative BC [31]. Additional data with regards to Overall Survival (OS) will be generated from an ongoing Phase III study (PALOMA 2, NCT01740427) (**Table 1**). As of October of 2018, the study did not highlight any evidences

regarding eventual cumulative or delayed toxicities arising from the combination of palbociclib and endocrine therapy in the long term [32].

On behalf of the described impressive results, the association of palbociclib and fulvestrant has been evaluated and compared with fulvestrant-based monotherapy in patients who progressed/relapsed after hormonal therapy (PALOMA 3 trial) [33, 34]. The combination of palbociclib with fulvestrant generated encouraging results in terms of longer PFS and a better quality of life in comparison to fulvestrant alone in the aforementioned category of patients, irrespective of menopausal status. The combination of palbociclib with fulvestrant documented a median PFS of 9.2 months, while the combination placebo and fulvestrant originated a 3.8 months PFS. On behalf of these results, the FDA approved the association of palbociclib and fulvestrant in early 2016 for treatment of advanced or metastatic hormone-positive/HER2-negative BC patients who progressed/relapsed after hormonal therapy [35].

Anti CDK4/6 in HER2 positive BC

Considering the results from preclinical studies and, in particular, the observed spectrum of sensitivity of diverse BC cell lines to palbociclib, it is of great interest to investigate the anti-tumor effect of CDK4/6 inhibition in combination with anti-HER2 therapy in this molecular subtype of BC.

Tumors carrying HER2 overexpression generally are characterized by biological aggressiveness and poor prognosis not only in breast, but also in other solid cancers [10, 36, 37]. HER2-positive BCs comprise a 15–20% of total cases, and the HER2 signaling downstream pathways involve several axes which ultimately modulate cell survival and proliferation [10, 36, 37].

De-regulation of the cell cycle machinery is commonly observed in HER2 positive BCs [10]. In 2001, Yu et al. highlighted the primary role of cyclin D1 for the development of HER2 positive murine BCs [38]. Accordingly, ablation of cyclin D1 in mice resulted in protection against HER2 positive tumor growth. In a pioneer paper, Finn et al. analysed the association of palbociclib and trastuzumab on three HER2 positive BC cell lines, ultimately documenting a synergistic anti-tumor activity *in vitro* [23]. Other preclinical studies then confirmed the effectiveness of the same combination, as well as the validity of palbociclib-based single

agent therapy [39].

The first clinical studies aiming to evaluate the combination of palbociclib and trastuzumab in advanced or metastatic cancers are currently ongoing (**Table 1**). The NA-PHER2 trial (NCT02530424) is meant to evaluate the combination of trastuzumab, pertuzumab, palbociclib and fulvestrant for treatment of ER-positive, HER2-positive invasive BC in the neoadjuvant setting. Primary endpoints of the study are represented by the determination of the effects of the combined drugs on tumor proliferation (Ki67) and apoptosis, meanwhile evaluating the safety and tolerability profile of the same pharmacological combination. Secondary endpoints include determination of pathological complete response (pCR) and clinical objective response [40].

The combination of palbociclib and trastuzumab plus or minus letrozole is then under evaluation in the PATRICIA study, a phase 2 trial designed to compare the two different therapeutic regimens for the treatment of HER2-positive, ER+ or ER-, locally advanced or metastatic BC in post-menopausal women who received prior treatments based on chemotherapy and trastuzumab. PFS at 6 months has been selected as the primary endpoint of this study [40].

Recently, in a very elegant paper, Goel et al. used a doxycyclin-inducible transgenic mouse model of HER2 positive BC to study the effect of the addition of a CDK4/6 inhibitor (adamaciclib) to anti-HER2 therapy (lapatinib) and the mechanisms involved with secondary resistance to anti-HER2 therapies [41]. The authors demonstrated that the cyclin D1/CDK4 axis mediates resistance to anti-HER2 therapy by showing that the tumor cells surviving HER2 blockade express very high levels of cyclin D1 and CDK4 in the nuclei. When the original driver of tumor formation (i.e. HER2) in this experimental setting is antagonised, a small number of cells are still able to survive by upregulating the cyclin D1/CDK4/Rb signalling pathway to start proliferating, regenerating a tumor [40].

Chapter 2

This first set of experiments created therefore the rationale for the use of a CDK4-abrogating agent for treating recurrent tumors. Combined inhibition of HER2 and cyclin D1/CDK4 showed synergistic anti-tumor activity, which resulted to be superior to both drugs used as single agents. Moreover, adding the CDK4/6 inhibitor restored sensitivity to HER2 blockade in cell lines previously shown to be resistant [41]. When the authors evaluated the mechanism by which abemaciclib exerts its anti-tumor activity, they found that the compound restores the signal by relieving the inhibitory feedback operated by mTOR on the EGFR family of kinases and their downstream effectors, via activation of TSC2 (Tuberin), a well-known inhibitor of mTOR and its substrate

p70s6s kinase. These findings validate previous reports on the interaction between cyclin D1 and TSC2 [42] (**Figure 1**).

The indirect effect of the CDK4/6 inhibitor on mTOR activity acts synergistically with the direct effect exerted by the drug on the cell cycle (cell cycle arrest), ultimately potentiating the “total” anti-tumor effect in the combination setting. It is rational to postulate that the addition of a PI3K/mTOR inhibitor would further increase this synergism [40].

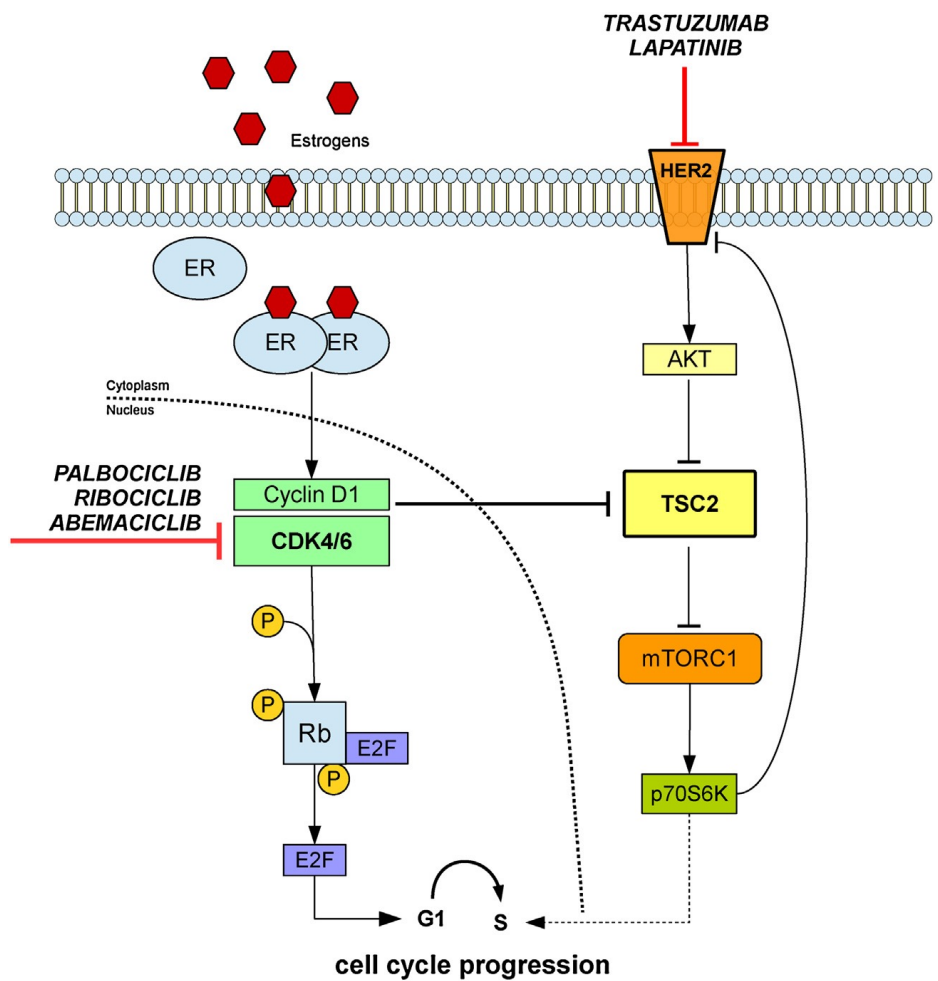


Figure 1 - Cross-talk between CyclinD1-CDK4/6 and the AKT/mTOR pathway via TSC2. The inhibitory feedback loop exerted by TSC2 on mTORC1 is normally inhibited by CyclinD1/CDK4/6, ultimately resulting in cell cycle progression from G1 phase to S phase. CDK4/6 inhibitors can therefore indirectly reduce mTORC1 activity, thus posing the rationale of overcoming resistance to HER2-inhibitors [40].

Other CDK4/6 inhibitors

LEE011 (ribociclib) and LY2835219 (abemaciclib) are the two other cell cycle inhibitors currently in clinical development targeting CDK4/6 in a highly specific fashion (**Figure 2**). In August 2016, ribociclib was granted “breakthrough therapy” designation by the FDA in view of the extremely encouraging results of the Phase 3 MONALEESA-2 trial. In that study, the combination of ribociclib and letrozole was found to significantly improve PFS compared with letrozole alone in first-line treatment of post-menopausal women with ER positive/HER2 negative advanced BC [43, 44]. The first interim analysis of data from the trial (presented at ESMO) showed a 44% augmentation of PFS with ribociclib plus letrozole as a first-line treatment association. The insurgence of toxicities was higher in the combination arm, mainly documenting the insurgence of neutropenia, leukopenia, lymphopenia and elevation of the levels of hepatic enzymes [44]. The compound was also observed to trigger anti-cancer activity as monotherapy in Rb positive solid malignancies and lymphomas, and also in melanoma when combined with letrozole [22, 45, 46].

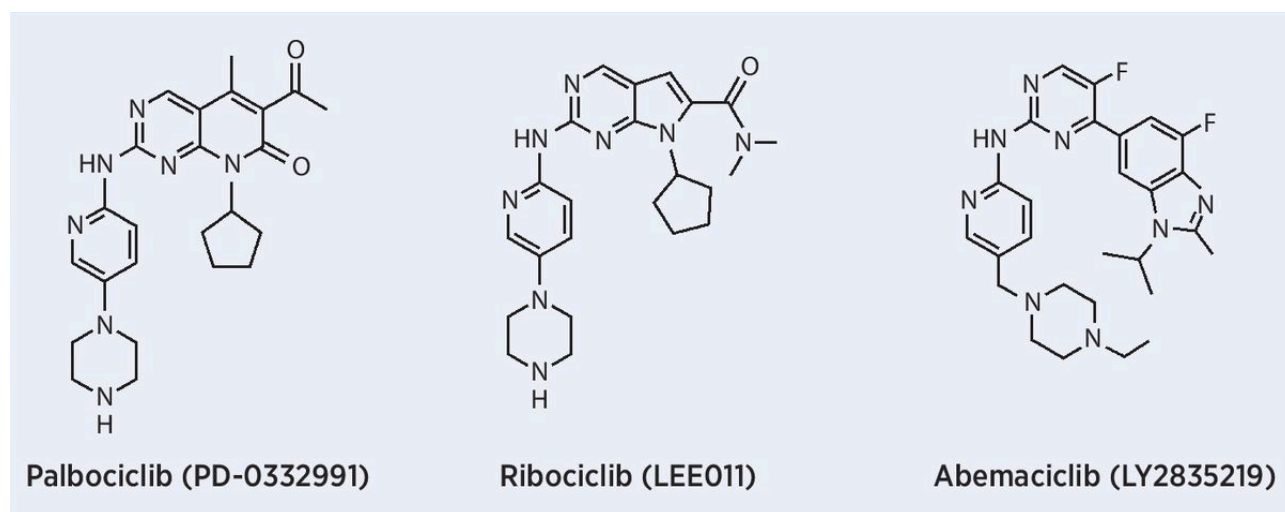


Figure 2 – Chemical structures of next-generation CDK4/6 inhibitors. © 2015 American Association for Cancer Research [6].

The molecular structure as well as the pharmacologic features of abemaciclib differ from both palbociclib and ribociclib (**Figure 2**). Compared to palbociclib, abemaciclib shows higher CDK4 selectivity, demonstrating a reduced incidence of neutropenia (21% versus 40% for both palbociclib and ribociclib) [46]. Due to its chemical characteristics, abemaciclib is able to cross the blood-brain barrier reaching the nervous system, thus opening new

Chapter 2

therapeutic employments of the drug including the treatment of glioblastoma, lung cancer, BC and other solid malignancies [47]. After generating impressive results from the MONARCH 1 clinical trial, abemaciclib monotherapy was designated as “breakthrough therapy” for treating patients with refractory hormone receptor-positive advanced or metastatic BC. The drug is currently being evaluated in two phase 3 trials in comparison with fulvestrant (MONARCH 2) and with a non-steroidal aromatase inhibitor (MONARCH 3) in post-menopausal patients with advanced or metastatic ER positive/HER2 negative BC [48, 49] (**Table 1**).

Both ribociclib and ademaciclib, with their very favourable safety and toxicity profile, as well as their differences in pharmacokinetics and pharmacodynamics, add new options to the treatment of advanced and metastatic hormone-positive BC and other solid tumors.

Chapter 2

Trial name	Phase	Administered drug(s)	Status	Notes	ID	Molecular subtype (BC)
Bardia et al. (2016) [50]	1b	Ribociclib + exemestane + everolimus	Recruiting	N/A	NCT01857193	ER+, HER2-
Yuric et al. (2016) [51]	1b/2	Letrozole + ribociclib + alpesilib	Recruiting	N/A	NCT01872260	ER+, HER2-
Tolaney et al.	1b/2	Ribociclib + trastuzumab or TDM1	Recruiting	N/A	NCT02657343	HER2+
JPBH (Tolaney et al., 2015a) [52]	1b	Abermaciclib + other anti-cancer therapies	Recruiting	N/A	NCT02057133	ER+, HER2-
monarchHER	2	Abermaciclib + other anti-cancer therapies	Recruiting	N/A	NCT02675231	ER+, HER2+
PALLET (Mangini et al., 2015) [53]	2	Palbociclib + letrozole	Recruiting	Neoadjuvant	NCT02296801	ER+, HER2-
MONALEESA-2	3	Letrozole ± ribociclib	Not Recruiting	First-line	NCT01958021	ER+, HER2-
MONALEESA-3	3	Fulvestrant ± ribociclib	Recruiting	First-line/prior endocrine therapy	NCT01958021	ER+, HER2-
MONALEESA-7	3	Tamoxifen or non-steroidal aromatase inhibitor + goserelin ± ribociclib	Recruiting	First-line	NCT02278120	ER+, HER2-
MONARCH-2	3	Fulvestrant ± abemaciclib	Not Recruiting	First-line/prior endocrine therapy	NCT02107703	ER+, HER2-
MONARCH-3	3	Non-steroidal aromatase inhibitor ± abemaciclib	Not Recruiting	First-line	NCT02246621	ER+, HER2-
PENELOPE-B	3	Placebo VS palbociclib	Recruiting	Adjuvant	NCT01864746	ER+, HER2 normal
PALOMA-1/TRIO-18	2	Letrozole ± palbociclib	Not Recruiting	First-line	NCT00721409	ER+, HER2-
PALOMA-2	3	Letrozole ± palbociclib	Not Recruiting	First-Line	NCT01740427	ER+, HER2-
PALOMA-3	3	Fulvestrant ± palbociclib: adding goserelin in premenopausal patients	Not Recruiting	Prior endocrine therapy	NCT01942135	ER+, HER2-
PALOMA-4	3	Letrozole ± palbociclib	Recruiting	First-line	NCT02297438	ER+, HER2-
PEARL	3	Exemestrane + palbociclib VS capecitabine	Recruiting	Prior non-steroidal aromatase inhibitor	NCT02530424	ER+, HER2-
NA-PHER2	2	Trastuzumab + pertuzumab + fulvestrant + palbociclib	Not Recruiting	Neoadjuvant	NCT02530424	ER+, HER2+
NeoPAL	2	Chemotherapy VS letrozole palbociclib	Recruiting	Neoadjuvant	NCT02400567	ER+
PARTICIA	2	Trastuzumab + pertuzumab ± letrozole	Recruiting	Prior chemotherapy and trastuzumab	NCT02448420	ER-, HER2+ (arm A) ER+, HER2+ (arm B)
PALLAS	3	Endocrine therapy (5 years) VS palbociclib (2 years)	Recruiting	Adjuvant	NCT02513394	ER+, HER2-
neoMONARCH	2	Anastrozole VS abemaciclib VS anastrozole + abemaciclib	Recruiting	Neoadjuvant	NCT02441946	ER+, HER2-

Table 1 - Clinical trials currently involving a CDK4/6 inhibitor in association with other compounds.

References

1. Siegel, R.L., K.D. Miller, and A. Jemal, *Cancer statistics, 2018*. CA Cancer J Clin, 2018. **68**(1): p. 7-30.
2. Hosford, S.R. and T.W. Miller, *Clinical potential of novel therapeutic targets in breast cancer: CDK4/6, Src, JAK/STAT, PARP, HDAC, and PI3K/AKT/mTOR pathways*. Pharmgenomics Pers Med, 2014. **7**: p. 203-15.
3. Holliday, D.L. and V. Speirs, *Choosing the right cell line for breast cancer research*. Breast Cancer Res, 2011. **13**(4): p. 215.
4. Hanahan, D. and R.A. Weinberg, *The hallmarks of cancer*. Cell, 2000. **100**(1): p. 57-70.
5. Hanahan, D. and R.A. Weinberg, *Hallmarks of cancer: the next generation*. Cell, 2011. **144**(5): p. 646-74.
6. VanArsdale, T., et al., *Molecular Pathways: Targeting the Cyclin D-CDK4/6 Axis for Cancer Treatment*. Clin Cancer Res, 2015. **21**(13): p. 2905-10.
7. Hartwell, L.H., J. Culotti, and B. Reid, *Genetic control of the cell-division cycle in yeast. I. Detection of mutants*. Proc Natl Acad Sci U S A, 1970. **66**(2): p. 352-9.
8. Nurse, P., *Finding CDK: linking yeast with humans*. Nat Cell Biol, 2012. **14**(8): p. 776.
9. Altenburg, J.D. and S.S. Farag, *The potential role of PD0332991 (Palbociclib) in the treatment of multiple myeloma*. Expert Opin Investig Drugs, 2015. **24**(2): p. 261-71.
10. Cancer Genome Atlas, N., *Comprehensive molecular portraits of human breast tumours*. Nature, 2012. **490**(7418): p. 61-70.
11. Peurala, E., et al., *The prognostic significance and value of cyclin D1, CDK4 and p16 in human breast cancer*. Breast Cancer Res, 2013. **15**(1): p. R5.
12. Ehab, M. and M. Elbaz, *Profile of palbociclib in the treatment of metastatic breast cancer*. Breast Cancer (Dove Med Press), 2016. **8**: p. 83-91.
13. Witkiewicz, A.K. and E.S. Knudsen, *Retinoblastoma tumor suppressor pathway in breast cancer: prognosis, precision medicine, and therapeutic interventions*. Breast Cancer Res, 2014. **16**(3): p. 207.
14. Zhang, S., et al., *QM-FISH analysis of the genes involved in the G1/S checkpoint signaling pathway in triple-negative breast cancer*. Tumour Biol, 2014. **35**(3): p. 1847-54.
15. Arima, Y., et al., *Loss of p16 expression is associated with the stem cell characteristics of surface markers and therapeutic resistance in estrogen receptor-negative breast cancer*. Int J Cancer, 2012. **130**(11): p. 2568-79.
16. Rocca, A., et al., *Progress with palbociclib in breast cancer: latest evidence and clinical considerations*. Ther Adv Med Oncol, 2017. **9**(2): p. 83-105.
17. Johnson, J., et al., *Targeting the RB-E2F pathway in breast cancer*. Oncogene, 2016. **35**(37): p. 4829-35.
18. Gallorini, M., A. Cataldi, and V. di Giacomo, *Cyclin-dependent kinase modulators and cancer therapy*. BioDrugs, 2012. **26**(6): p. 377-91.
19. Jessen, B.A., et al., *Peripheral white blood cell toxicity induced by broad spectrum cyclin-dependent kinase inhibitors*. J Appl Toxicol, 2007. **27**(2): p. 133-42.
20. Fournier, M.N., et al., *Phase I dose-finding study of weekly docetaxel followed by flavopiridol for patients with advanced solid tumors*. Clin Cancer Res, 2007. **13**(19): p. 5841-6.
21. Fry, D.W., et al., *Specific inhibition of cyclin-dependent kinase 4/6 by PD 0332991 and associated antitumor activity in human tumor xenografts*. Mol Cancer Ther, 2004. **3**(11): p. 1427-38.

Chapter 2

22. Finn, R.S., A. Aleshin, and D.J. Slamon, *Targeting the cyclin-dependent kinases (CDK) 4/6 in estrogen receptor-positive breast cancers*. *Breast Cancer Res*, 2016. **18**(1): p. 17.
23. Finn, R.S., et al., *PD 0332991, a selective cyclin D kinase 4/6 inhibitor, preferentially inhibits proliferation of luminal estrogen receptor-positive human breast cancer cell lines in vitro*. *Breast Cancer Res*, 2009. **11**(5): p. R77.
24. Dean, J.L., et al., *Therapeutic CDK4/6 inhibition in breast cancer: key mechanisms of response and failure*. *Oncogene*, 2010. **29**(28): p. 4018-32.
25. Lehn, S., et al., *A non-functional retinoblastoma tumor suppressor (RB) pathway in premenopausal breast cancer is associated with resistance to tamoxifen*. *Cell Cycle*, 2011. **10**(6): p. 956-962.
26. Schwartz, G.K., et al., *Phase I study of PD 0332991, a cyclin-dependent kinase inhibitor, administered in 3-week cycles (Schedule 2/1)*. *Br J Cancer*, 2011. **104**(12): p. 1862-8.
27. Clark, A.S., et al., *Palbociclib (PD0332991)-a Selective and Potent Cyclin-Dependent Kinase Inhibitor: A Review of Pharmacodynamics and Clinical Development*. *JAMA Oncol*, 2016. **2**(2): p. 253-60.
28. Asghar, U., et al., *The history and future of targeting cyclin-dependent kinases in cancer therapy*. *Nat Rev Drug Discov*, 2015. **14**(2): p. 130-46.
29. DeMichele, A., et al., *CDK 4/6 inhibitor palbociclib (PD0332991) in Rb+ advanced breast cancer: phase II activity, safety, and predictive biomarker assessment*. *Clin Cancer Res*, 2015. **21**(5): p. 995-1001.
30. Slamon, D.J., et al., *Phase I study of PD 0332991, cyclin-D kinase (CDK) 4/6 inhibitor in combination with letrozole for first-line treatment of patients with ER-positive, HER2-negative breast cancer*. 2010. **28**(15_suppl): p. 3060-3060.
31. Finn, R.S., et al., *The cyclin-dependent kinase 4/6 inhibitor palbociclib in combination with letrozole versus letrozole alone as first-line treatment of oestrogen receptor-positive, HER2-negative, advanced breast cancer (PALOMA-1/TRIO-18): a randomised phase 2 study*. *The Lancet Oncology*, 2015. **16**(1): p. 25-35.
32. Dieras, V., et al., *Long-term Pooled Safety Analysis of Palbociclib in Combination With Endocrine Therapy for HR+/HER2- Advanced Breast Cancer*. *J Natl Cancer Inst*, 2018.
33. Verma, S., et al., *Palbociclib in Combination With Fulvestrant in Women With Hormone Receptor-Positive/HER2-Negative Advanced Metastatic Breast Cancer: Detailed Safety Analysis From a Multicenter, Randomized, Placebo-Controlled, Phase III Study (PALOMA-3)*. *Oncologist*, 2016. **21**(10): p. 1165-1175.
34. Turner, N.C., et al., *Palbociclib in Hormone-Receptor-Positive Advanced Breast Cancer*. *N Engl J Med*, 2015. **373**(3): p. 209-19.
35. Barroso-Sousa, R., G.I. Shapiro, and S.M. Tolane, *Clinical Development of the CDK4/6 Inhibitors Ribociclib and Abemaciclib in Breast Cancer*. *Breast Care (Basel)*, 2016. **11**(3): p. 167-73.
36. English, D.P., D.M. Roque, and A.D. Santin, *HER2 expression beyond breast cancer: therapeutic implications for gynecologic malignancies*. *Mol Diagn Ther*, 2013. **17**(2): p. 85-99.
37. Yan, M., et al., *HER2 aberrations in cancer: implications for therapy*. *Cancer Treat Rev*, 2014. **40**(6): p. 770-80.
38. Yu, Q., Y. Geng, and P. Sicinski, *Specific protection against breast cancers by cyclin D1 ablation*. *Nature*, 2001. **411**(6841): p. 1017-21.
39. Witkiewicz, A.K., D. Cox, and E.S. Knudsen, *CDK4/6 inhibition provides a potent adjunct to Her2-targeted therapies in preclinical breast cancer models*. *Genes Cancer*, 2014. **5**(7-8): p. 261-72.
40. Corona, S.P., et al., *CDK4/6 inhibitors in HER2-positive breast cancer*. *Crit Rev Oncol Hematol*, 2017. **112**: p. 208-214.

Chapter 2

41. Goel, S., et al., *Overcoming Therapeutic Resistance in HER2-Positive Breast Cancers with CDK4/6 Inhibitors*. *Cancer Cell*, 2016. **29**(3): p. 255-269.
42. Zacharek, S.J., Y. Xiong, and S.D. Shumway, *Negative regulation of TSC1-TSC2 by mammalian D-type cyclins*. *Cancer Res*, 2005. **65**(24): p. 11354-60.
43. Munster, P.N., et al., *Phase Ib study of LEE011 and BYL719 in combination with letrozole in estrogen receptor-positive, HER2-negative breast cancer (ER+, HER2- BC)*. 2014. **32**(15_suppl): p. 533-533.
44. Hortobagyi, G.N., et al., *First-line ribociclib (RIB) + letrozole (LET) in hormone receptor-positive (HR+), HER2-negative (HER2-) advanced breast cancer (ABC): MONALEESA-2 biomarker analyses*. 2018. **36**(15_suppl): p. 1022-1022.
45. Murphy, C.G. and M.N. Dickler, *The Role of CDK4/6 Inhibition in Breast Cancer*. *Oncologist*, 2015. **20**(5): p. 483-90.
46. Sherr, C.J., D. Beach, and G.I. Shapiro, *Targeting CDK4 and CDK6: From Discovery to Therapy*. *Cancer Discov*, 2016. **6**(4): p. 353-67.
47. Patnaik, A., et al., *Efficacy and Safety of Abemaciclib, an Inhibitor of CDK4 and CDK6, for Patients with Breast Cancer, Non-Small Cell Lung Cancer, and Other Solid Tumors*. *Cancer Discov*, 2016. **6**(7): p. 740-53.
48. Lu, E.P., et al., *Caspase-9 is required for normal hematopoietic development and protection from alkylator-induced DNA damage in mice*. *Blood*, 2014. **124**(26): p. 3887-95.
49. Tolaney, S.M., et al., *Abstract P5-19-13: Clinical activity of abemaciclib, an oral cell cycle inhibitor, in metastatic breast cancer*. 2015. **75**(9 Supplement): p. P5-19-13-P5-19-13.
50. Bardia, A., et al., *Abstract P6-13-01: Triplet therapy with ribociclib, everolimus, and exemestane in women with HR+/HER2- advanced breast cancer*. 2016. **76**(4 Supplement): p. P6-13-01-P6-13-01.
51. Juric, D., et al., *Ribociclib (LEE011) and letrozole in estrogen receptor-positive (ER+), HER2-negative (HER2-) advanced breast cancer (aBC): Phase Ib safety, preliminary efficacy and molecular analysis*. 2016. **34**(15_suppl): p. 568-568.
52. Tolaney, S.M., et al., *A phase Ib study of abemaciclib with therapies for metastatic breast cancer*. 2015. **33**(15_suppl): p. 522-522.
53. Mangini, N.S., et al., *Palbociclib: A Novel Cyclin-Dependent Kinase Inhibitor for Hormone Receptor-Positive Advanced Breast Cancer*. *Ann Pharmacother*, 2015. **49**(11): p. 1252-60.

Chapter 3

The anti-tumor efficacy of CDK4/6 inhibition is enhanced by the combination with PI3K/AKT/mTOR inhibitors through impairment of glucose metabolism in TNBC cells

Preliminary data and rationale of the present work

The results described in the present Chapter have been published in 2018 on an international scientific journal and reflect the experimental work performed in the first half of the doctorate course [1].

As described previously, palbociclib is undoubtedly the most extensively-studied anti CDK4/6-abrogating agent to date. The drug is orally-administered and its mechanism of action is based on the inhibition of CDK4/6-cyclin D1-mediated phosphorylation of Rb, which in turn prevents the subsequent release of the transcription factor E2F. Thus, palbociclib is defined as a cytostatic drug, efficiently blocking cell cycle progression from G1 to S phase [2]. As mentioned, palbociclib was granted accelerated approval in 2015 for the treatment of ER-positive, HER2-negative advanced BC in association with letrozole, and in combination with fulvestrant in patients with ER-positive/ HER2-negative advanced BC with disease progression following endocrine therapy [3-5]. However, a few early preclinical evidences have been highlighting a potential utilization of palbociclib for treating TNBC cell lines [6]. Based on the aforementioned molecular characteristics of BC which are typically associated with palbociclib-mediated anti-tumor response, TNBC with a Rb- positive, p16INK4-negative profile might rationally represent a suitable candidate for treatment with CDK4/6 inhibitors.

The mechanism of action of palbociclib also poses the bases for its possible employment in combinatory schedules of treatment: the recently described activation of Protein Kinase B (AKT) signaling which is triggered by the administration of palbociclib highlights a solid rationale for the combination of this drug with inhibitors of the phosphoinositide 3-kinase/AKT/mammalian target of rapamycin (PI3K/AKT/mTOR) pathway, being this last strictly implicated in the control of cell growth, proliferation, migration, and metabolism [7]. Because this pathway is also found to be frequently deregulated in BC cells, the utilization of PI3K/mTOR inhibitors is being currently investigated in several clinical trials [8].

These preliminary findings pose the basis of the present experimental study, which aims to investigate the anti-tumor activity of palbociclib on a panel of TNBC cell lines by considering a utilization of the compound also in combination with PI3K/mTOR inhibitors. Our observations show that the association of palbociclib with PI3K/mTOR inhibitors potentiates the anti-proliferative effect of the single drugs, also triggering an impairment of tumor cell metabolism, suggesting new therapeutic strategies to combat the aggressive behaviour of TNBC.

Materials and methods

Cell culturing

Human BC cell lines MDA-MB-231, MDA-MB-468, HCC-38 (all triple negative) and MCF-7 (ER α -positive) were cultured in RPMI supplemented with 2 mM glutamine, 10% fetal bovine serum (FBS), and 100 U/ml penicillin/100 μ g/ml streptomycin. Cells were purchased from the American Type Culture Collection (Manassas, VA), which authenticates the phenotypes of these cell lines on a regular basis ([http:// www.lgcstandards-atcc.org](http://www.lgcstandards-atcc.org)). Hypoxic conditions were established by placing the cells in a tissue culture incubator with controlled O₂ levels (Binder GmbH, Tuttlingen, Germany).

Drug treatment

Palbociclib (PD-0332991) was provided by Pfizer (New York City, NY); NVP-BEZ235, NVP-BYL719, and NVP- BKM120 (hereafter, referred to as BEZ235, BYL719, and BKM120) were provided by Novartis Institutes for Bio- Medical Research (Cambridge, MA). Drugs were prepared in DMSO, and DMSO concentration never exceeded 0.1% (v/v); equal amounts of the solvent were added to control cells.

Evaluation of cell proliferation, cell death, and cell cycle

Cell proliferation was evaluated by counting the cells in a Bürker hemocytometer with trypan blue exclusion method and by Crystal Violet (CV) staining. The nature of the interaction between palbociclib and PI3K inhibitors was calculated using the Bliss additivity model. A theoretical dose-response curve was calculated for combined inhibition using the equation of Bliss = EA + EB-EA*EB, where EA and EB are the percent of inhibition versus control obtained by BYL719, BEZ235 or BKM120 (A) and palbociclib (B) alone and the E Bliss is the percent of inhibition that would be expected if the combination was exactly additive. If the combination effect is higher than the expected Bliss equation value, the interaction is

Chapter 3

synergistic, while if the effect is lower, the interaction is antagonistic. Otherwise, the effect is additive and there is no interaction between the drugs. Cell death was analysed by fluorescence microscopy after staining with Hoechst 3342 and Propidium Iodide (PI). Distribution of the cells in the cell cycle was determined as follows: briefly, 5×10^5 cells were incubated overnight at 4 °C in 1 ml of hypotonic fluorochrome solution. Analysis was performed with Coulter EPICS XL-MCL cytometer (Coulter Co., Miami, FL, USA). Cell-cycle-phase distributions were analysed by MultiCycle DNA Content and FCS Express Software (De Novo Software, Glendale, CA 91203).

Western blotting

Antibodies against p-Rb^{Ser780} (#9307), Rb (#9309), cyclin D1 (#2926), CDK6 (#3136), c-myc (#9402), p-AKT^{Ser473} (#9271), AKT (#9272), p-mTOR^{Ser2448} (#2971), mTOR (#2972), p-ERK1/2^{Thr202/Tyr204} (#4370), ERK1/2 (#4695), were from CST (Danvers, MA); anti-p-CDK6^{Tyr24} (sc- 293,097) was from Santa Cruz Biotechnology, Incorporated (Dallas, TX). Anti CDKN2A/p16^{INK4a} (ab81278) and anti-GLUT-1 (ab40084) were from Abcam (Cambridge, UK). Antibody against HIF-1 α (#610959) was from BD Biosciences (Franklin Lakes, NJ). Anti- β -actin (#3598) was from BioVision (Milpitas, CA). All the antibodies were used at the recommended dilution of 1:1000. Horseradish peroxidase-conjugated secondary antibodies (1:10,000) and chemiluminescence system were from Millipore (Millipore, MA). Reagents for electrophoresis and blotting analysis were from BIO-RAD Laboratories (Hercules, CA).

Quantitative real-time PCR

Total RNA was isolated by RNeasy Mini Kit (Qiagen, Venlo, Netherlands) and the quantitative real-time Polymerase Chain Reaction (PCR) was performed using the StepOne system instrument (Applied Biosystems). Briefly, samples were amplified using the following thermal profile: 95 °C for 20 s and 40 cycles of denaturation at 95 °C for 3 s followed by annealing and extension at 60 °C for 30 s. The primer to specifically amplify GLUT-1

Chapter 3

(QT00068957) was obtained from Qiagen. HPRT1 (QT00059066) and PGK1 (QT00013776) were used as housekeeping genes and were purchased from Qiagen. The fold change was calculated by the $\Delta\Delta\text{CT}$ method.

Glucose uptake and consumption

Briefly, cells were rinsed with Kreb's Ringer HEPES buffer (KRH) and incubated in KRH containing 1 $\mu\text{Ci/ml}$ Deoxy-D-glucose-2-[1,2- $^3\text{H}(\text{N})$] (2DG, PerkinElmer, Waltham, MA) at 37 °C for 5 min. Then, the cells were quickly rinsed three times in fresh cold Earle's solution containing 0.1 mM phloretin (Sigma-Aldrich). Ice-cold trichloroacetic acid (TCA, 5%) was added and radioactivity in the acid extracts was measured by liquid-scintillation. Cell proteins, precipitated by TCA, were dissolved in 0.5 N NaOH and their concentration determined by a dye-fixation method (Bio-Rad, Hercules, CA). Glucose uptake was calculated as pmol of 2DG/mg protein/ 5 min and expressed as percent vs control condition. Glucose levels in the media were determined using a Glucose (HK) Assay Kit (product code GAHK-20) (Sigma-Aldrich, St. Louis, MI), according to the manufacturer's instruction. Glucose consumption was calculated subtracting the glucose amount in the spent media to glucose in cell-free media. Data were calculated as mg glucose/mg protein and expressed as percent vs control.

Statistical analysis

Statistical analyses were carried out using GraphPad Prism 6.00 software. Statistical significance of differences among data was estimated by two-tailed Student's t test. Comparison among groups was made using analysis of variance (one-way ANOVA, repeated measures) followed by Tukey's post-test.

Results

Effects of palbociclib on cell proliferation and cell cycle distribution in TNBC cells

As a first task, the effect of palbociclib on cell proliferation has been evaluated on the following panel of TNBC cell lines: MDA-MB-231, MDA-MB-468, HCC38. For comparison purposes, ER+ luminal-A BC cell line MCF-7 has been selected for drug testing as it represents the BC cancer histotype for which palbociclib is currently approved and administered in clinics.

As reported in literature, cell sensitivity to the drug can be predicted by the presence of detectable levels of p-Rb and cyclin D1, in parallel to a reduced expression of the cell cycle inhibitor p16^{INK4} [9]. As shown in **Figure 1A**, MDA-MB-231, HCC38, and MCF-7 cell lines expressed detectable levels of both p-Rb and cyclin D1, whereas p16^{INK4} was not present in sufficient amounts to be measured; in accordance, palbociclib inhibited cell proliferation in these cell models with EC₅₀ (referring to as the concentration of palbociclib at which the drug is able to trigger a 50% of the maximum effect) values ranging from 0.3 to 1.4 μM (**Figure 1B**).

Conversely, MDA-MB-468 cells, associated with the loss of Rb, low expression of cyclin D1 and presence of p16^{INK4} expression, resulted to be less sensitive to palbociclib (**Figure 1B**).

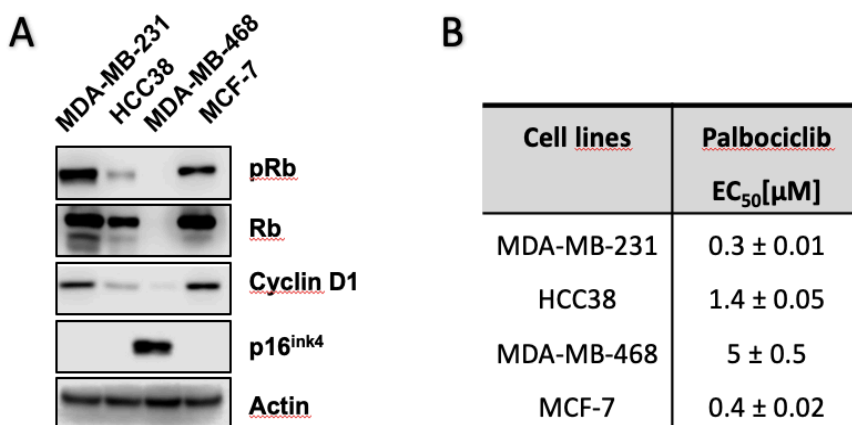


Figure 1 - (A) Expression levels of cell cycle proteins in TNBC and ER+ cell lines. Cells were seeded and after 24 h the expression of the indicated proteins was analysed by Western blotting. **(B)** TNBC and ER+ cell lines were treated with increased concentration of palbociclib (0.01-10 μM) and after 72 h cell proliferation was evaluated by crystal violet staining. The EC₅₀ values are expressed as mean \pm SD of three independent experiments.

Regarding the effect of palbociclib on cell-cycle inhibition, the drug was found to trigger a robust cell cycle blockade in G0/G1 phase only with regards to sensitive cell models. Specifically, 80% and 70% of MDA-MB-231 and HCC38 cell lines, respectively, resulted to be blocked in G0/G1 phase, whereas no alteration of cell distribution within cell cycle phases was observed on MDA-MB-468 cells (**Figure 2**).

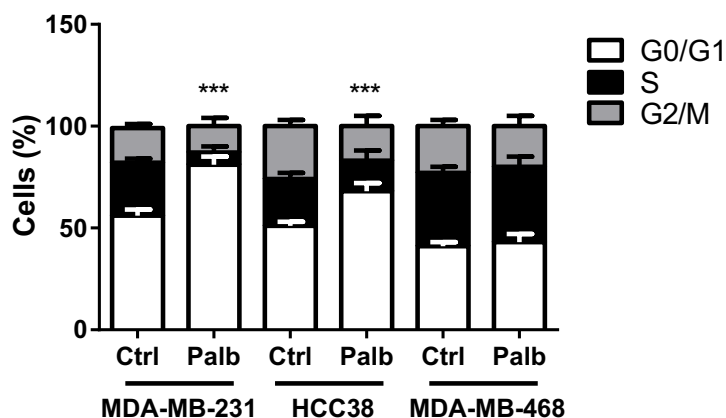


Figure 2 - Palbociclib inhibits cell proliferation only in sensitive cell lines through cell cycle arrest in G0/G1 phase. TNBC cell lines were treated in absence (ctrl) or in presence (palb) of palbociclib 0.5 μ M. After 24 h cells were stained with propidium iodide and cell cycle phases distribution were determined by flow cytometry analysis. Data were expressed as percentage of distribution in each cell cycle phase. Results are representative of three independent experiments. *** $p < 0.001$ vs G0/G1 ctrl, t-Student's Test.

The next task of the present study aimed to evaluate the nature of CDK4/6 abrogation on TNBC cell lines. In order to analyse the reversibility of palbociclib-mediated inhibition of the cell cycle, MDA-MB-231 and HCC38 cells have been treated with palbociclib for 24 hours. At the end of the treatment, the compound has been removed and cell distribution within cell cycle phases has been assessed at increasing time intervals. As a result, the initial blockade in G0/G1 phase was progressively lost following drug removal, with restoration of normal distribution of cells in each cell cycle phase after 24 hours for both cell lines. Therefore, this finding confirms that the nature of palbociclib-mediated abrogation of CDK4/6 on TNBC cells is reversible (**Figure 3**).

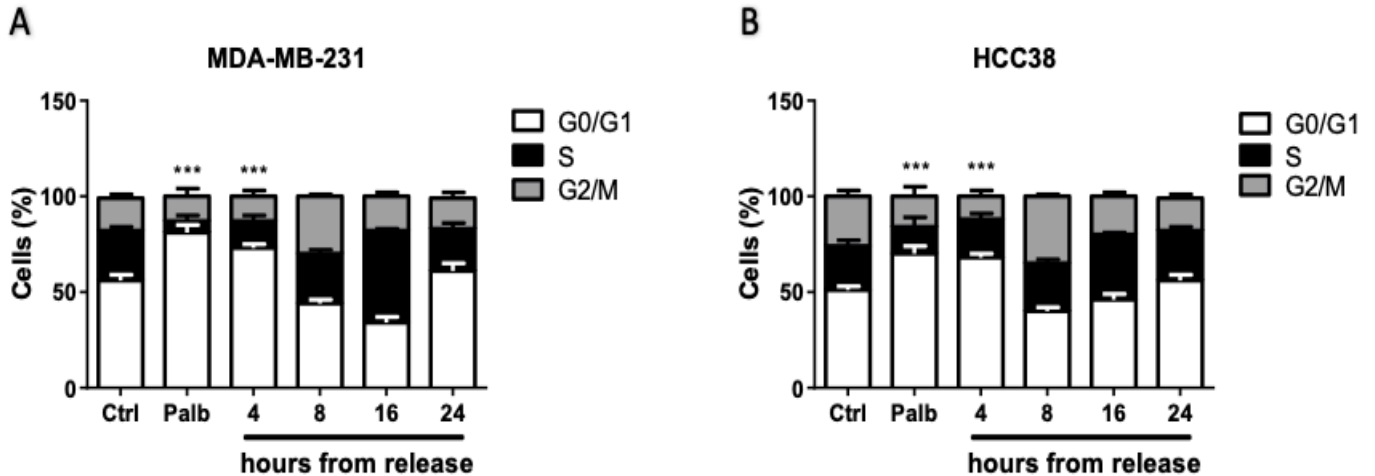


Figure 3 - Reversible effects of palbociclib on cell cycle phases distribution. MDA-MB-231 (**A**) and HCC38 cell lines (**B**) were treated with palbociclib 0.5 μ M (MDA-MB-231) or 1 μ M (HCC38) for 24 h and cell cycle phases distribution was evaluated after the indicated recovery periods.

To further corroborate these data, then, the effect of palbociclib on the expression of cell cycle-related proteins has been investigated. As a result, we observed that the drug was able to mediate a decrease of the levels of p-Rb, Rb and p-CDK6, alongside to a concomitant increase of cyclin D1. This drug-induced modulation has been highlighted as both dose- and time- dependent (**Figure 4A-B**, respectively). As reported in literature, the hypophosphorylation of Rb protein due to CDK4/6 inhibition has been documented to trigger an activation of Rb itself, which in turn keeps E2F in a repressed state, ultimately leading to the inhibition of downstream gene transcription [10]. Accordingly, this finding was confirmed in the present study as palbociclib treatment of MDA-MB-231 and HCC38 cells down-regulated the expression of myc, which is known to comprise E2F- binding sites in its regulatory domain (**Figure 4A-B**).

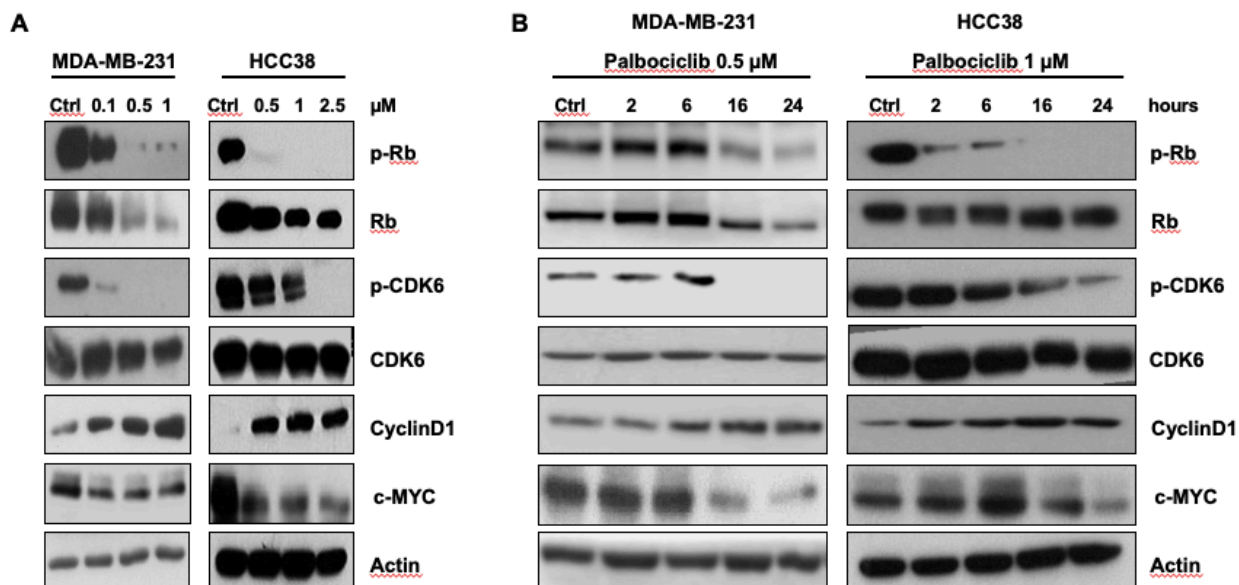


Figure 4 - Palbociclib induces a regulation of cell cycle-related proteins both in a dose- and -time dependent manner. **(A)** Dose-dependent levels of cell cycle protein in TNBC cell lines. Cells were seeded and treated with increasing doses of palbociclib (0.1, 0.5, 1 or 0.5, 1, 2.5 μM); after 24 h the expression levels of the indicated proteins were analyzed by Western blotting. **(B)** Time-dependent levels of cell cycle protein in TNBC cell lines. Cells were seeded and treated with a fixed dose (0.5 or 1 μM) of palbociclib; after 2, 6, 16 and 24 hours the expression levels of the indicated proteins were analyzed by Western blotting. Results are representative of three independent experiments.

Effects of palbociclib in combination with PI3K/mTOR inhibitors

As recently reported in literature, the AKT/mTOR signalling pathway can be positively modulated by palbociclib-based treatment [7, 8]. Based on these preliminary observations, the activation status of this pathway has been investigated on MDA-MB-231 and HCC38 cell lines by meanwhile administering palbociclib in a dose- and time- dependent fashion (**Figure 5A-B**, respectively). As a result, the drug triggered a dose-dependent up-regulation of the phosphorylation levels of AKT proteins and mTOR, whereas no modulation was noticed with regards to ERK-1/2 pathway. Also, the same modulation has been observed in a time-dependent fashion for up to 24 hours.

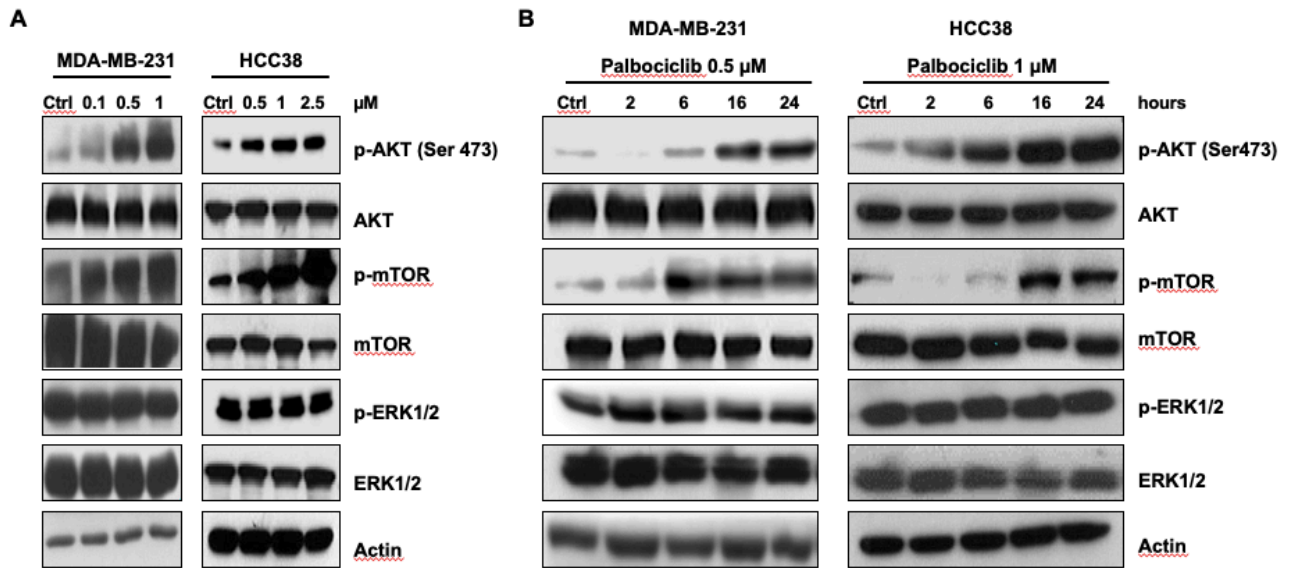


Figure 5 - Palbociclib induces an up-regulation of PI3K/AKT/mTOR pathway in TNBC cell lines. **(A)** Dose-dependent levels of PI3K/AKT pathway in TNBC cell lines. Cells were seeded and treated with an increasing dose of palbociclib (0.1, 0.5, 1 or 0.5, 1, 2.5 μM); after 24 h the expression of the indicated proteins were analyzed by Western blotting. **(B)** Time-dependent levels of PI3K/AKT pathway in TNBC cell lines. Cells were seeded and treated with a fixed dose (0.5 or 1 μM) of palbociclib; after 2, 6, 16 and 24 h the expression of the indicated proteins were analyzed by Western blotting. Results are representative of three independent experiments.

After these initial observations, we proceeded to evaluate the combination of palbociclib with three PI3K/mTOR inhibitors on TNBC cell lines. Specifically, the following compounds have been selected for testing: BYL719, an abrogating agent targeting the p110 α catalytic subunit of PI3K, BEZ235, a dual PI3K and mTORC1–2 inhibitor, and BKM120, a pan-class I PI3K inhibitor. The administration of PI3K/mTOR inhibitors as single-agents on the proliferation of TNBC cell lines gave rise to an inhibitory effect (**Table 1**).

Drug	MDA-MB-231 (EC_{50})	HCC38 (EC_{50})
BYL719 (μM)	2.5 ± 0.2	7.5 ± 0.25
BEZ235 (nM)	6 ± 0.1	2.6 ± 0.06
BKM120 (μM)	5 ± 0.5	0.3 ± 0.01

Table 1 - Sensitivity of TNBC cells to PI3K/mTOR inhibitors. HCC38 cells and MDA-MB-231 cells were treated with increasing concentrations of the indicated PI3K/mTOR inhibitors. After 72h cell proliferation was evaluated by CV staining. Data are expressed as EC_{50} values and are means \pm SD of three independent experiments (n=5).

Chapter 3

As a first task, the *simultaneous* association of a fixed concentration of palbociclib (0.5 μ M) combined with increasing concentrations of the PI3K/mTOR inhibitors has been evaluated on MDA-MB-231 and HCC-38 cell lines. According to Bliss experimental model, this type of schedule gave rise to an additive effect (**Figure 6**).

Because AKT activation was observed to be positively modulated for up to 24 hours as a result of palbociclib-based treatment, we proceeded to investigate the efficacy of a schedule of treatment involving a pre-incubation with palbociclib for 24 hours followed by a simultaneous administration of the PI3K inhibitors plus palbociclib for additional 48 hours. This type of schedule has been named *sequential* combined treatment. As shown in **Figure 7**, this last therapeutic approach resulted in a synergistic inhibition of cell proliferation in both MDA-MB-231 and HCC-38 cells.

Importantly, when palbociclib was removed during treatment with PI3K inhibitors, the synergistic effect was lost, leading to an additive inhibition of cell proliferation (**Figure 8**).

The sequential combined treatment resulted in a greater increase of the proportion of cells accumulating in the G0/G1 phase of the cell cycle (**Figure 9A**), with percentages of $\sim 90\%$ for each administered PI3K inhibitor. Moreover, the sequential combined treatment triggered a significant down-regulation of the PI3K/AKT/mTOR pathway; as shown in **Figure 9B**, this schedule of treatment triggered the inactivation of mTOR and a complete dephosphorylation of p-Rb, as compared with the single drug treatments. To note, the same type of treatment schedule led to a strong inhibition of myc expression due to Rb inactivation.

Chapter 3

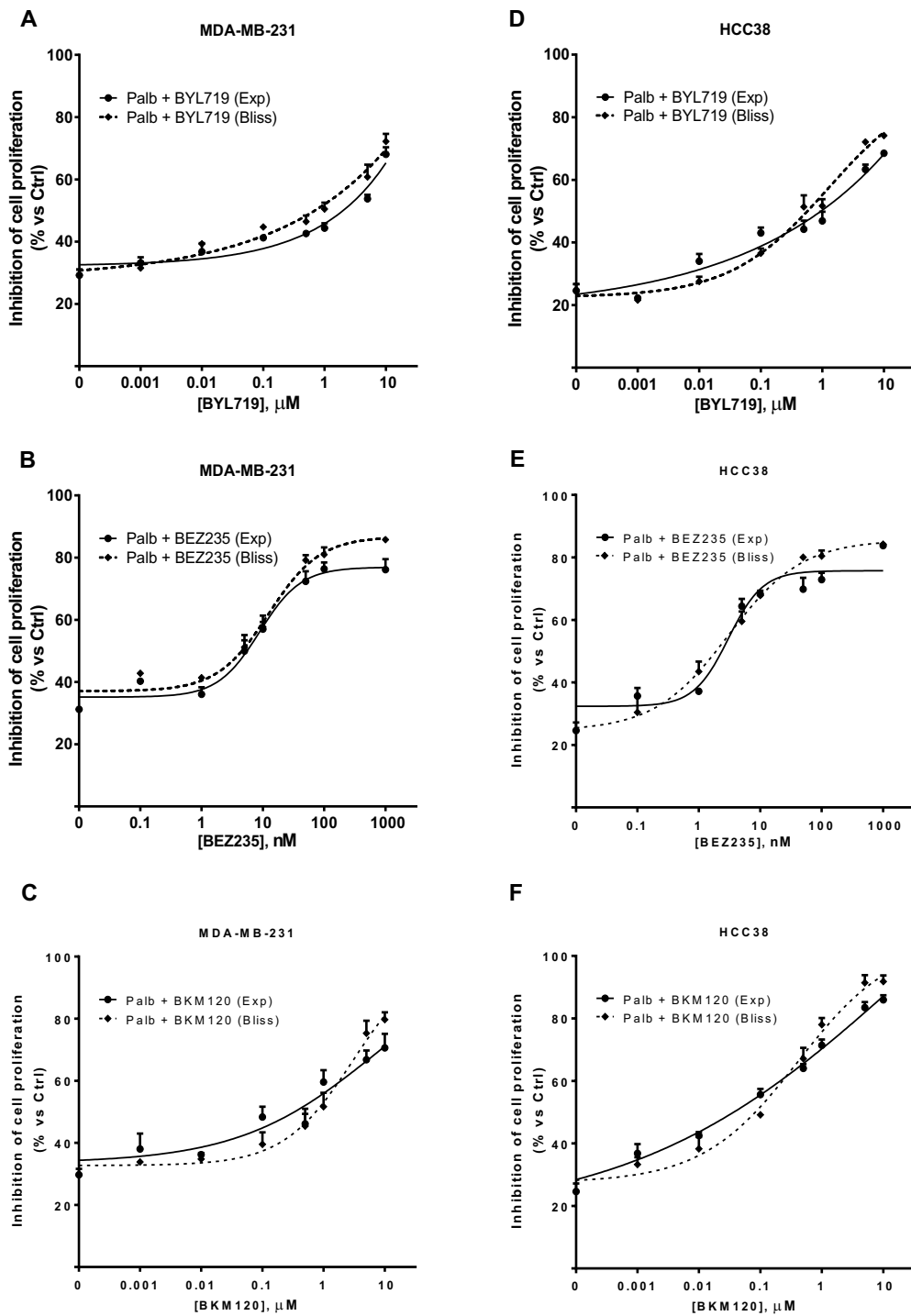


Figure 6 - A simultaneous treatment with palbociclib and PI3K/AKT/mTOR inhibitors induces additive effects. MDA-MB-231 (**A-C**) and HCC38 cells (**D-F**) were treated with 0.5 μ M palbociclib alone or in combination with increasing concentrations of BYL719, BEZ235 or BKM120. After 72 h cell proliferation was assessed by CV assay. The effect of the drug combinations was evaluated using the Bliss interaction model. Data are mean values \pm SD of three independent experiments ($n = 5$).

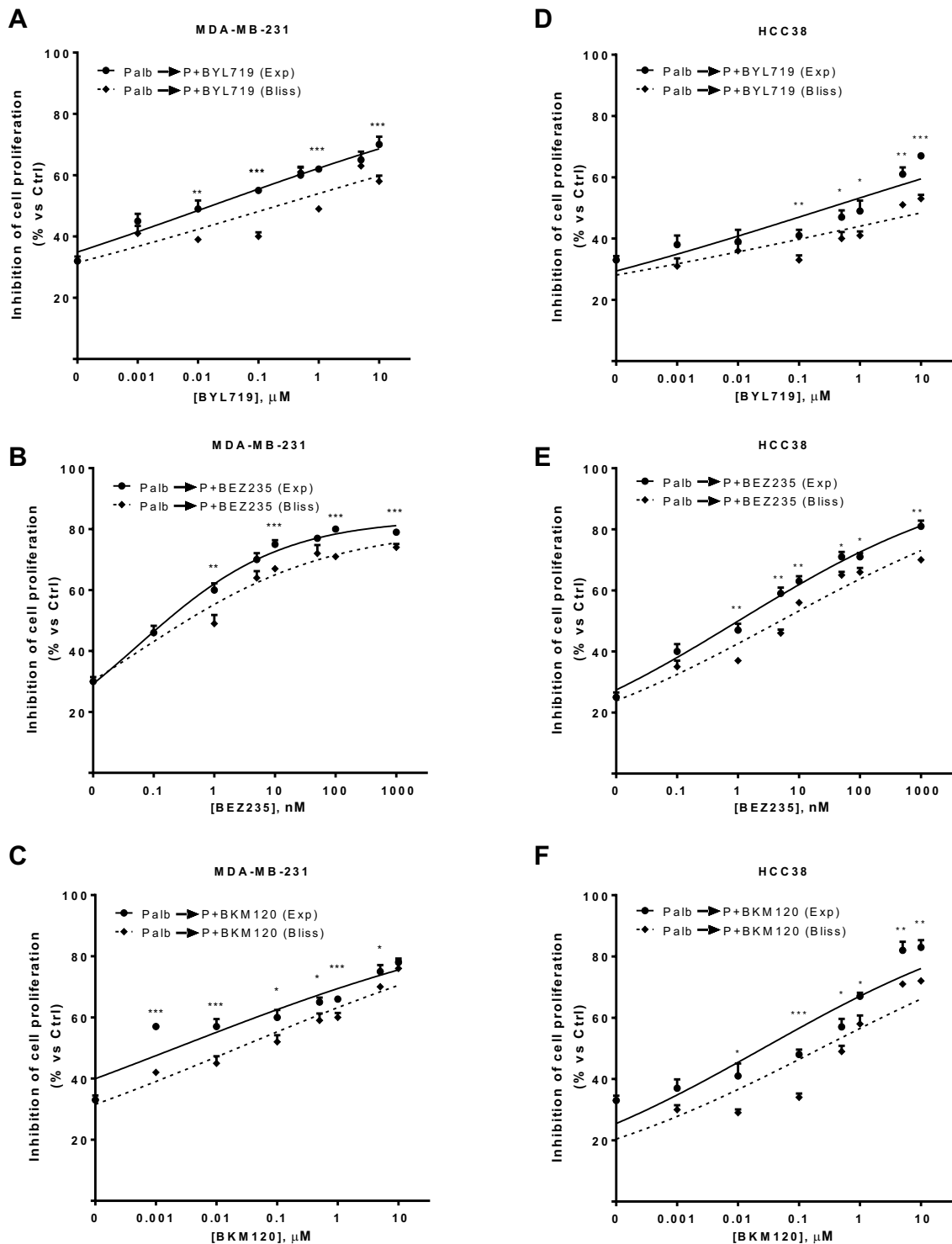


Figure 7 - A sequential exposure to palbociclib and PI3K/AKT/mTOR inhibitors, with palbociclib maintained during all the treatment, induces synergistic effects. MDA-MB-231 (**A-C**) and HCC38 cells (**D-F**) were pre-incubated with 0.5 μM palbociclib for 24 h. Then, the cells were treated with increasing concentrations of BYL719, BEZ235 or BKM120 alone or in combination with palbociclib. After 48 h cell proliferation was assessed by CV assay. The effect of the drug combinations was evaluated using the Bliss interaction model. Data are mean values \pm SD of three independent experiments ($n = 5$).

Chapter 3

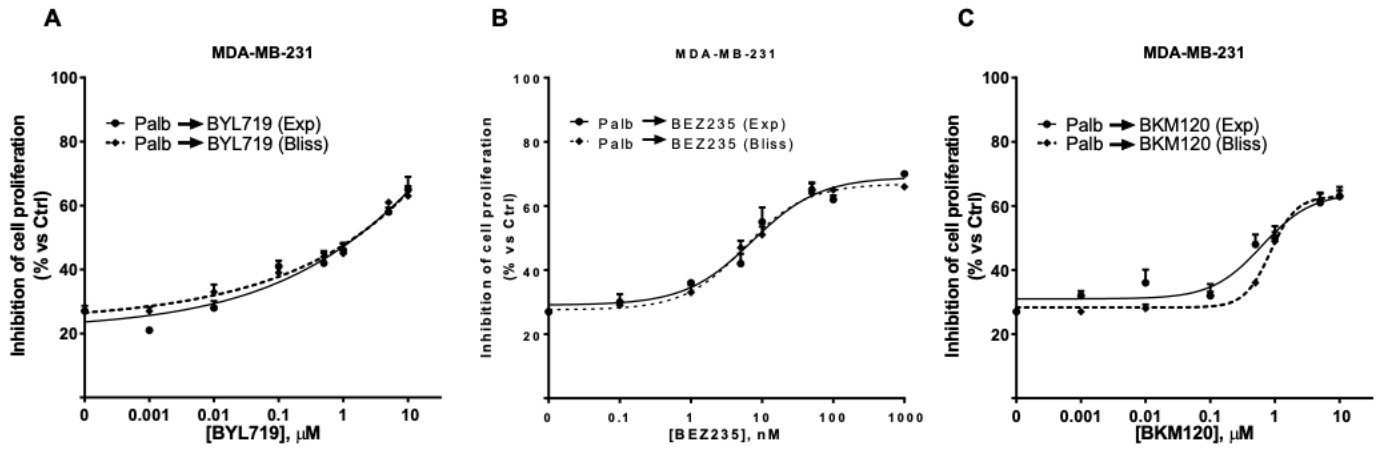


Figure 8 - A sequential exposure to palbociclib followed by PI3K/AKT/mTOR inhibitors alone induces additive effects. MDA-MB-231 were pre-incubated with 0.5 μ M palbociclib for 24h and then treated with increasing concentrations of BYL719 (**A**), BEZ235 (**B**) or BKM120 (**C**) alone. After 48h cell proliferation was assessed by CV assay. The effect of the drug combinations was evaluated using the Bliss interaction model. Data are mean values \pm SD of three independent experiments (n=5).

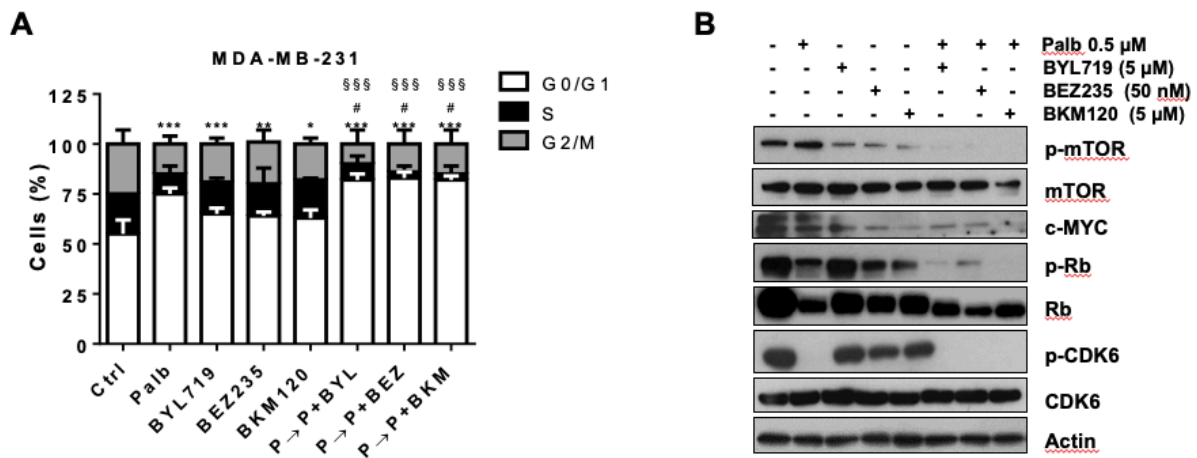


Figure 9 – (**A**) MDA-MB-231 cells were treated with 0.5 μ M palbociclib for 48 h, 2.5 μ M BYL719, 2.5 μ M BKM120 or 50 nM BEZ235 for 24 h or were pre-incubated with palbociclib for 24 hours and then with palbociclib combined with the PI3K/mTOR inhibitors for further 24 hours. Then the cells were stained with PI and the distribution of cells in cell cycle phases was determined by flow cytometry. Results are representative of three independent experiments (n = 5). * p < 0.05, ** p < 0.01, *** p < 0.001 vs G0/G1 ctrl; # p < 0.05 vs G0/G1 Palb; §§§ p < 0.001 vs G0/G1 BYL719, BEZ235 or BKM120. (**B**) The cells were treated as in (**A**) and the expression of the indicated proteins was evaluated on cell protein extracts by Western blotting. Results are representative of two independent experiments.

By comparing the tumor growth-inhibitory effects documented by the administration of three diverse schedules of treatment, the increased anti-proliferative efficacy of the sequential combined treatment was confirmed (**Figure 10A**); moreover, palbociclib alone did not induce cell death, as expected, mainly documenting a cytostatic activity on tumor cells; however, the association of palbociclib with BEZ235 was seen to potentiate the effects of PI3K/AKT/mTOR inhibitor on the induction of apoptosis, with the sequential combined treatment documenting the highest rate of cell death (31% of cell death versus 15% and 21% for the combined and the sequential treatment, respectively) (**Figure 10B**).

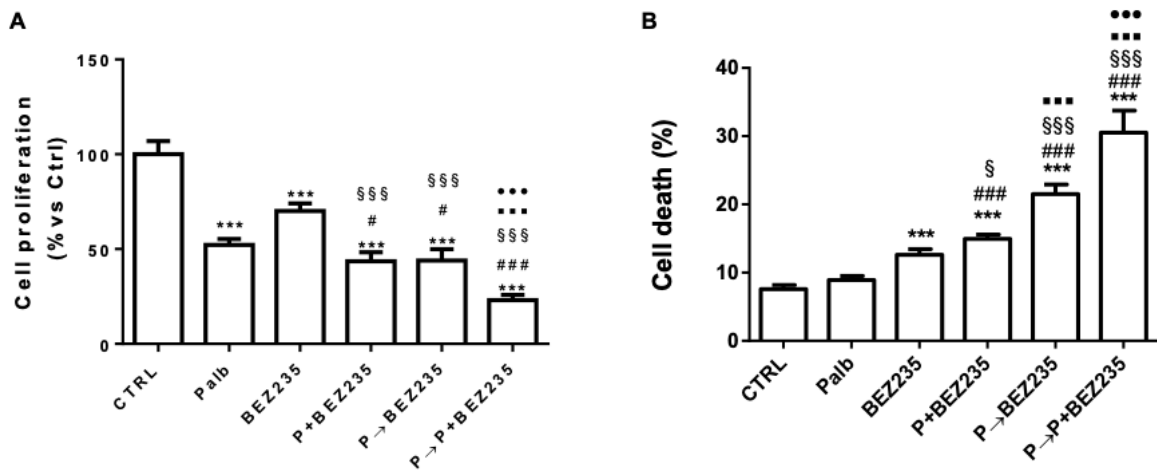


Figure 10 - The combination of palbociclib with BEZ235 enhances cell death. MDA-MB-231 cells were treated with 0.5 μ M palbociclib, 50 nM BEZ235 or with three schedules of treatments: simultaneous, sequential or sequential combined. After 72 h, cell proliferation was evaluated by cell counting with trypan blue exclusion (**A**) and cell death was assessed by fluorescence microscopy after Hoechst 3342/PI staining (**B**). Results are representative of three independent experiments (n = 5). ***p < 0.001 vs ctrl; # p < 0.05, ### p < 0.001 vs palb; § p < 0.05, \$\$\$ p < 0.001 vs BEZ235; *** p < 0.001 vs P + BEZ235; ●●● p < 0.001 vs P→BEZ235.

Altogether, these findings demonstrate that palbociclib may be used to boost the anti-tumor activity of PI3K inhibitors, and indicates that the maintainment of palbociclib during treatment with these inhibitors can be the best choice.

Effect of palbociclib and PI3K/mTOR inhibition on glucose energy metabolism

The direct involvement of cell cycle-related proteins in the regulation of cell energy metabolism is currently supported by several evidences in literature [11]. In the present task, the effect of palbociclib, alone or combined with BYL719, on cell glucose metabolism has been investigated under both normoxic and hypoxic conditions. As a result, palbociclib is shown to down-regulate glucose uptake and consumption, as well as the expression of GLUT-1 glucose transporter in MDA-MB-231 cells (**Figure 11**).

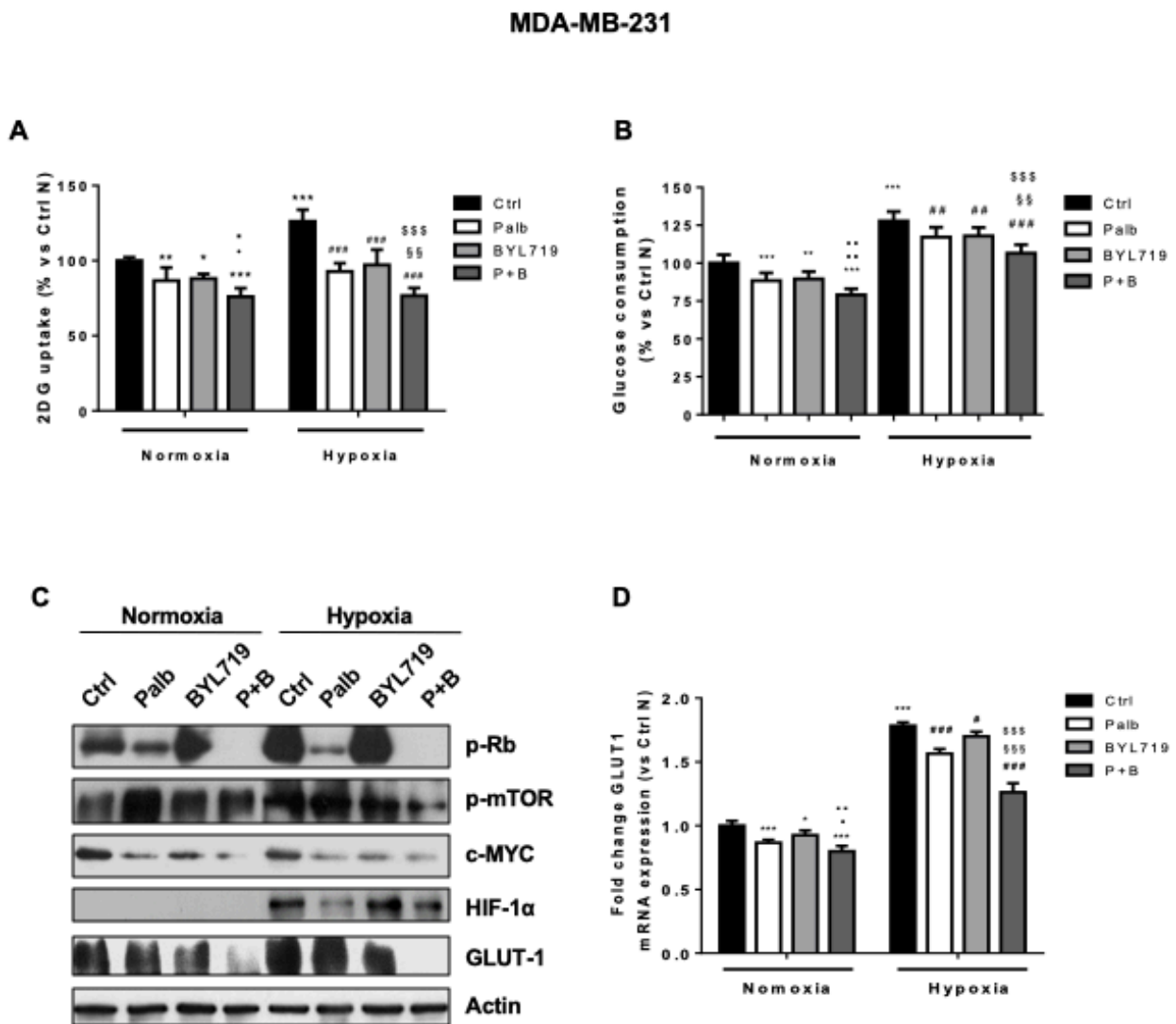


Figure 11 - Palbociclib combined with the PI3K/AKT inhibitor BYL719 hinders glucose metabolism under normoxic and hypoxic conditions. MDA-MB- 231 cells were treated with 0.5 μ M palbociclib and 5 μ M BYL719 alone or in combination under normoxic or hypoxic (1% O₂) conditions for 24 h. Glucose uptake (**A**) and glucose consumption (**B**) were measured. *p < 0.05, **p < 0.01, ***p < 0.001 vs ctrl Normoxia (N); •p < 0.05, ••p < 0.01 vs palb N; •p < 0.05, ••p < 0.01 vs BYL N; ##p < 0.01, ###p < 0.001 vs ctrl Hypoxia (H); §§p < 0.01 vs Palb H; \$\$\$p < 0.001 vs BYL H. (**C**) The expression of the indicated proteins was analysed by Western blotting. (**D**) GLUT-1 mRNA levels were analysed by RT-PCR. Results are plotted as 2^{-ΔΔCT} ± SD.

The greater efficacy of the combination of palbociclib with BYL719 is putatively due to the inhibition of both PI3K/mTOR signaling and c-myc expression (see **Figure 9B**), whose involvement in the regulation of glucose metabolism is today ascertained [12]. Interestingly, the sequential combined treatment with palbociclib maintained during the incubation with BYL719 promoted a ~ 50% decrease of glucose uptake as compared to control (**Figure 12A**), which was associated with a significant inhibition of GLUT-1 expression (**Figure 12B**).

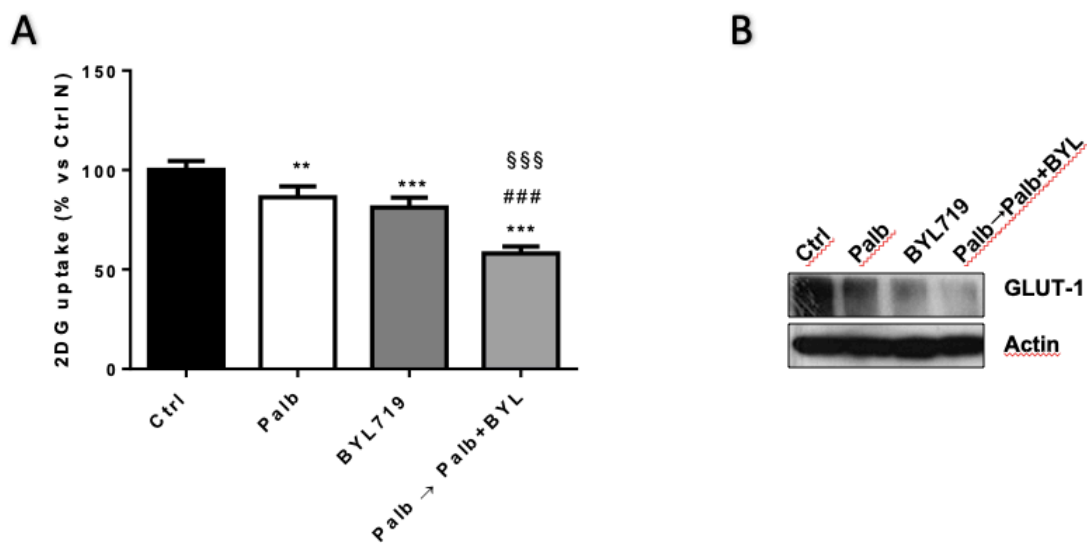


Figure 12 – **(A)** MDA-MB-231 cells were treated with 0.5 μ M palbociclib for 48 h and 5 μ M BYL719 for 24 h alone or were pre-incubated with palbociclib for 24 h and then with palbociclib combined with BYL719 for further 24 h. Glucose uptake was then evaluated. ** $p < 0.01$, *** $p < 0.001$ vs ctrl; #### $p < 0.001$ vs palb; \$\$\$ $p < 0.001$ vs BYL. **(B)** The cells were treated as in e and GLUT-1 expression was evaluated by Western blotting on cell protein extracts.

Altogether, these results suggest that inhibition of PI3K/mTOR signaling may improve the efficacy of palbociclib also through a negative modulation of glucose metabolism.

Conclusion

This first part of the present doctorate study highlights that the utilization of palbociclib in association with PI3K/mTOR inhibitors possesses solid preclinical bases that might be translated for the treatment of Rb- proficient TNBC on behalf of the highlighted effects on both cell proliferation/viability and energy metabolism.

As described in the previous Chapter, CDK4/6 inhibitors demonstrated to be highly effective for the treatment of Rb-functional BCs, especially with regards to hormone-positive subtypes [9]. On the other hand, TNBC is considered a potentially non-responding type of tumor as it is frequently associated with Rb loss [13]. However, a series of early evidences suggested a possible utilization of CDK4/6 inhibitors also for the treatment of a portion of TNBC cell lines, posing the bases of the rationale of the present work [6, 9, 14].

This study demonstrates that palbociclib as a single-agent treatment is able to reduce cell proliferation in TNBC cell models, by eliciting reversible blockade of the cell cycle in G1 phase. This effect has been documented only in cell lines expressing detectable levels of the predictive markers of response to palbociclib, i.e. Rb, cyclin D1, and CDK6 proteins, associated with negligible expression levels of p16. Palbociclib-based treatment in TNBC cell lines inhibited p-Rb, Rb, and p-CDK6 levels, and down-regulated the expression of c-myc, a direct target of E2F transcription factor.

Recent findings highlighted that CDK4 can be highly expressed in TNBC, especially with regards to the basal-like subtype [14]. The analysis of the expression levels of CDK4 might therefore serve as a predictive biomarker of response to palbociclib-based therapies. Moreover, the blockade of CDK4 has been shown to prevent cancer stemness by reducing the self-renewal potential of TNBC cells [15]. Furthermore, CDK4/6 abrogation has been shown to enhance tumor-antigen presentation and to meanwhile suppress regulatory T cell proliferation on different types of BC cell lines, including TNBC: this very recent finding provides a brand-new rationale for the evaluation of novel therapeutic regimens based on the combination of palbociclib and immunotherapies [14, 15].

The present results show that palbociclib-based treatment can trigger the best results in terms of anti-tumor activity when combined with PI3K/mTOR inhibitors.

Chapter 3

One of the key characteristics of palbociclib-based treatment is represented by the ability of the drug to induce AKT activation by releasing p-Rb- mediated inhibition of mTORC2. When found in a hyperphosphorylated form, Rb suppresses the activity of the mTORC2 complex, by directly binding to the complex component Sin1. Since AKT is a substrate of mTORC2, the inhibition of Rb phosphorylation, subsequent to CDK4/6 inhibition, results in mTORC2 activation, thus increasing AKT phosphorylation [7]. This finding served us as a rationale for testing the anti-tumor activity of PI3K/mTOR inhibitors in combination with palbociclib, with special regards to three schedules of treatment:

- Simultaneous combination, referring to as a schedule of treatment in which the compounds are administered at the same time and maintained during the whole treatment time.
- Sequential combination I, involving a 24 hours pre-treatment with palbociclib followed by a replacement of this drug with PI3K/mTOR inhibitors alone.
- Sequential combination II, or sequential combined treatment, based on a pre-treatment with palbociclib and followed by the addition of PI3K/mTOR inhibitors while maintaining palbociclib exposure.

As shown in the results, the first two schedules of treatment gave rise to an additive effect, as calculated using the Bliss experimental model. The last type of schedule of treatment, however, was observed to trigger a synergistic inhibitory effect on the proliferation of TNBC cells. In line with our findings, recent evidences indicate TNBC cell lines with luminal androgen receptor-positive features as synergistically responsive to the combination of palbociclib and PI3K/mTOR inhibitors. The recorded response was also associated with low level of CDK2 activity, p16^{INK4} loss and cyclin D1 expression [6].

With the results of the present preclinical study, we translationally indicate that treatment based on the combination between palbociclib and PI3K/mTOR inhibitors can be of relevant benefit also for the treatment of other TNBC subtypes, i.e. mesenchymal and basal-like subgroups, represented by MDA-MB-231 and HCC38 cell models respectively [16]. To note, the best combination schedule resulted to be represented by the sequential combined treatment, highlighting a possible novel therapeutic approach for the treatment of TNBC.

Chapter 3

The present study also highlights that the anti-tumor activity of palbociclib on TNBC cells can be also due to an inhibitory effect on glucose metabolism. The interdependence between proliferation stimuli and metabolic responses is supported by several evidences in literature, including the finding showing that cyclin D1/CDK6/Rb/E2F pathway is implicated in the modulation of several metabolic processes [17]. Moreover, further evidences highlight that E2F pathway can negatively modulate energy expenditure, through the inhibition of mitochondrial oxidative metabolism [11, 18]; E2F has also been shown to be able to stimulate the glycolytic flux by regulating the expression of phosphofructokinase enzyme [11]. Furthermore, downstream of E2F, cancer metabolic reprogramming might be affected by c-myc transcription factor, which has been shown to regulate glucose metabolism in TNBC cells [19].

With the present study, a palbociclib-mediated detrimental effect on glucose metabolism has been documented. In particular, the drug has been shown to exert an inhibitory activity on E2F/c-myc resulting in a reduction of GLUT-1 expression and glucose uptake. All together, these findings highlight that palbociclib hinders glucose metabolism in TNBC cells under both normoxic and hypoxic conditions, an effect supported by the observation that c-myc cooperates with Hypoxia-Induced Factor (HIF)-1 α to induce the expression of glycolytic enzymes [20]. To note, the accumulation of HIF-1 α was destabilized in an inhibitory fashion by palbociclib administration, an evidence already reported in literature that can contribute to explain the reduction of glucose utilization under hypoxia [21]. As shown in the results section, the detrimental effect of palbociclib on glucose metabolism was especially observed when the drug was combined with PI3K/mTOR inhibitors, with particular emphasis to the schedules of treatment involving a pre-incubation with palbociclib. This finding can be supported by published evidences documenting that the AKT/ mTOR signalling axis plays a primary role in cancer metabolic reprogramming [22]. In the clinical setting, the association between palbociclib and the mTOR inhibitor everolimus has been shown to inhibit aerobic glycolysis in glioblastoma cells, further adding translational value to the present study [23].

Acknowledgements

The author of this thesis wishes to thank Prof. Pier Giorgio Petronini and Prof. Roberta Alfieri and the whole lab team for providing structures and resources to perform the present study. The author also thanks Prof. Daniele Generali for the scientific support provided during the doctorate course. Special thanks to Dr. Daniele Cretella for providing tutoring activity and for the kind professionalism demonstrated during the time spent in Parma.

This work was supported by Associazione per la Ricerca in Campo Oncologico – ARCO, Cremona; A.VO.PRO.RI.T., Parma; Di mano in mano Onlus, Parma; Fondazione Italiana Biologi – Ordine Nazionale dei Biologi, Roma. The funders had no role in study design, data collection and analysis, decision to publish, or preparation of the manuscript.

References

1. Cretella, D., et al., *The anti-tumor efficacy of CDK4/6 inhibition is enhanced by the combination with PI3K/AKT/mTOR inhibitors through impairment of glucose metabolism in TNBC cells*. J Exp Clin Cancer Res, 2018. **37**(1): p. 72.
2. DeMichele, A., et al., *CDK 4/6 inhibitor palbociclib (PD0332991) in Rb+ advanced breast cancer: phase II activity, safety, and predictive biomarker assessment*. Clin Cancer Res, 2015. **21**(5): p. 995-1001.
3. Finn, R.S., et al., *Palbociclib and Letrozole in Advanced Breast Cancer*. N Engl J Med, 2016. **375**(20): p. 1925-1936.
4. Finn, R.S., et al., *Efficacy and safety of palbociclib in combination with letrozole as first-line treatment of ER-positive, HER2-negative, advanced breast cancer: expanded analyses of subgroups from the randomized pivotal trial PALOMA-1/TRIO-18*. Breast Cancer Res, 2016. **18**(1): p. 67.
5. Finn, R.S., et al., *The cyclin-dependent kinase 4/6 inhibitor palbociclib in combination with letrozole versus letrozole alone as first-line treatment of oestrogen receptor-positive, HER2-negative, advanced breast cancer (PALOMA-1/TRIO-18): a randomised phase 2 study*. The Lancet Oncology, 2015. **16**(1): p. 25-35.
6. Asghar, U.S., et al., *Single-Cell Dynamics Determines Response to CDK4/6 Inhibition in Triple-Negative Breast Cancer*. Clin Cancer Res, 2017. **23**(18): p. 5561-5572.
7. Zhang, J., et al., *Inhibition of Rb Phosphorylation Leads to mTORC2-Mediated Activation of Akt*. Mol Cell, 2016. **62**(6): p. 929-942.
8. Dey, N., P. De, and B. Leyland-Jones, *PI3K-AKT-mTOR inhibitors in breast cancers: From tumor cell signaling to clinical trials*. Pharmacol Ther, 2017. **175**: p. 91-106.
9. Finn, R.S., et al., *PD 0332991, a selective cyclin D kinase 4/6 inhibitor, preferentially inhibits proliferation of luminal estrogen receptor-positive human breast cancer cell lines in vitro*. Breast Cancer Res, 2009. **11**(5): p. R77.
10. Johnson, J., et al., *Targeting the RB-E2F pathway in breast cancer*. Oncogene, 2016. **35**(37): p. 4829-35.
11. Fajas, L., *Re-thinking cell cycle regulators: the cross-talk with metabolism*. Front Oncol, 2013. **3**: p. 4.
12. Fan, Y., K.G. Dickman, and W.X. Zong, *Akt and c-Myc differentially activate cellular metabolic programs and prime cells to bioenergetic inhibition*. J Biol Chem, 2010. **285**(10): p. 7324-33.
13. Cancer Genome Atlas, N., *Comprehensive molecular portraits of human breast tumours*. Nature, 2012. **490**(7418): p. 61-70.
14. Dai, M., et al., *CDK4 regulates cancer stemness and is a novel therapeutic target for triple-negative breast cancer*. Scientific Reports, 2016. **6**: p. 35383.
15. Goel, S., et al., *CDK4/6 inhibition triggers anti-tumour immunity*. Nature, 2017. **548**(7668): p. 471-475.
16. Lehmann, B.D., et al., *Identification of human triple-negative breast cancer subtypes and preclinical models for selection of targeted therapies*. The Journal of Clinical Investigation, 2011. **121**(7): p. 2750-2767.
17. Fritz, V. and L. Fajas, *Metabolism and proliferation share common regulatory pathways in cancer cells*. Oncogene, 2010. **29**(31): p. 4369-77.
18. Bonelli, M.A., et al., *Combined Inhibition of CDK4/6 and PI3K/AKT/mTOR Pathways Induces a Synergistic Anti-Tumor Effect in Malignant Pleural Mesothelioma Cells*. Neoplasia, 2017. **19**(8): p. 637-648.

Chapter 3

19. Shen, L., et al., *Metabolic reprogramming in triple-negative breast cancer through Myc suppression of TXNIP*. Proc Natl Acad Sci U S A, 2015. **112**(17): p. 5425-30.
20. Kim, J.W., et al., *Hypoxia-inducible factor 1 and dysregulated c-Myc cooperatively induce vascular endothelial growth factor and metabolic switches hexokinase 2 and pyruvate dehydrogenase kinase 1*. Mol Cell Biol, 2007. **27**(21): p. 7381-93.
21. Zhang, J., et al., *The CDK4/6 inhibitor palbociclib synergizes with irinotecan to promote colorectal cancer cell death under hypoxia*. Cell Cycle, 2017. **16**(12): p. 1193-1200.
22. DeBerardinis, R.J., et al., *The biology of cancer: metabolic reprogramming fuels cell growth and proliferation*. Cell Metab, 2008. **7**(1): p. 11-20.
23. Olmez, I., et al., *Combined CDK4/6 and mTOR Inhibition Is Synergistic against Glioblastoma via Multiple Mechanisms*. Clin Cancer Res, 2017. **23**(22): p. 6958-6968.

Chapter 4

Immune-related therapeutic approaches for the treatment of solid tumors

Introduction

In recent years, the immune system has become a key subject of investigation for its central role in cancer development and progression. It is generally accepted that immune cells can exert both anti-tumor and tumor-promoting activities, and their role in the eradication of transforming cells during carcinogenesis is the focus of intense research [2].

The early observation of immune infiltrates within tumor niches and tumor-associated stroma suggested that lymphocytes may have been able to recognize and potentially eliminate malignant cells, but the presence of ineffective, anergic lymphocytes prompted investigators to hypothesize the existence of mechanisms of immune escape that allowed tumor cells to survive.

Today, immunotherapy has emerged as a tremendously powerful therapeutic approach for the treatment of different types of solid tumors, and the steady progress in the field is further expanding the current therapeutic inventory and the types of tumors which can be treated [1, 2].

The role of the immune system in the context of cancer

It is well known that diverse lymphocytic subpopulations can exert remarkably different effects *in vivo* [3-5]. For instance, the function of various classes of immune effector cells (referred to as immune surveillance lymphocytes) can be kept under control by other populations of immune cells, referred to as immunosuppressive lymphocytes [3, 4, 6]. The physiological brake exerted by this last type of immune cells is indispensable to avoid over-activation of cytotoxic cells and to prevent potentially fatal auto-immune reactions.

In the context of cancer, CD8⁺ cytotoxic T lymphocytes, alongside with Natural Killer (NK) cells and in concert with CD4⁺ type-1 T lymphocytes, have been shown to be able to recognize malignant cells and to subsequently eliminate them, thus representing the immune surveillance arm [5]. These types of cells have been shown to be able to shape tumor immunogenicity and combat early-phase tumor development through the production of IFN- γ [7, 8].

Conversely, other lymphocyte subpopulations have been observed to put a brake to the anti-tumor activity of the immune surveillance compartment, thus representing the immunosuppressive arm. Amongst them, FOXP3⁺ CD25^{high} CD4⁺ T-regulatory lymphocytes (Tregs), Myeloid-Derived Suppressor Cells (MDSC) and CD4⁺ type-2 T lymphocytes are considered the most important subpopulations involved in suppression of anti-tumor activity [5].

Although the balance between the immune surveillance and immunosuppressive arms is highly regulated in physiological conditions, the immune homeostasis of the tumor microenvironment (TME) is systematically lost during tumor progression and the immunosuppressive arm becomes dominant.

Immunoediting and TIL

The process by which tumor cells acquire the ability to escape from immune recognition and eradication is referred to as immunoediting, a multistep phenomenon described for the first time by Dunn et al. in 2004 [9, 10].

During the early stages of this process, immune surveillance-related lymphocytes can recognize and eliminate malignant cells, thus efficiently blocking cancer progression (*elimination* phase). However, this immunological evolutionary pressure favours selection of malignant clones which are more likely to evade immune recognition and consequent elimination. This selection can occur through the following biological mechanisms:

- Cancer cells become “invisible” to host recognition by reducing the expression levels of Major Histocompatibility Complex type – 1 (MHC-1) / Human Leukocyte Antigen (HLA) molecules and reducing the presentation of tumor antigens, therefore drastically decreasing the immunogenicity of the lesion [11, 12].
- Cancer cells become increasingly able to directly inhibit the activity of immune surveillance-related lymphocytes (CD8⁺ cytotoxic T lymphocytes, and NKs) by overexpressing immune-checkpoint ligands which bind immune-checkpoint molecules at the surface of immune cells inhibiting their function. For instance, PD-L1, one of the most extensively studied and clinically relevant inhibitory ligand blocks the activation

Chapter 4

and proliferation of immune cells by binding to PD1, a checkpoint molecule expressed at the surface of a variety of immune cells [13, 14].

- Cancer cells, in addition to upregulating PD-L1 expression, release massive amounts of interleukin (IL)-10, IL-35, and transforming growth factor (TGF)- β , which trigger the proliferation and survival of immunosuppressive cells including Tregs and MDSCs) [15, 16]. This mechanism further inhibits T cell activity and increases the overall immunosuppression level in the TME [15, 16].
- Transformed cells have been shown to be able to inhibit T cell priming against tumor-associated antigens *in vivo*. Spranger et al. showed that this inhibitory mechanism is driven by the activation of the Wnt/ β -catenin pathway in tumor cells which leads to defective recruitment of CD103+ Dendritic Cells (DCs) in the TME, and subsequent inhibition of T cell priming and trafficking [17, 18]. In addition, the same authors demonstrate that CD103+ DCs recruit T effector cells via CXCL9/10, a potent T cell chemoattractant present in T cell- enriched inflamed tissues, highlighting novel mechanisms of immune evasion and new therapeutic ways to circumvent immunosuppression in TME [18] .

The aforementioned mechanisms of immune evasion require some time and usually progress in a stepwise fashion. At certain stages, the activation of immune escape mechanisms may still not be strong enough to completely inhibit T cell recognition and early tumor elimination, giving rise to an *equilibrium* phase in which anti-tumor and tumor-promoting mechanisms are present in equal proportion [10].

Eventually, immune escape mechanisms take control by establishing the strong immunosuppressive environment commonly found in tumors. At this last step, referred to as *escape* phase, the malignancy is largely composed of transformed cells with low immunogenicity. In this scenario, malignancies are usually characterized by the presence of ineffective (or anergic) TIL, which reflect the initial attempt of the host to eliminate tumor outgrowth.

Early immunotherapy and immune checkpoint inhibition

Novel immune-based therapies can exploit several mechanisms involved in the immune response to cancer; overall, the rationale that drives them is to boost and restore a physiological machinery whose baseline function represents a natural defence line against malignancies. Hence, modern immunotherapy makes it possible to revert the immunosuppressive features which are typical of immunoedited TMEs. The first clear success of immunotherapy in clinic was observed in trials using a high-dose IL-2 regimen (bolus HD IL-2) to treat renal cell cancer and metastatic melanoma [19, 20]; Although these results were exciting, the treatment was not devoid of side effects, as it was accompanied by the manifestation of transient but severe drug-related toxicities.

During the same time period, a growing body of evidence begun accumulating supporting the idea that immune infiltrates play a major role in the modulation of response to conventional treatments [21-34]. The discovery and characterization of immune regulatory checkpoints, such as PD-1/PD-L1 and CTLA-4, represented perhaps the most significant step in the evolution of immunotherapy as it introduced novel revolutionary ways to modulate the function of the immune system to combat cancer [35, 36].

Both the CTLA-4 and PD1/PDL1 inhibitory pathways represent some of the most important mechanisms exploited by malignant cells to take advantage over the immune system. Many solid neoplasms have indeed been observed to express both PD1 and its ligand PDL1 at high levels, often with the contemporary presence of anergic infiltrating CD8+ T lymphocytes [37, 38]. Furthermore, immune regulatory checkpoints can act as positive proliferation modulators for FOXP3 Treg cells [36, 39].

CTLA-4

The result of the inhibition of an immune-inhibitory pathway is theoretically an immune-stimulating effect: this hypothesis was initially investigated in preclinical models by the pioneering work of Dr. Allison and colleagues. In his pivotal study, the immune checkpoint CTLA-4 was firstly described as a negative regulator of T cell activation. This finding ultimately led to the development of ipilimumab, an anti CTLA-4 abrogating agent in clinical use for the treatment of advanced melanoma [40]. The discovery of CTLA-4 granted the

2018 Nobel prize for Medicine to James Allison, as ipilimumab generated high clinical success demonstrating a high anti-tumor efficacy in the clinical setting [41, 42]. Currently, ipilimumab shows documented antitumor activity with an optimal dose of 3 mg/kg and exhibits a relatively low toxicity spectrum, particularly if compared with classic chemotherapeutics [43].

PD-1/PD-L1

The clinical potential of anti PD-1/PD-L1 agents arises from the fact that a great number of solid tumors express PD-L1, including breast, colorectal, lung, renal-cell, and pancreatic carcinomas [44-46]. In human hepatocellular carcinoma, overexpression of PDL1 is associated with worst prognoses, reflecting the influence of the highly immunosuppressive microenvironment [47]. Regarding breast cancer, up-regulation of PDL1 has been shown to be clearly predictive of worst clinical outcomes, and has been found to be typical of the more aggressive tumor subtypes, especially of the triple-negative basal-like subtypes [48]. The overexpression of PDL1 is often correlated with the contemporary presence of high PD1-expressing TIL within the tumor microenvironment, and analysis of PD1/ PDL1 expression could predict patient's prognosis and provide information about the ongoing immunoediting phenomenon [49].

Immune checkpoint inhibition: critical aspects

The applicability and efficacy of immune checkpoint blockade relies on several key aspects:

- The immunogenicity of the tumor to be treated, which depends on the level of expression of MHC-1 molecules and their associated tumor antigens. The presence of a large number of tumor neoantigens is generally associated to tumors with high mutational load which are more immunogenic and are commonly referred to as immunologically "hot" tumors. Although often strongly reduced due to immunoediting, the immunogenicity of these types of tumors makes possible to restore anti-tumor

immunological activity via checkpoint blockade and/or any other pharmacological approaches aimed at reactivating the immune system [50].

- The presence of immune surveillance-related immune cells within the TME, which is typical of immunogenic lesions and which represents a major requirement for the efficacy of immune checkpoint inhibitors [51]. Preclinically, this finding is supported by the observation that the reactivation of anergic T cells within the TME is directly required for the therapeutic efficacy of immune checkpoint inhibition [52].

The success of therapies based on the abrogation of immune regulatory checkpoints is being considered as one of the latest therapeutic frontiers in the fight against cancer, retrieving impressive results in the clinical setting. However, a proportion of patients still does not benefit from immune checkpoint-based therapies, and novel immune-related approaches might be of high benefit.

Adoptive Cell Therapies (ACTs)

Immunotherapies based on the infusion of autologous T lymphocytes - Adoptive T Cell Therapies (ACT) - have been shown to be able to produce strong clinical responses in specific types of solid tumors – first of all metastatic melanoma – in patients who do not respond to immune checkpoint inhibitors.

These techniques differ according to the compartment from which T cells are harvested and the type of molecules used to define T cell specificity. Currently, there are at least three general approaches to perform ACT;

- 1- ACT based on the infusion of T cells which have been genetically engineered to express an antigen-specific T cell receptor (TCR T cells) [53];
- 2- ACT based on the infusion of T cells expressing a chimeric antigen receptor (CAR T cells), a single-chain variable domain linked to an intracellular T cell signaling domain [53];
- 3- ACT based on adoptive transfer of TIL (TIL therapy). This represents a technique aiming to infuse autologous T lymphocytes isolated from immune infiltrates found in the tumor and in the surrounding stroma. Due to the intrinsic nature of this type of cellular therapy, T lymphocytes isolated from neoplastic lesions are likely to possess

a broad spectrum of antigen recognition activity, and their reactivity is not restricted to one type of MHC molecules only.

Today, TIL therapy represents an highly viable therapeutic option for the treatment of melanoma, showing robust and reproducible anti-tumor efficacy in clinical trials [54]. The clinical development of this therapeutic approach, ideated for the first time by Rosenberg and colleagues for the treatment of metastatic melanoma, will be described in greater detail in Chapter 5. TIL therapy is also the object of the experimental work described in Chapter 6 in the context of the ICON study.

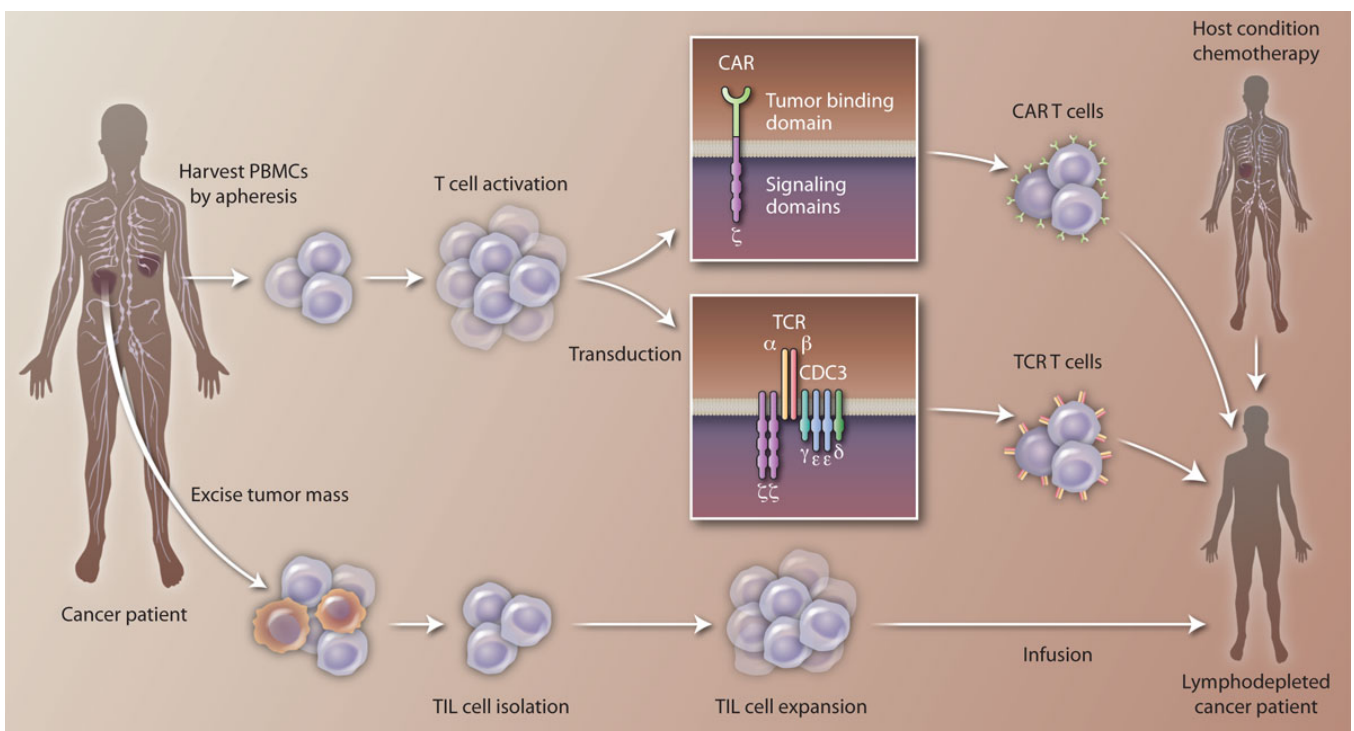


Figure 1 – Representation of current adoptive cell therapies (ACT) [55].

Cancer vaccines

Traditionally, a vaccine is a harmful portion of a pathogen agent which, after inoculation, stimulates the establishment of a specific adaptive immunity without eliciting any damage to the host. Today, cancer has become the new frontier for vaccine-based therapies. While an anticancer vaccine would be unlikely to totally eradicate a bulky tumor, it may more realistically reduce the risk of relapse after surgery or the probabilities of developing metastases, with obvious enormous benefits for patients.

Chapter 4

To set up an antitumor vaccine, identification of tumor antigens (TAs) is firstly required. TAs can be expressed by a unique tumor type and be restricted to a few individuals, or they can be found on all kinds of malignancies. Among TAs, tumor-specific TAs – also referred to as cancer/testis (CT) antigens – are characterized by exclusive expression on malignancies only. TAs can be viral antigens, which are generated in response to viral infections, or can be neo-antigens, which are originated from DNA damage. Diversely, tumor-associated antigens (TAAs) are defined as antigens that are found to be overexpressed on cancer cells, but are observed at lower levels also on healthy tissues. Therefore, their presence on uninvolved tissues is not ideal for a vaccine-based therapy.

An ideal vaccine should target antigens uniquely expressed in cancer cells such as CT-like tumor-specific antigens and should be directed against more than one of them: tumor cells can indeed delete or down-regulate genes encoding for TAs, and as a result they can escape immune recognition. Targeting multiple TAs, especially neo-antigens, can therefore improve the probabilities of success for a vaccine [56].

As of now, an example of TAA is represented by MUC-1, a widely expressed mucine typical of the majority of epithelial cells. MUC-1 is the target of Stimuvax[®](L-BLP25), a liposome-based vaccine which elicits an immunogenic action majorly through a peptide derived from MUC-1, BLP25. Its effectiveness, alone or in association with standard treatments, was evaluated through a series of Phase II/III clinical trials in NSCLC, resulting in a general OS increase especially for combinatorial therapy [57]. As of today, a cancer vaccine is clinically available for asymptomatic or weakly symptomatic metastatic castration-resistant prostate carcinoma: Sipuleucel-T consists of autologous Antigen-Presenting Cells (APCs) targeting a prostatic acid phosphatase, which is found to be overexpressed on the majority of prostate cancer cells [58].

References

1. *Trial watch: ipilimumab success in melanoma provides boost for cancer immunotherapy.* Nat Rev Drug Discov, 2010. **9**(8): p. 584.
2. Letendre, P., et al., *Ipilimumab: from preclinical development to future clinical perspectives in melanoma.* Future Oncol, 2017. **13**(7): p. 625-636.
3. Denburg, J.A. and J. Bienenstock, *Physiology of the immune response.* Can Fam Physician, 1979. **25**: p. 301-7.
4. Schultz, K.T. and F. Grieder, *Structure and function of the immune system.* Toxicol Pathol, 1987. **15**(3): p. 262-4.
5. Schreiber, R.D., L.J. Old, and M.J. Smyth, *Cancer immunoediting: integrating immunity's roles in cancer suppression and promotion.* Science, 2011. **331**(6024): p. 1565-70.
6. McComb, S., et al., *Introduction to the immune system.* Methods Mol Biol, 2013. **1061**: p. 1-20.
7. Shankaran, V., et al., *IFN γ and lymphocytes prevent primary tumour development and shape tumour immunogenicity.* Nature, 2001. **410**(6832): p. 1107-11.
8. Shankaran, V., et al., *Pillars Article: IFN γ and Lymphocytes Prevent Primary Tumour Development and Shape Tumour Immunogenicity.* Nature. 2001. 410: 1107-1111. J Immunol, 2018. **201**(3): p. 827-831.
9. Dunn, G.P., L.J. Old, and R.D. Schreiber, *The three Es of cancer immunoediting.* Annu Rev Immunol, 2004. **22**: p. 329-60.
10. Dunn, G.P., L.J. Old, and R.D. Schreiber, *The immunobiology of cancer immunosurveillance and immunoediting.* Immunity, 2004. **21**(2): p. 137-48.
11. McGranahan, N., et al., *Allele-Specific HLA Loss and Immune Escape in Lung Cancer Evolution.* Cell, 2017. **171**(6): p. 1259-1271 e11.
12. Morita, R., Y. Hirohashi, and T. Torigoe, *Mechanism of immune escape of cancer and its regulation.* Rinsho Ketsueki, 2009. **50**(5): p. 375-80.
13. Vinay, D.S. and B.S. Kwon, *Harnessing immune checkpoints for cancer therapy.* Immunotherapy, 2018. **10**(14): p. 1265-1284.
14. Shi, T., et al., *Cancer Immunotherapy: A Focus on the Regulation of Immune Checkpoints.* Int J Mol Sci, 2018. **19**(5).
15. Sanjabi, S., et al., *Anti-inflammatory and pro-inflammatory roles of TGF- β , IL-10, and IL-22 in immunity and autoimmunity.* Curr Opin Pharmacol, 2009. **9**(4): p. 447-53.
16. Wu, H., et al., *Aberrant expression of Treg-associated cytokine IL-35 along with IL-10 and TGF- β in acute myeloid leukemia.* Oncol Lett, 2012. **3**(5): p. 1119-1123.
17. Spranger, S., R. Bao, and T.F. Gajewski, *Melanoma-intrinsic beta-catenin signalling prevents anti-tumour immunity.* Nature, 2015. **523**(7559): p. 231-5.
18. Spranger, S., et al., *Tumor-Residing Batf3 Dendritic Cells Are Required for Effector T Cell Trafficking and Adoptive T Cell Therapy.* Cancer Cell, 2017. **31**(5): p. 711-723 e4.
19. McDermott, D.F. and M.B. Atkins, *Interleukin-2 therapy of metastatic renal cell carcinoma--predictors of response.* Semin Oncol, 2006. **33**(5): p. 583-7.
20. Atkins, M.B., et al., *High-dose recombinant interleukin 2 therapy for patients with metastatic melanoma: analysis of 270 patients treated between 1985 and 1993.* J Clin Oncol, 1999. **17**(7): p. 2105-16.
21. Jass, J.R., *Lymphocytic infiltration and survival in rectal cancer.* J Clin Pathol, 1986. **39**(6): p. 585-9.

Chapter 4

22. Clemente, C.G., et al., *Prognostic value of tumor infiltrating lymphocytes in the vertical growth phase of primary cutaneous melanoma*. *Cancer*, 1996. **77**(7): p. 1303-10.
23. Galon, J., et al., *Type, density, and location of immune cells within human colorectal tumors predict clinical outcome*. *Science*, 2006. **313**(5795): p. 1960-4.
24. Mlecnik, B., et al., *Histopathologic-based prognostic factors of colorectal cancers are associated with the state of the local immune reaction*. *J Clin Oncol*, 2011. **29**(6): p. 610-8.
25. Galon, J., W.H. Fridman, and F. Pages, *The adaptive immunologic microenvironment in colorectal cancer: a novel perspective*. *Cancer Res*, 2007. **67**(5): p. 1883-6.
26. Leffers, N., et al., *Prognostic significance of tumor-infiltrating T-lymphocytes in primary and metastatic lesions of advanced stage ovarian cancer*. *Cancer Immunol Immunother*, 2009. **58**(3): p. 449-59.
27. Sato, E., et al., *Intraepithelial CD8+ tumor-infiltrating lymphocytes and a high CD8+/regulatory T cell ratio are associated with favorable prognosis in ovarian cancer*. *Proc Natl Acad Sci U S A*, 2005. **102**(51): p. 18538-43.
28. Denkert, C., et al., *Tumor-associated lymphocytes as an independent predictor of response to neoadjuvant chemotherapy in breast cancer*. *J Clin Oncol*, 2010. **28**(1): p. 105-13.
29. Martinet, L., et al., *Human solid tumors contain high endothelial venules: association with T- and B-lymphocyte infiltration and favorable prognosis in breast cancer*. *Cancer Res*, 2011. **71**(17): p. 5678-87.
30. Marrogi, A.J., et al., *Study of tumor infiltrating lymphocytes and transforming growth factor-beta as prognostic factors in breast carcinoma*. *Int J Cancer*, 1997. **74**(5): p. 492-501.
31. Al-Shibli, K.I., et al., *Prognostic effect of epithelial and stromal lymphocyte infiltration in non-small cell lung cancer*. *Clin Cancer Res*, 2008. **14**(16): p. 5220-7.
32. Karja, V., et al., *Tumour-infiltrating lymphocytes: A prognostic factor of PSA-free survival in patients with local prostate carcinoma treated by radical prostatectomy*. *Anticancer Res*, 2005. **25**(6C): p. 4435-8.
33. Fridman, W.H., et al., *The immune contexture in human tumours: impact on clinical outcome*. *Nat Rev Cancer*, 2012. **12**(4): p. 298-306.
34. Adotevi, O., et al., *A decrease of regulatory T cells correlates with overall survival after sunitinib-based antiangiogenic therapy in metastatic renal cancer patients*. *J Immunother*, 2010. **33**(9): p. 991-8.
35. Pardoll, D.M., *The blockade of immune checkpoints in cancer immunotherapy*. *Nat Rev Cancer*, 2012. **12**(4): p. 252-64.
36. Rotte, A., J.Y. Jin, and V. Lemaire, *Mechanistic overview of immune checkpoints to support the rational design of their combinations in cancer immunotherapy*. *Ann Oncol*, 2018. **29**(1): p. 71-83.
37. Quezada, S.A. and K.S. Peggs, *Exploiting CTLA-4, PD-1 and PD-L1 to reactivate the host immune response against cancer*. *Br J Cancer*, 2013. **108**(8): p. 1560-5.
38. Taube, J.M., et al., *Colocalization of inflammatory response with B7-h1 expression in human melanocytic lesions supports an adaptive resistance mechanism of immune escape*. *Sci Transl Med*, 2012. **4**(127): p. 127ra37.
39. Wing, K., et al., *CTLA-4 control over Foxp3+ regulatory T cell function*. *Science*, 2008. **322**(5899): p. 271-5.
40. Naidoo, J., D.B. Page, and J.D. Wolchok, *Immune checkpoint blockade*. *Hematol Oncol Clin North Am*, 2014. **28**(3): p. 585-600.
41. Chambers, C.A., T.J. Sullivan, and J.P. Allison, *Lymphoproliferation in CTLA-4-deficient mice is mediated by costimulation-dependent activation of CD4+ T cells*. *Immunity*, 1997. **7**(6): p. 885-95.

Chapter 4

42. Tivol, E.A., et al., *Loss of CTLA-4 leads to massive lymphoproliferation and fatal multiorgan tissue destruction, revealing a critical negative regulatory role of CTLA-4*. *Immunity*, 1995. **3**(5): p. 541-7.
43. Hodi, F.S., et al., *Improved survival with ipilimumab in patients with metastatic melanoma*. *N Engl J Med*, 2010. **363**(8): p. 711-23.
44. Gatalica, Z., et al., *Programmed cell death 1 (PD-1) and its ligand (PD-L1) in common cancers and their correlation with molecular cancer type*. *Cancer Epidemiol Biomarkers Prev*, 2014. **23**(12): p. 2965-70.
45. Droeser, R.A., et al., *Clinical impact of programmed cell death ligand 1 expression in colorectal cancer*. *Eur J Cancer*, 2013. **49**(9): p. 2233-42.
46. Konishi, J., et al., *B7-H1 expression on non-small cell lung cancer cells and its relationship with tumor-infiltrating lymphocytes and their PD-1 expression*. *Clin Cancer Res*, 2004. **10**(15): p. 5094-100.
47. Gao, Q., et al., *Overexpression of PD-L1 significantly associates with tumor aggressiveness and postoperative recurrence in human hepatocellular carcinoma*. *Clin Cancer Res*, 2009. **15**(3): p. 971-9.
48. Soliman, H., F. Khalil, and S. Antonia, *PD-L1 expression is increased in a subset of basal type breast cancer cells*. *PLoS One*, 2014. **9**(2): p. e88557.
49. Muenst, S., et al., *The presence of programmed death 1 (PD-1)-positive tumor-infiltrating lymphocytes is associated with poor prognosis in human breast cancer*. *Breast Cancer Res Treat*, 2013. **139**(3): p. 667-76.
50. Rodriguez, J.A., *HLA-mediated tumor escape mechanisms that may impair immunotherapy clinical outcomes via T cell activation*. *Oncol Lett*, 2017. **14**(4): p. 4415-4427.
51. Tumeh, P.C., et al., *PD-1 blockade induces responses by inhibiting adaptive immune resistance*. *Nature*, 2014. **515**(7528): p. 568-71.
52. Spranger, S., et al., *Mechanism of tumor rejection with doublets of CTLA-4, PD-1/PD-L1, or IDO blockade involves restored IL-2 production and proliferation of CD8(+) T cells directly within the tumor microenvironment*. *J Immunother Cancer*, 2014. **2**: p. 3.
53. June, C.H., S.R. Riddell, and T.N. Schumacher, *Adoptive cellular therapy: a race to the finish line*. *Sci Transl Med*, 2015. **7**(280): p. 280ps7.
54. Rohaan, M.W., et al., *Adoptive transfer of tumor-infiltrating lymphocytes in melanoma: a viable treatment option*. *J Immunother Cancer*, 2018. **6**(1): p. 102.
55. Radvanyi, L.G., et al., *Specific lymphocyte subsets predict response to adoptive cell therapy using expanded autologous tumor-infiltrating lymphocytes in metastatic melanoma patients*. *Clin Cancer Res*, 2012. **18**(24): p. 6758-70.
56. Dougan, M. and G. Dranoff, *Immune therapy for cancer*. *Annu Rev Immunol*, 2009. **27**: p. 83-117.
57. Butts, C., et al., *Updated survival analysis in patients with stage IIIB or IV non-small-cell lung cancer receiving BLP25 liposome vaccine (L-BLP25): phase IIB randomized, multicenter, open-label trial*. *J Cancer Res Clin Oncol*, 2011. **137**(9): p. 1337-42.
58. Patel, P.H. and D.R. Kockler, *Sipuleucel-T: a vaccine for metastatic, asymptomatic, androgen-independent prostate cancer*. *Ann Pharmacother*, 2008. **42**(1): p. 91-8.

Chapter 5

TIL therapy

Introduction

Less than a decade ago, melanoma was characterized by high rates of mortality associated with limited therapeutic options [1]. Thanks to the development of immune-checkpoint inhibitors, survival rates in terms of OS have been drastically increasing from values ranging around 9-28% to up to 58% - a more than 30% increase -, whereas incidence rates have been growing [2-4]. Notwithstanding these huge progresses, a large portion of patients still results to not respond to immune checkpoint inhibition or develops resistance after documenting initial clinical response [5].

TIL therapy already demonstrated to be of high clinical benefit for metastatic melanoma patients, with demonstrated response rate of 42% at the MD Anderson Cancer Center including 20% of very long term durable responses (potential cures). Patients who have progressed on checkpoint blockade treatments may still respond to TIL therapy albeit with more modest response rate and shorter duration, even in heavily pretreated patients [6]. The present Chapter will highlight the most important characteristics of TIL therapy by mentioning the historical pathway which led to the current clinical success and by describing the immunological features associated with optimal response to this type of treatment.

TIL therapy: the melanoma experience

The advent of ACT based on the utilization of autologous *ex vivo*-expanded TIL – more simply referred to as TIL therapy – for the treatment of metastatic melanoma provided an additional therapeutic option for those patients failing to respond to immune checkpoint inhibition, originating impressive results in first clinical trials. In particular, the first major clinical successes with TIL therapy were observed by Rosenberg et al. in a series of phase I/II trials documenting impressive complete responses with the infusion of autologous TIL in association with HD IL-2 and previous lymphodepleting treatment [7, 8]. The administration of HD IL-2 was necessary in order to maintain T cell activity after autologous transfer, as well as lymphodepletion was a required pre-requisite in order to prepare the patient for TIL infusion by decreasing the number of immunosuppressive cells, especially Tregs [7, 8].

In the following years, several consecutive clinical trials were performed documenting stable long-term responses following TIL therapy also in the setting of heavily pretreated patients, irrespective of the type of prior treatment received [9]. Altogether, the results from these trials consistently highlighted an Objective Response Rate (ORR) of 72%, with 40% of patients documenting durable clinical responses and 10-20% achieving Complete Remission (CR) [10-14]. To note, early responders reaching CR were not influenced by previous therapy, and therefore failure to respond to immune checkpoint inhibitors was not seen to affect response to TIL therapy [5, 10]. However, recent evidence suggest that treatment-naïve patients may respond better to TIL therapy (47%), although previous immunotherapy regimens do not affect dramatically response rates (38% with previous anti CTLA-4 blockade and 33% with previous PD-1 blockade) [6].

Altogether the clinical success of TIL therapy paved the way for further development of new clinical trials worldwide aiming to optimize critical steps of the procedure, especially regarding the composition of the final TIL product, the intensity of lymphodepleting regimens, and the dose of IL-2. In general, in these trials TIL therapy was administered to patients failing to respond to systemic treatment, including dacarbazine, interferon- α , HD IL-2, and ipilimumab (CTLA-4 abrogating agent) [9-11, 13, 14].

Today, the first-line treatment for advanced melanoma involves the utilization of an anti PD-1 inhibitor (nivolumab) often combined with other immunotherapeutics including ipilimumab. This type of treatment generated striking results in the clinical setting, documenting a 3-year OS of about 50% [4]. However, a fraction of patients is still seen to not respond to systemic immunotherapy, and additional pharmacological options are lacking; in this scenario, TIL therapy might represent an additional tool for the treatment of patients whose disease is shown to progress after PD-1 blockade. Moreover, the latest clinical trials are aiming to evaluate whether TIL therapy, administered either in combination with PD-1 inhibitors or as single treatment, can be of clinical benefit as first-line therapy.

TIL as prognostic factors

TIL have been at the centre of the scientific attention since quite a long time mainly on behalf of their prognostic relevance: in 1986, the presence of TIL in rectal cancers was associated with an improvement in PFS for the first time [15]. In the following years, confirmations of the prognostic value of TIL have been accruing for several types of solid tumors, including

melanoma [16], colorectal cancer [17-19], ovarian cancer [20, 21], breast cancer [22-24], non-small cell lung cancer [25], renal-cell carcinoma [24], prostate carcinoma [26], and other less common types of malignancies [27]. Furthermore, while tumors with high CD8+ T infiltration were typically associated with improved prognoses, Treg infiltration was correlated with worse clinical outcomes [21, 27, 28].

TIL therapy: main advantages

TIL therapy is a labor-intensive procedure but can undoubtedly trigger impressive responses in the long run. The response to TIL therapy is however durable in a relevant fraction of treated patients, rendering this therapeutic approach very intriguing.

Immunologically talking, TIL have been shown to possess an extremely broad range of antigen-recognition. On behalf of their former presence *within* the tumor lesions and their surroundings, TIL have the chance to encounter a great variety of tumor antigens, both known and not known, reflecting ultimately the real antigenic landscape of the tumor [5]. In addition, antigen recognition is extended to all possible kinds of MHC/HLA molecules, highlighting one key advantage over engineered T cells (CAR and TCR T cells) [5].

Toxicities related to TIL therapy are generally very limited and easily manageable, and they are seen to arise as a consequence of lymphodepleting regimens or IL-2 administration [29]. However, a few transient TIL-related toxicities have been reported, including chills, fever, and dyspnea in the short term and autoimmune diseases in the medium term, including vitiligo and uveitis [11]. To note, non-transient TIL-related toxicities have been recently documented in a case report regarding a patient experiencing full-body rash, non-transient panuveitis and hearing loss. The same patient, however, documented a durable complete response lasting for two years after TIL-based treatment; as an intriguing fact, biopsy of the rash highlighted an high presence of infiltrating CD8+ T cells [5, 30].

TIL therapy: critical aspects

The success of TIL therapy depends on a series of factors which must be kept in strict consideration.

- In first place, the feasibility of the technique requires the presence of a surgically-resectable tissue fragment in order to set up TIL cultures; the details of TIL culturing will be described in the Materials and Methods section of this thesis. As reported in the landmark study by Rosenberg et al, the success of TIL therapy in the setting of metastatic melanoma required the presence of metastatic nodules of at least 2 cm diameter which can be accessed for resection [9]. More recently, however, it has been shown that TIL can be grown *ex vivo* starting from tumor lesions of at least 1 cm³ [13]. Process development in this area now makes it possible to grow enough TIL for therapeutic use from two core needle biopsies [31].
- Clinical response strictly depends on the total number of autologous TIL. Indeed, it has been shown that response occurs in patients infused on average with almost twice the number of lymphocytes administered to non-responders, indicating that the growth of TIL *ex vivo* is an extremely important parameter to consider [12, 13]. Therefore, novel techniques and/or pharmacological treatments aiming to increase the number of TIL available for infusion remain the subject of intense investigation in the area of TIL therapy.
- The composition of the TIL product has been observed to be essential for the obtainment of durable, objective clinical responses in the long run. Specifically, the composition of the TIL product requires a higher proportion of CD8+ T lymphocytes and a minimum number of CD4+ T lymphocytes. An increased number of CD8+ T lymphocytes has been indeed shown to be a major factor for the obtainment of durable responses, in conjunction with the total number of infused lymphocytes and their differentiation status [12]. The persistence of TIL after infusion, as well as the maintainment of their effector function, strictly depends on the differentiation stage and on the differential expression of activating or inhibiting costimulatory receptors on T lymphocytes [12]. Therefore, the characterization of immune infiltrates (immunomonitoring) is fundamental for the feasibility of the whole technique.

Chapter 5

Nonetheless, the activation status of CD8+ T lymphocytes has been shown to trigger the best clinical responses. Typically, T cell activation relies on three different signals:

- T Cell Receptor (TCR) engagement of MHC/HLA-antigen (signal 1);
- Engagement of co-stimulator molecules and their ligands such as B7 and CD28, 4-1BB (CD137), CD27 and others (signal 2) [31];
- Presence of inflammatory cytokines, including IL-12 and IFN- γ (signal 3)

Today, techniques aiming to improve the number of activated CD8+ T cells in the TIL product are being developed, and novel improvements in this sense have been already published [31, 32].

- A critical parameter is also given by the necessity of lymphodepleting regimens prior to actual TIL infusion [29]. The first evidences regarding the importance of lymphodepletion prior to TIL product administration in order to obtain improved responses were documented in preclinical murine models in the 1980s [33, 34].

Briefly, lymphodepletion is performed in order to obtain three major effects:

- To deplete the patient from immunosuppressive lymphocytes such as FOXP3+ CD4+ T-regs [35];
- To reduce the number of endogenous lymphocytes which can compete with infused TIL for cytokines such as IL-7 and IL-15 [36]. Biologically, these cytokines have been shown to boost the proliferation and survival of T lymphocytes, and are seen to be released by non-lymphoid cells as a consequence of lymphopenia to maintain homeostasis (cytokine sinks) [37, 38];
- To increase the “physical space” for infused TIL within the tumor microenvironment [5].

In early clinical trials, lymphodepletion was performed by administering a schedule of treatment based on cyclophosphamide (60 mg/kg, 2 days of treatment) followed by fludarabine (25 mg/m², 5 days of treatment). Twenty-four hours after the last dose of fludarabine, TIL infusion was performed [7, 9, 11]. In other studies, lymphodepletion has been performed by Total Body Irradiation (TBI), or using a combination of TBI and chemotherapy [14, 29].

As lymphodepleting regimens have been shown to trigger the onset of several toxicities, especially transient pancytopenia and febrile neutropenia, the evaluation of reduced intensity lymphodepletion regimens is currently ongoing (**Table 1**). As an example, a phase II clinical trial is investigating whether the utilization of attenuated lymphodepletion regimens based on fludarabine 25 mg/m² administered for only 3 days followed by TBI (NCT03166397) may be of clinical benefit for patients undergoing TIL therapy.

- In parallel to previous lymphodepleting treatments, a systemic administration of IL-2 is required after TIL infusion in order to maintain T cell reactivity and persistence. In first clinical trials, IL-2 was infused at high-doses (720,000 IU/kg) every 8 hours for a maximum total amount of 15 doses or until the development of toxicities [7, 9, 11]. The dose of IL-2 in conjunction with TIL infusion has been at the center of scientific interest as it is considered alongside with lymphodepletion as the main responsible for the development of transient toxicities, including angioedema, hypotension, fever, nausea, myalgia, rigor, and reduced urine output [39]. Promisingly, recent evidences suggest that it is possible to obtain durable responses with TIL also in presence of lower doses of IL-2 administered in a continuous decrescendo regimen [13]. For these reasons, current clinical trials are exploring different regimens of IL-2 alongside with TIL therapy (**Table 1**).

- One last important feature related to the success of TIL therapy is the recognition of neoantigens by infused TIL. In particular, it has been demonstrated that the success of immunotherapies and TIL therapy in melanoma was especially due to the recognition of MART-1 and gp100 antigens by the wide majority of TIL products [40]. Neoantigens are defined as mutated peptides generated as a consequence of DNA damage [5].

As an implication, tumors harboring high levels of mutational load, such as melanoma and lung cancer, carry the potential of being successfully treated with TIL therapy on behalf of the supposed high rate of neoantigens expressed by tumor cells. As mentioned in the previous chapter, the correlation between high mutational load and improved response to immune checkpoint inhibitors has been demonstrated with regards to lung cancer, melanoma, and on other solid tumors harboring mismatch repair deficiencies [41-44]. For TIL therapy, a recent study from

Rosenberg et al. suggested that tumor regression can be obtained subsequently to adoptive therapies based on T cell products enriched with neoantigen specific T cells [45]. The last part of Chapter 6 shows that TIL expanded *ex vivo* from a total of 4 non-small cell lung cancer patients are able to recognize neoantigens *in vitro* when their autologous reactivity is measured.

TIL therapy: how is it performed?

The details regarding the materials and methods used to isolate and expand TIL regarding the present work will be better described in the dedicated section of Chapter 6.

Briefly, the process at the base of TIL isolation, expansion and final infusion can be divided into three main phases: pre-REP, REP (Rapid Expansion Protocol), and infusion (**Figure 1**) [46].

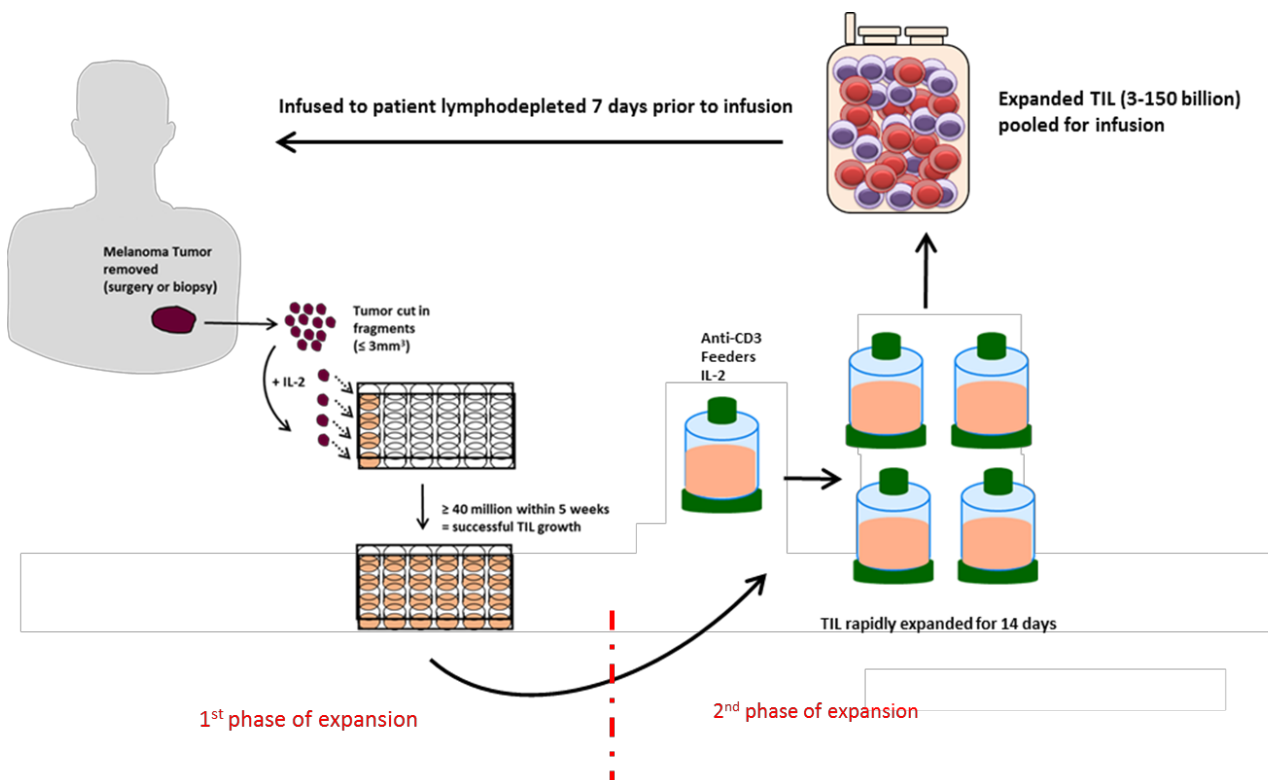


Figure 1 – Representation of three phases of TIL therapy: pre-REP phase, Rapid Expansion Protocol (REP) phase, and infusion phase.

Chapter 5

In the pre-REP phase, freshly-resected tumor samples are initially cut into smaller fragments (1-3 mm²); alternatively, tumor samples can be enzymatically digested to obtain a single cell suspension. Fragments (or digests) are subsequently placed into multi-well culture plates in presence of fresh medium and IL-2. Tumor fragments are left in culture for a period of time ranging between 3 to 5 weeks, with fresh medium + IL-2 replacement performed every 2-3 days until a sufficient number of pre-REP TIL is obtained (12×10^6). The second phase (REP phase) involves a two-weeks long expansion process performed by culturing the obtained pre-REP TIL product in presence of IL-2, anti CD-3 antibody, and feeder cells. These last are represented by irradiated Peripheral Blood Mononuclear Cells (PBMCs) obtained either autologously or allogeneically (normal donors), and serve as a source of growth factors which are released in massive amount in the culture medium. Altogether, these procedures allow the pre-REP TIL product to expand over 1,000 folds, ultimately obtaining the REP TIL product. Due to the massive cellular density generated, the REP phase is usually performed in special culturing bioreactors allowing gas recirculation (G-Rex bottles).

Although the continuous administration of IL-2 can support T cell expansion, at the same time it has been observed that it also leads to the obtainment of exhausted T cells; moreover, the relatively long time required for TIL expansion to be completed further decreases T cell activation. It is possible that switching to the use of IL-7 and IL-15 may be a solution, as documented preclinically, but currently this does not represent a feasible approach yet [47]. To overcome this issue, diverse monoclonal antibodies can be administered to boost T cell activation pharmacologically: in particular, soluble 4-1bb agonist (Urelumab) has been shown to be able to select the most reactive T cell clones by stimulating the 4-1BB (CD137) receptor on T cells. This in turn has been documented to boost T cell proliferation, survival, activation, and IL-2 production [31], and to give rise to TIL products enriched for activated T cells, thus further improving the potential clinical success of the procedure [31].

Chapter 5

Trial	Phase	Lymphodepletion regimen	IL-2 regimen	Disease Stage	NCT ID
A Phase I Study to Evaluate Safety, Feasibility and Immunologic Response of Adoptive T Cell Transfer With or Without Dendritic Cell Vaccination in Patients With Metastatic Melanoma	I	Cy 60 mg/kg i.v. (d - 7&-6) + Flu 25 mg/m ² i.v. (d - 5 to - 1)	100,000 IU/kg t.i.d., maximum 14 doses	Inoperable stage III or stage IV melanoma	NCT01946373
Phase I Study to Assess Feasibility and Safety of Adoptive Transfer of Autologous Tumor- infiltrating Lymphocytes in Combination With Interleukin-2 Followed by Nivolumab Rescue for Advanced Metastatic Melanoma	I	Cy i.v. for 2d and Flu i.v. 5d (not otherwise specified)	HD IL-2 t.i.d. max 8 doses	Stage IV melanoma	NCT03475134
A Phase 2, Single-Center, Open Label Study of Autologous, Adoptive Cell Therapy Following a Reduced Intensity, Non-myeloablative, Lymphodepleting Induction Regimen in Metastatic Melanoma Patients	II	Flu (25 mg/m ² for 3 d) + TBI (2 Gy as single treatment)	720,000 IU/kg t.i.d., until tolerable toxicity, max 10 doses	Measurable metastatic melanoma	NCT03166397
Combined Therapy of Nivolumab and Adoptive T Cell Therapy in Metastatic Melanoma Patients: Pilot Study Phase I/II	I/II	Not described	600,000 IU/kg/d for 5d	Stage IIIB, IIIC or IV melanoma	NCT03374839
A Pilot Clinical Trial Combining PD-1 Blockade, CD137 Agonism and Adoptive Cell Therapy for Metastatic Melanoma	Pilot	Cy 2 d beginning 3–6 w after tumor collection for TIL growth + Flu for 5 d	Unspecified	Unresectable cutaneous or mucosal stage III/IV	NCT02652455
Phase Ib Trial of Pembrolizumab Administered in Combination With or Following Adoptive Cell Therapy- A Multiple Cohort Study; The ACTIVATE (Adoptive Cell Therapy InVigorated to Augment Tumor Eradication) Trial	Ib	Cohort 1: Cy i.v. 60 mg/kg/d for 2d + Flu 25 mg/m ² for 5 d Cohort 2: Cy i.v. 30 mg/kg per day for 2 days	Cohort 1 + 2: 125,000 IU/kg s.c./d	Unresectable stage III/IV melanoma or Platinum resistant ovarian cancer	NCT03158935
A Pilot Study of Lymphodepletion Plus Adoptive Cell Transfer With T cells Transduced With CXCR2 and NGFR Followed by High Dose Interleukin-2 in Patients With Metastatic Melanoma	Pilot	Cy 60 mg/kg for 2d + Flu 25 mg/m ² for 5d	720,000 IU/kg i.v. every 8–16 h, max 15 doses	Metastatic melanoma or stage III in-transit, subcutaneous, or regional nodal disease	NCT01740557
T cell Therapy in Combination With Vemurafenib for Patients With BRAF Mutated Metastatic Melanoma	I/II	Cy 60 mg/kg for 2d + Flu 25 mg/m ² for 5 d	Decrescendo regimen (18 MIU/m ² for 6 h, 18 MIU/m ² for 12 h, 18 MIU/m ² for 24 h followed by 4,5 MIU/m ² for another 3 × 24 h)	Unresectable stage III/IV melanoma	NCT02354690
Randomized Phase III Study Comparing a Non- myeloablative Lymphocyte Depleting Regimen of Chemotherapy Followed by Infusion of Tumor Infiltrating Lymphocytes and Interleukin-2 to Standard Ipilimumab Treatment in Metastatic Melanoma	III	Cy 60 mg/kg iv for 2d + Flu 25 mg/m ² for 5d	600,000 IU/kg t.i.d., max 15 doses	Unresectable stage III/IV melanoma	NCT02278887
A Pilot Study of Lymphodepletion Plus Adoptive Cell Transfer With TGF-beta Resistant (DNRII) and NGFR Transduced T cells Followed by High Dose Interleukin-2 in patients With Metastatic Melanoma	Pilot	Cy 60 mg/kg i.v. for 2d + Flu 25 mg/m ² i.v. for 5d	720,000 IU/kg i.v. every 8–16 h max 15 doses on d 1–5+ 22–26	Metastatic melanoma or stage III in-transit, subcutaneous, or regional nodal disease (turnstile I)	NCT01955460
Phase II Study Evaluating the Infusion Of Autologous TIL And Low-Dose Interleukin-2 (IL-2) Therapy Following A Preparative Regimen Of Non-Myeloablative Lymphodepletion Using cyclophosphamide And Fludarabine In Patients With Metastatic Melanoma	II	Cy 60 mg/kg i.v. for 2 d + Flu 25 mg/m ² i.v. for 5 d	125,000 IU/kg/d for 2 w (2 d rest between each w)	Measurable, unresectable stage III/IV melanoma	NCT01883323
A Phase II Study for Metastatic Melanoma Using High Dose Chemotherapy Preparative Regimen Followed by Cell Transfer Therapy Using Tumor Infiltrating Lymphocytes Plus IL-2 With the Administration of Pembrolizumab in the Retreatment Arm	II	Cy 60 mg/kg/day for 2 d + Flu 25 mg/m ² i.v. for 5 d	720,000 IU/kg i.v. t.i.d., max 12 doses	Measurable metastatic melanoma	NCT01993719
A Prospective Randomized and Phase 2 Trial for Metastatic Melanoma Using Adoptive Cell Therapy With Tumor Infiltrating Lymphocytes Plus IL-2 Either Alone or Following the Administration of Pembrolizumab	II	Cohort 1 + 2: Cy 60 mg/kg i.v. for 2d + Flu 25 mg/m ² for 5d	Cohort 1 + 2: 720,000 IU/kg i.v. t.i.d., max 12 doses	Measurable metastatic melanoma	NCT02621021
A Phase 2, Multicenter Study to Assess the Efficacy and Safety of Autologous Tumor Infiltrating Lymphocytes (LN-144) for Treatment of Patients With Metastatic Melanoma	II	Lymphodepleting chemotherapy, not otherwise specified	Unspecified	Unresectable metastatic melanoma	NCT02360579
Lymphodepletion Plus Adoptive Cell Transfer with or Without Dendritic Cell Immunization in Patients With Metastatic Melanoma	II	Cy 60 mg/kg for 2 d + Flu 25 mg/m ² for 5d	Cohort 1–3: 720,000 IU/kg every 8–16 h, max doses on d 1–5+ 22–26 (+/- 7 d), as tolerated Cohort 4: 1.2 MIU of IL-2 on d 2, 4, 9, 11, 16 and 18 as tolerated. Subsequently 2x/w	Metastatic melanoma, uveal melanoma or stage III in-transit or regional nodal disease	NCT00338377

Table 1 – Ongoing clinical trials (currently recruiting) aiming to evaluate and improve TIL therapy for the treatment of solid tumors.

References

1. Karimkhani, C., et al., *The global burden of melanoma: results from the Global Burden of Disease Study 2015*. Br J Dermatol, 2017. **177**(1): p. 134-140.
2. Luke, J.J., et al., *Targeted agents and immunotherapies: optimizing outcomes in melanoma*. Nat Rev Clin Oncol, 2017. **14**(8): p. 463-482.
3. Svedman, F.C., et al., *Stage-specific survival and recurrence in patients with cutaneous malignant melanoma in Europe - a systematic review of the literature*. Clin Epidemiol, 2016. **8**: p. 109-22.
4. Wolchok, J.D., et al., *Overall Survival with Combined Nivolumab and Ipilimumab in Advanced Melanoma*. N Engl J Med, 2017. **377**(14): p. 1345-1356.
5. Rohaan, M.W., et al., *Adoptive transfer of tumor-infiltrating lymphocytes in melanoma: a viable treatment option*. J Immunother Cancer, 2018. **6**(1): p. 102.
6. Forget, M.A., et al., *Prospective Analysis of Adoptive TIL Therapy in Patients with Metastatic Melanoma: Response, Impact of Anti-CTLA4, and Biomarkers to Predict Clinical Outcome*. Clin Cancer Res, 2018. **24**(18): p. 4416-4428.
7. Rosenberg, S.A., et al., *Treatment of patients with metastatic melanoma with autologous tumor-infiltrating lymphocytes and interleukin 2*. J Natl Cancer Inst, 1994. **86**(15): p. 1159-66.
8. Dudley, M.E., et al., *Cancer regression and autoimmunity in patients after clonal repopulation with antitumor lymphocytes*. Science, 2002. **298**(5594): p. 850-4.
9. Rosenberg, S.A., et al., *Durable complete responses in heavily pretreated patients with metastatic melanoma using T-cell transfer immunotherapy*. Clin Cancer Res, 2011. **17**(13): p. 4550-7.
10. Besser, M.J., et al., *Adoptive transfer of tumor-infiltrating lymphocytes in patients with metastatic melanoma: intent-to-treat analysis and efficacy after failure to prior immunotherapies*. Clin Cancer Res, 2013. **19**(17): p. 4792-800.
11. Dudley, M.E., et al., *Adoptive cell therapy for patients with metastatic melanoma: evaluation of intensive myeloablative chemoradiation preparative regimens*. J Clin Oncol, 2008. **26**(32): p. 5233-9.
12. Radvanyi, L.G., et al., *Specific lymphocyte subsets predict response to adoptive cell therapy using expanded autologous tumor-infiltrating lymphocytes in metastatic melanoma patients*. Clin Cancer Res, 2012. **18**(24): p. 6758-70.
13. Andersen, R., et al., *Long-Lasting Complete Responses in Patients with Metastatic Melanoma after Adoptive Cell Therapy with Tumor-Infiltrating Lymphocytes and an Attenuated IL2 Regimen*. Clin Cancer Res, 2016. **22**(15): p. 3734-45.
14. Dudley, M.E., et al., *Adoptive cell transfer therapy following non-myeloablative but lymphodepleting chemotherapy for the treatment of patients with refractory metastatic melanoma*. J Clin Oncol, 2005. **23**(10): p. 2346-57.
15. Jass, J.R., *Lymphocytic infiltration and survival in rectal cancer*. J Clin Pathol, 1986. **39**(6): p. 585-9.
16. Clemente, C.G., et al., *Prognostic value of tumor infiltrating lymphocytes in the vertical growth phase of primary cutaneous melanoma*. Cancer, 1996. **77**(7): p. 1303-10.
17. Galon, J., et al., *Type, density, and location of immune cells within human colorectal tumors predict clinical outcome*. Science, 2006. **313**(5795): p. 1960-4.
18. Mlecnik, B., et al., *Histopathologic-based prognostic factors of colorectal cancers are associated with the state of the local immune reaction*. J Clin Oncol, 2011. **29**(6): p. 610-8.

Chapter 5

19. Galon, J., W.H. Fridman, and F. Pages, *The adaptive immunologic microenvironment in colorectal cancer: a novel perspective*. *Cancer Res*, 2007. **67**(5): p. 1883-6.
20. Leffers, N., et al., *Prognostic significance of tumor-infiltrating T-lymphocytes in primary and metastatic lesions of advanced stage ovarian cancer*. *Cancer Immunol Immunother*, 2009. **58**(3): p. 449-59.
21. Sato, E., et al., *Intraepithelial CD8+ tumor-infiltrating lymphocytes and a high CD8+/regulatory T cell ratio are associated with favorable prognosis in ovarian cancer*. *Proc Natl Acad Sci U S A*, 2005. **102**(51): p. 18538-43.
22. Denkert, C., et al., *Tumor-associated lymphocytes as an independent predictor of response to neoadjuvant chemotherapy in breast cancer*. *J Clin Oncol*, 2010. **28**(1): p. 105-13.
23. Martinet, L., et al., *Human solid tumors contain high endothelial venules: association with T- and B-lymphocyte infiltration and favorable prognosis in breast cancer*. *Cancer Res*, 2011. **71**(17): p. 5678-87.
24. Marrogi, A.J., et al., *Study of tumor infiltrating lymphocytes and transforming growth factor-beta as prognostic factors in breast carcinoma*. *Int J Cancer*, 1997. **74**(5): p. 492-501.
25. Al-Shibli, K.I., et al., *Prognostic effect of epithelial and stromal lymphocyte infiltration in non-small cell lung cancer*. *Clin Cancer Res*, 2008. **14**(16): p. 5220-7.
26. Karja, V., et al., *Tumour-infiltrating lymphocytes: A prognostic factor of PSA-free survival in patients with local prostate carcinoma treated by radical prostatectomy*. *Anticancer Res*, 2005. **25**(6C): p. 4435-8.
27. Fridman, W.H., et al., *The immune contexture in human tumours: impact on clinical outcome*. *Nat Rev Cancer*, 2012. **12**(4): p. 298-306.
28. Adotevi, O., et al., *A decrease of regulatory T cells correlates with overall survival after sunitinib-based antiangiogenic therapy in metastatic renal cancer patients*. *J Immunother*, 2010. **33**(9): p. 991-8.
29. Goff, S.L., et al., *Randomized, Prospective Evaluation Comparing Intensity of Lymphodepletion Before Adoptive Transfer of Tumor-Infiltrating Lymphocytes for Patients With Metastatic Melanoma*. *J Clin Oncol*, 2016. **34**(20): p. 2389-97.
30. Yeh, S., et al., *Ocular and systemic autoimmunity after successful tumor-infiltrating lymphocyte immunotherapy for recurrent, metastatic melanoma*. *Ophthalmology*, 2009. **116**(5): p. 981-989 e1.
31. Tavera, R.J., et al., *Utilizing T-cell Activation Signals 1, 2, and 3 for Tumor-infiltrating Lymphocytes (TIL) Expansion: The Advantage Over the Sole Use of Interleukin-2 in Cutaneous and Uveal Melanoma*. *J Immunother*, 2018. **41**(9): p. 399-405.
32. Forget, M.A., et al., *A Novel Method to Generate and Expand Clinical-Grade, Genetically Modified, Tumor-Infiltrating Lymphocytes*. *Front Immunol*, 2017. **8**: p. 908.
33. Rosenberg, S.A., P. Spiess, and R. Lafreniere, *A new approach to the adoptive immunotherapy of cancer with tumor-infiltrating lymphocytes*. *Science*, 1986. **233**(4770): p. 1318-21.
34. Mills, C.D. and R.J. North, *Expression of passively transferred immunity against an established tumor depends on generation of cytolytic T cells in recipient. Inhibition by suppressor T cells*. *J Exp Med*, 1983. **157**(5): p. 1448-60.
35. Antony, P.A., et al., *CD8+ T cell immunity against a tumor/self-antigen is augmented by CD4+ T helper cells and hindered by naturally occurring T regulatory cells*. *J Immunol*, 2005. **174**(5): p. 2591-601.
36. Gattinoni, L., et al., *Removal of homeostatic cytokine sinks by lymphodepletion enhances the efficacy of adoptively transferred tumor-specific CD8+ T cells*. *J Exp Med*, 2005. **202**(7): p. 907-12.

Chapter 5

37. Schluns, K.S., et al., *Interleukin-7 mediates the homeostasis of naive and memory CD8 T cells in vivo*. Nat Immunol, 2000. **1**(5): p. 426-32.
38. Schluns, K.S., et al., *Cutting edge: requirement for IL-15 in the generation of primary and memory antigen-specific CD8 T cells*. J Immunol, 2002. **168**(10): p. 4827-31.
39. Marabondo, S. and H.L. Kaufman, *High-dose interleukin-2 (IL-2) for the treatment of melanoma: safety considerations and future directions*. Expert Opin Drug Saf, 2017. **16**(12): p. 1347-1357.
40. Kvistborg, P., et al., *TIL therapy broadens the tumor-reactive CD8(+) T cell compartment in melanoma patients*. Oncoimmunology, 2012. **1**(4): p. 409-418.
41. Rizvi, N.A., et al., *Cancer immunology. Mutational landscape determines sensitivity to PD-1 blockade in non-small cell lung cancer*. Science, 2015. **348**(6230): p. 124-8.
42. Snyder, A., et al., *Genetic basis for clinical response to CTLA-4 blockade in melanoma*. N Engl J Med, 2014. **371**(23): p. 2189-2199.
43. Le, D.T., et al., *Mismatch repair deficiency predicts response of solid tumors to PD-1 blockade*. Science, 2017. **357**(6349): p. 409-413.
44. Le, D.T., et al., *PD-1 Blockade in Tumors with Mismatch-Repair Deficiency*. N Engl J Med, 2015. **372**(26): p. 2509-20.
45. Tran, E., et al., *Cancer immunotherapy based on mutation-specific CD4+ T cells in a patient with epithelial cancer*. Science, 2014. **344**(6184): p. 641-5.
46. Dudley, M.E., et al., *Generation of tumor-infiltrating lymphocyte cultures for use in adoptive transfer therapy for melanoma patients*. J Immunother, 2003. **26**(4): p. 332-42.
47. Kaneko, S., et al., *IL-7 and IL-15 allow the generation of suicide gene-modified alloreactive self-renewing central memory human T lymphocytes*. Blood, 2009. **113**(5): p. 1006-15.

Chapter 6

CD8⁺ TIL isolated and expanded from a NSCLC immunosuppressive tumor microenvironment exhibit neoantigen-specific activation *in vitro*

Introduction

The present Chapter describes the experimental work performed during the second part of the doctorate course at the Melanoma Medical Oncology department of the MD Anderson Cancer Center in Houston, USA. The study aims to test whether TIL therapy may be extended also for the treatment of NSCLC, on behalf of the results obtained in the setting of metastatic melanoma in recent times. As of today, the response rate to immune-checkpoint inhibitors with regards to NSCLC is limited to a 20% portion of patients. Latest clinical trials are aiming to overcome this limited response rate by combining novel immune-related therapeutic approaches with immune-checkpoint inhibitors. With this regard, it becomes fundamental to evaluate and to understand the molecular features associated to immunological diversity within tumor infiltrates [1-3].

As lung cancer is on the way to be the next solid tumor to be treated with TIL therapy, one key aspect posing the bases for further immune-related approaches is represented by the systematic characterization of immune infiltrates with regards to the latest prognostic and clinically-relevant findings. Nonetheless, the understanding of the heterogeneity associated with NSCLC microenvironment represents a crucial step for the development of personalized therapeutic schemes based on immune-related approaches [3]. To this regard, the determination of novel robust biomarkers helping clinicians to predict response to anti PD-1 drugs is strongly needed [3].

Lung cancer statistics and histological subtypes

Lung and bronchus cancer nowadays represents the principal cause of cancer-related death among both man and women worldwide [4-10].

Lung cancer can be categorized into two main histological subtypes: small-cell lung carcinoma (SCLC), and NSCLC [11].

NSCLC represents 85% of total diagnoses, and can be further categorized into three histological subgroups: adenocarcinoma, large-cell carcinoma, and squamous-cell carcinoma [11]. Among them, adenocarcinoma represented in the last decade the most prevalent histological subtype in Western Countries, mainly due to high pollution rates in urban areas and tobacco smoking. However, significant changes in social behaviors have led to a decrease of this trend due to a diminished utilization of tobacco smoking, especially

with regards to male individuals from United States, United Kingdom, and Australia [6, 12]. However, low- and middle-income Countries are today assisting to a major increase of lung cancer-related deaths, as heavy industrialization is taking place in these years [4].

In 2018, a total of 234,030 new lung and bronchus cancer cases is likely to be diagnosed in the United States. Among them, male and female diagnoses are estimated to account for a total of 121,680 and 112,350 cases, respectively [6].

The probabilities of developing lung cancer have been estimated to be strictly associated with cigarette smoking (both active and passive), radon exposure, asbestos inhalation, pollution in urban areas, and a personal family history of this type of cancer [13-18].

During the last decades, progresses have been made to improve the early diagnosis of lung cancer which, however, is often detected at late stages (especially stage IV), where chemotherapy and/or radiotherapy-based therapeutic schemes represent the most feasible treatment approach [19].

However, during the last decade, the characterization of specific molecular targets paved the way for the development of novel personalized therapeutic approaches (e.g. small-molecule inhibitors) which significantly improved the prognoses of patients affected by lung cancer, especially regarding NSCLC [20]. Novel therapeutic targets reflect a new way to characterize lung cancers based on the expression of specific biomarkers, including:

- Mutations of epidermal growth factor receptor (EGFR). *EGFR* gene mutations, which are found on 10–15% of lung cancer adenocarcinomas, can be targeted pharmacologically with novel tyrosine kinase inhibitors such as erlotinib, afatinib, gefitinib, osimertinib, and dacomitinib [20]. Of note, osimertinib has been ideated to target the T790M mutation of the EGFR gene, an aberration which has been correlated with the development of resistance to EGFR inhibitors [21].
- Mutations of KRAS are detected more frequently in adenocarcinomas and in individuals with a smoking history [22]. Recently, a study highlighted a possible therapeutic targeting of mutated KRAS with small-molecule inhibitors, without affecting non-mutated KRAS [23].
- Mutations of Anaplastic Lymphoma Kinase (ALK), found on 3-7% of lung tumors. ALK can also rearrange into diverse fusion product, among which the most typical is given by EML4-ALK [24]. This last product is the therapeutic target of crizotinib, a FDA-

approved drug which today is the standard of care for patients with previously untreated, advanced ALK-positive NSCLC [25].

- Mutations of BRAF arise in 2-4% of adenocarcinomas [26]. Mutation of BRAF has been associated with development of resistance to EGFR inhibitors in 1-2% of cases [27]. Mutant BRAF is the pharmacological target of vemurafenib, dabrafenib, and sorafenib: although recent data indicate that the pharmacological targeting of BRAF can give rise to promising clinical anti-tumor efficacy, new clinical trials are currently evaluating this new therapeutic approach [28, 29].

Immunotherapies for lung cancer

Aside from the clear therapeutic improvements generated by the introduction of small-molecule inhibitors, the treatment of lung cancer has greatly benefitted from the advent of immunotherapy. As of today, several immune-related pharmacologic approaches have been approved for the treatment of NSCLC, especially those targeting the PD-1/PD-L1 immune regulatory checkpoint. In general, the evaluation of PD-L1 expression levels on tumor cells by immunohistochemistry represents the main criterion for the selection of patients receiving immune checkpoint inhibitors [30]. Recently, it has been proposed that the evaluation of the expression levels on TIL might further enhance therapy prediction [31].

Regarding PD-1 inhibitors, nivolumab was approved by FDA in October of 2015 as a second-line therapy for treating non-squamous chemo-refractory NSCLC, and on March 2015 for the treatment of advanced squamous NSCLC patients who do not respond to chemotherapy. As a first-line treatment, pembrolizumab has been approved on October 2016 for treating advanced NSCLC showing expression levels of PD-L1 on tumor cells of at least 50% (tumor proportion score) [30]. Of note, pembrolizumab was previously approved for the treatment of chemo-refractory metastatic NSCLC with PD-L1 expression levels higher than 1%. Moreover, the same drug was FDA-approved in May 2017 as a first-line treatment in combination with chemotherapy for patients affected by metastatic NSCLC.

Regarding PD-L1 abrogating agents, atezolizumab received FDA approval in October of 2016 for the treatment of advanced NSCLC refractory to previous chemotherapy. Very recently (February 2018), the approval of durvalumab introduced an additional therapeutic

tool for the treatment of locally advanced, unresectable stage III NSCLC patients who did not show progression following chemotherapy/radiotherapy. A recent phase 3 study compared the anti-tumor efficacy of durvalumab with placebo in patients with stage III NSCLC who did not have disease progression after two or more cycles of platinum-based chemoradiotherapy [32]. Altogether, the results of this trial highlighted a clinical benefit arising from the introduction of durvalumab in terms of PFS: median PFS was evaluated as 16.8 months versus 5.6 months with regards to the durvalumab treatment arm and placebo, respectively [32].

Lung cancer: the next candidate for TIL therapy?

In spite of a significant improvement in patient's prognosis obtained by the introduction of immune checkpoint inhibitors, however, a far too high proportion of patients are seen to not responding to such treatment options, whereas other patients develop resistance after an initial response.

Considering the clinical benefit reported with the utilization of TIL therapy for the treatment of metastatic melanoma patients who progressed after immune checkpoint inhibition, it is reasonable to consider TIL therapy for NSCLC [33, 34].

In particular:

- Both NSCLC and metastatic melanoma result to be two immunologically “hot” types of solid tumors, meaning that immune infiltrates are often seen to be enriched for anergic T cells with cytotoxic potential. The clinical success of TIL therapy in melanoma has been shown to be due to the presence of highly tumor-reactive TIL in the infused product [34-37]. In particular, one of the first observations in this sense came from the work of Dr. Yang et al on melanoma, which demonstrated that CD8+ T-lymphocytes expressing high levels of PD-1 prior to expansion were more likely to generate a tumor-specific reactivity after expansion. This finding implied that the highly-reactive clones responsible for tumor regression were once part of the CD8+ PD1+ TIL population and that, in spite of the original immunosuppressive tumor microenvironment, the *ex vivo* expansion process was able to restore lymphocytic reactivity [38]. In addition, Rosenberg et al. demonstrated that, within the PD1+ CD8+ T-population, the expression levels of LAG-3 and TIM-3 were positively associated with the obtainment of tumor-reactive TIL after expansion [39]. For NSCLC, an

increased presence of infiltrating T CD8+ lymphocytes expressing high levels of PD-1 and TIM-3 has been documented in literature [3, 40].

- Both NSCLC and metastatic melanoma result to be associated with high mutational loads, resulting into an increased expression of mutated peptides (neoantigens) as a consequence of DNA damage. Recent evidences suggest that TIL can recognize neoantigens resulting from cancer-specific mutations, and that this phenomenon is at the base of improved clinical outcomes with TIL therapy [41-44].

Therefore, the rationale of administering TIL products for the treatment of NSCLC is supported by concrete evidences, suggesting that TIL therapy might represent a significant therapeutic improvement, especially for those patients who develop resistance to systemic immunotherapy.

Outline of the project

The ICON study (ImmunogenomiC profiling of early stage NNSCLC) has been ideated in order to perform a comprehensive immunogenomic characterization of early stage localized NSCLC. The ICON study is currently ongoing and aims to pave the way for the molecular identification of phenomena related to tumor immunity that may be targeted in future trials. The ICON study is currently ongoing thanks to the multidisciplinary participation of several working groups at the University of Texas MD Anderson Cancer Center in Houston, USA, involving tissue and blood profiling, genomics, development of PDX models, evaluation of intratumoral heterogeneity and TCR sequencing, and characterization of TIL from freshly-resected tumor samples.

The results hereby presented have been generated by the TIL characterization working group on NSCLC, where the author of this thesis spent a period of time of about 18 months.

The present results can be divided into the following tasks:

- TIL immunophenotyping in fresh tissues (immunomonitoring);
- Immunosignatures detection using clustering of flow data and clinical parameters;
- Evaluation of the feasibility of TIL expansion *ex vivo*;

- Evaluation of autologous reactivity of expanded TIL with a pool of predicted neoantigens.

Earlier work has demonstrated the prognostic significance of TIL in localized NSCLC [45-48]. This section of the work evaluates the functional status of T cells infiltrating NSCLC tumors and their capacity to expand *ex-vivo* and perform effector function.

Moreover, the present work involved an evaluation of autologous tumor reactivity of TIL with a pool of peptides which were previously identified as potential neoantigens from mutations identified in the tumor tissue and based on an *in silico* prediction.

The ICON study: patient population

A total of 141 patients have been enrolled in the ongoing ICON study (**Table 1**). Among them, 75 were female individuals and 66 male subjects. The median age was assessed as 68 years, ranging between 38 and 85 years. Mean age has been recorded as 67 years. For each patient enrolled, smoking status has been retrieved, resulting in a total of 7 subjects who were smokers at the moment of enrollment and a total of 112 who declared a previous history of smoking. A total of 22 patients have been recorded as never smokers.

The majority of cases were assessed as stage I (51 cases), followed by stage II (52 cases), and stage III (33 cases). One stage IV case was present, as well as two patients documenting complete response after chemotherapy (stage 0).

Previous neoadjuvant chemotherapy was administered in a minority of cases (33 subjects), while the majority of cases were chemotherapy-naïve (106 cases). Two patients underwent targeted therapy before surgery.

Chapter 6

Cohort size	N=141	Histology		Pathologic State	
		Adenocarcinomas	N=89	Stage 0*	N=2
Gender		Squamous Cell Carcinomas	N=37	Stage 1	N=51
F	N=75	Small cell	N=4	Stage 2	N=52
M	N=66	Large Cell	N=3	Stage 3	N=33
Mean	67	Pleomorphic	N=3	Stage 4	N=1
Median	68	Adenosquamous	N=2	Data N/A	N=2
Range	38-85	Carcinosarcoma	N=1		
		Adenosarcoma	N=1	Clinical Tumor Size	
Smoking Status		SCC/Large cell	N=1	Mean	4.2
Former	N=112			Median	3.6
Current	N=7	Vital Status		Range	1.4-11
Never	N=22	No Recurrence	N=11 3		
		Recurrence	N=26	Path Tumor Size	
Neoadjuvant Therapy		Dead	N=14 N=12	Mean	4.8
None	N=106	Alive	5	Median	4.1
Chemo	N=33	Data N/A	N=2	Range	0-12
Targeted Therapy	N=2				

*(post-chemo Path CR)

Table 1 – Patient population of the ICON study: characteristics.

Task 1: TIL immunophenotyping in fresh tumor tissues

Introduction

Since the translational evaluation of TIL from fresh tumor samples has been a proven tool to improve the clinical efficacy of TIL therapy, this section of the present thesis describes the results obtained from the systematic characterization through multiparametric flow-cytometry of immune infiltrates from surgically-resected fresh lung tumor cores. In addition, samples from matched uninvolved lung tissues have been characterized in parallel for comparison purposes.

Materials and methods

Staining and flow cytometry evaluation

Fresh tumor samples were manually disaggregated to obtain a single-cell suspension for analysis. Both the disaggregated tissue samples and expanded TIL were stained in FACS Wash Buffer (Dulbecco's Phosphate Buffered Saline 1 x with 1% Bovine Serum Albumin) for 30 min using fluorochrome-conjugated monoclonal antibodies including CD3, CD4, CD8, CD16, CD56, CD57, Granzyme B, CD27, CD28, CD45, CD45RA, CD45RO, CCR7, BTLA (clone J168) (BD Bioscience), PD-1. Details regarding the types of antibodies and their conjugated fluorochromes are shown in **Table 2**. Stained cells were fixed in 1% paraformaldehyde solution for 20 min. Intracellular staining was performed using eBioscience transcription factor staining kit according to the manufacturer's instructions. Samples were acquired using the BD FACSCanto™ II or BD LSRFortessa X-20 and analyzed using FlowJo Software v10.2 (Tree Star). Dead cells were excluded using an AQUA or Yellow live/dead staining (Invitrogen).

Chapter 6

Panel	CD Designation	Marker	Fluorophore
Panel #1 - T cellular activation	CD45	--	BUV395
	CD4	--	BUV496
	CD278	ICOS	BV421
	CD366	TIM-3	BV605
	CD279	PD-1	BV650
	CD103	ITGAE	BV711
	CD152	CTLA-4	BV786
	CD357	GITR	Alexa Fluor 488
	CD3	--	PerCP-Cy5.5
	CD223	LAG-3	PE
	--	FoxP3	PE-eFluor610 **
	CD56	--	PE-Cy7
	--	Ki67	APC
	CD8	--	Alexa 700
	CD25	IL-2R α	APCFire/750 *
Panel #2 - Memory panel	CD4	--	BUV496
		Live/dead	AmCyan
	CD45RA	--	V450
	CD27	--	FITC
	CCR7	--	PerCP-Cy5.5
	BTLA	--	PE
	CD28	--	PE-Cy7
	CD3	--	APC
	CD8	--	AF700
	CD45RO	--	APC-H7
Panel #3 - T cellular functionality	Perforin	--	FITC
	IFN- γ	--	PE
	CD3	--	PE-Cy7
	TIM3	--	APC
	CD8	--	APC-Cy7
	GrzB V450	--	(PB)
	PD-1	--	PerCP-Cy5.5

Table 2 – Fluorochrome-conjugated monoclonal antibodies and panels used to characterize immune infiltrates from freshly-disaggregated tissue samples.

Results

As of October 2018, flow-cytometry characterization of immune infiltrates in freshly disaggregated lung cancers and from matched adjacent uninvolved tissues has been performed on a total of 141 samples (**Table 3**). However, at the moment data are available for subgroup of patients of 53 individuals. Each tumor tissue sample and selected normal tissues were also used for *ex-vivo* T-cell expansion.

PERFORMED ASSAY	NUMBER OF FRESH TUMOR SAMPLES STAINED BY FLOW CYTOMETRY	SUCCESSFUL TIL (OR NORMAL T CELL) GROWTH (>12 MILLION)	NUMBER OF EXPANDED TIL CULTURES STAINED BY FLOW CYTOMETRY
Fresh tumor tissue	120/141	90/133	42/121
Fresh adjacent normal tissue	120/141	26/39 (>12 million)	36/39

Table 3 – Information about the total number of samples for which flow cytometry analyses have been performed and for which it has been possible to obtain successful TIL growth.

NSCLC immune infiltrates are enriched for CD3+ T lymphocytes, depleted for NK cells, and show a reduced number of CD8+ T cells as compared with uninvolved tissue.

As a first observation, CD3+ T-lymphocytes appear to be mostly prevalent among the total immune cells in immune infiltrates from NSCLC samples as compared with uninvolved tissue samples. Specifically, the lung tumor fraction results to be enriched for CD45+ CD3+ lymphocytes (62.4%), whereas uninvolved lung infiltrates possess a smaller proportion of the same lymphocytic population (47.2%) (**Figure 1A**).

When the CD45+ population is gated for the CD3- CD56+ population (commonly referring to as NK cells), the uninvolved lung tissue results to be mostly enriched for this type of

immune cells (54.1%); conversely, matched tumor samples show a minor proportion of infiltrating NK cells (19.2%) (**Figure 1B**).

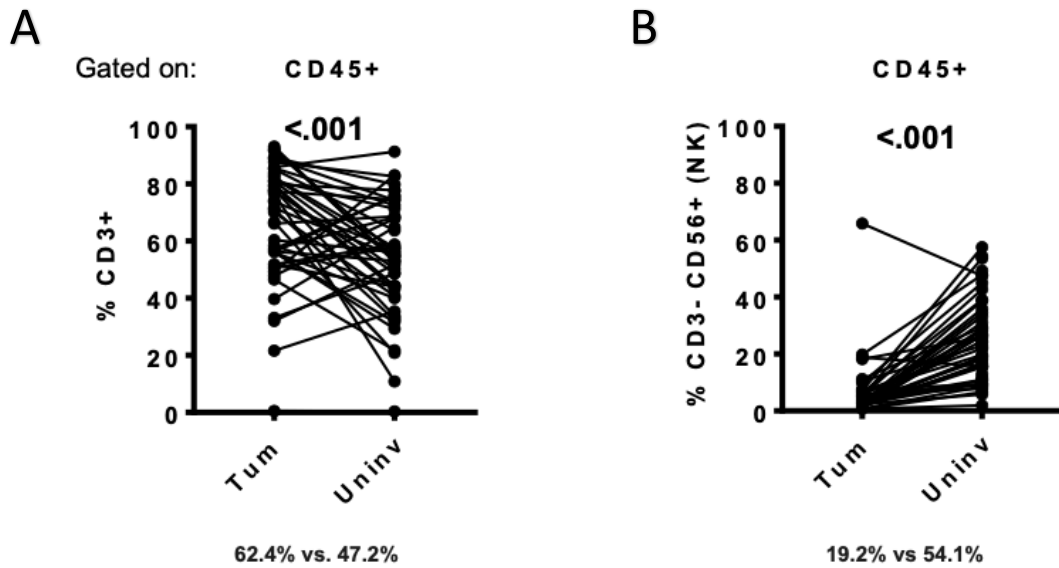


Figure 1 - Immune fraction is enriched for CD3⁺ T cells and poor in NK cells in tumor. Results have been originated by evaluating NSCLC fresh samples and their matched uninvolved tissues by multiparametric flow cytometry on a subgroup of patients (N=53) from the ongoing ICON study.

When looking at the CD8⁺ T cell population within CD3⁺ gate, uninvolved tissues appear to possess the highest proportion of infiltrating cytotoxic CD8⁺ T lymphocytes (52%), whereas tumor samples show an infiltration level of the same lymphocytic population of 44% (**Figure 2A**). On the contrary, Tregs, gated as FOXP3⁺ CD4⁺ T cells, result to infiltrate tumor samples at higher proportions as compared with uninvolved lung tissues (8.2% versus 3.0%, respectively) (**Figure 2B**). Moreover, the evaluation of the CD8⁺/CD4⁺ ratio reveals similar values for both tumor samples and uninvolved lung tissues (1.6 versus 1.7, respectively) (**Figure 2C**).

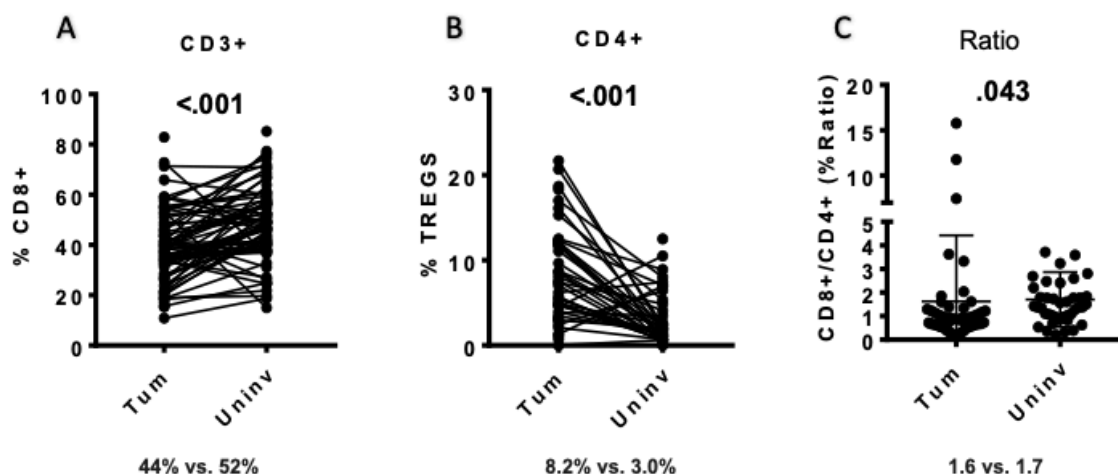


Figure 2 – (A) Infiltrating T cell populations are depleted of CD8+ T lymphocytes and (B) exhibit higher proportion of infiltrating Tregs. (C) The CD8⁺/CD4⁺ T cell fractional ratio measured in the CD3⁺ cell infiltrate population was on average significantly reduced in the tumor as compared to matched uninvolved lung tissue. Results have been originated by evaluating NSCLC fresh samples and their matched uninvolved tissues by multiparametric flow cytometry on a subgroup of patients (N=53) from the ongoing ICON study.

TIL isolated from NSCLC show activation but lack cytotoxic potential

After an initial evaluation of the diverse lymphocytic components that infiltrate lung cancer and matched uninvolved lung tissues, this part of the present study proceeds to focus on the CD8+ T cellular population, as it has been demonstrated to be majorly responsible for anti-tumor response in the clinical setting. In particular, the present section involves a characterization of the activation status, proliferation status, and functional status of the CD8+ lymphocytic compartment within immune infiltrates from lung tumor and matched uninvolved tissue samples.

The activation status of CD8+ T cells has been retrieved by evaluating the expression levels of immune-checkpoints PD1, TIM3, and LAG3 [49]. In addition, the expression levels of co-stimulatory molecule ICOS have been analysed on CD8+ T-lymphocytes to further investigate the level of activation of TIL [50].

Chapter 6

The analysis of the expression levels of PD1 on CD8+ T lymphocytes reveals that NSCLC samples are significantly enriched for this type of immune cells as compared with adjacent uninvolved tissue samples. In tumors, PD1+ CD8+ T lymphocytes represent the 57.9% of the total CD8+ T cell population, whereas immune infiltrates from uninvolved tissues show a reduced proportion of the same population (32.5%) (**Figure 3A**).

Similarly, the expression levels of TIM3 appear to be higher on CD8+ T cells from tumor samples than what is observed in CD8+ T-lymphocytes infiltrating the adjacent uninvolved tissue (7.1% versus 3.0%, respectively) (**Figure 3B**). The proportion of LAG3+ CD8+ T lymphocytes, then, results to be higher on immune infiltrates obtained from tumor samples as compared with uninvolved tissue (3.7% versus 0.4%, respectively) (**Figure 3C**).

Lastly, the evaluation of the expression levels of ICOS on CD8+ T-lymphocytes reveals an important increase in the tumor compartment as compared with the uninvolved counterpart. Thus, ICOS+ CD8+ T-lymphocytes appear to infiltrate lung tumors at a significantly higher rate as compared with adjacent uninvolved lung samples (37.6% versus 11.2%, respectively) (**Figure 3D**).

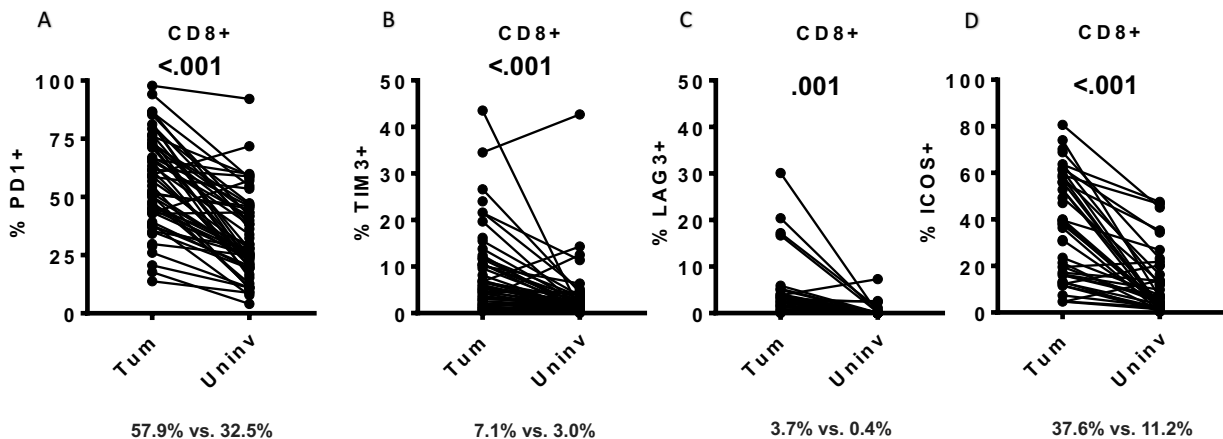


Figure 3 – Cytofluorimetric evaluation of the activation status of CD8+ T-lymphocytes isolated from freshly-resected NSCLC samples and compared with adjacent uninvolved lung tissue samples. CD8⁺ TIL showed fractional enrichment in **(A)** PD1 (57.9% vs 32.5%), **(B)** TIM3 (7.1% vs 3.0%), **(C)** LAG3 (3.7% vs 0.4%), and **(D)** ICOS (37.6% vs. 11.2%) expression. Results have been originated by evaluating NSCLC fresh samples and their matched uninvolved tissues by multiparametric flow cytometry on a subgroup of patients (N=53) from the ongoing ICON study.

Regarding the proliferation status of TIL, the expression levels of Ki67 have been evaluated on CD8⁺ T-lymphocytes. As shown in **Figure 4A**, the proportion of Ki67⁺ CD8⁺ T cells is higher in the NSCLC side (17.3%), while normal tissues exhibit a lower rate of proliferating TIL (6.4%).

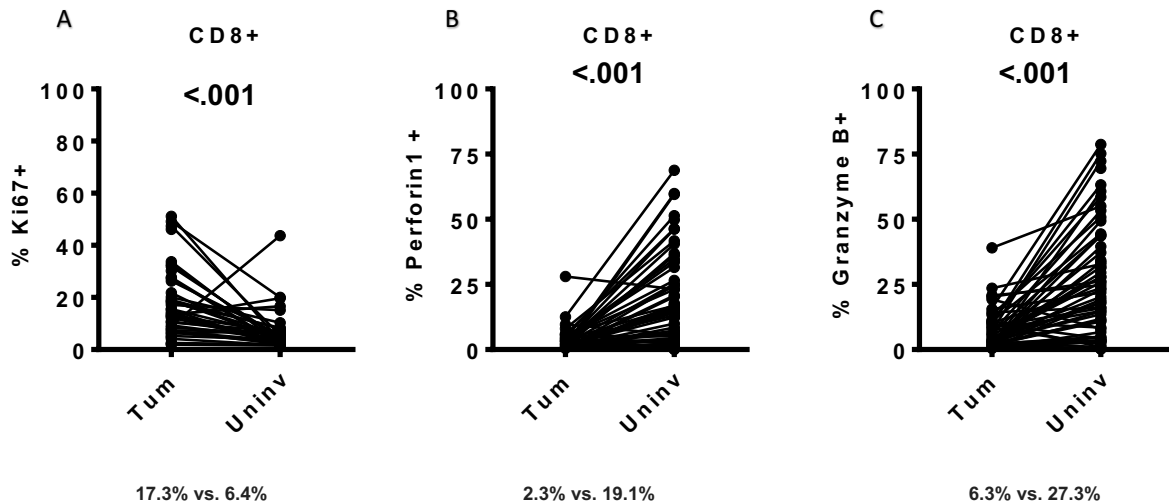


Figure 4 – Comparison of cytofluorimetric data in a subgroup of tumor and matched uninvolved lung tissues (N=53) from the ongoing ICON study. **(A)** Evaluation of the proliferation status of CD8⁺ T-lymphocytes isolated from freshly-resected lung tumor samples and compared with adjacent uninvolved lung tissue samples revealing that CD8⁺ TIL showed fractional enrichment of Ki67 (17.3% vs. 6.4%). **(B)** CD8⁺ TIL contained a significantly less cells expressing perforin (2.3% vs. 19.1%) and **(C)** granzyme (6.3% vs. 27.3%).

The functional status of infiltrating CD8⁺ T lymphocytes has been analysed by measuring the expression levels of perforin-1 and granzyme B. As illustrated in **Figure 4B**, the proportion of CD8⁺ T cells expressing high levels of perforin-1 is remarkably augmented in lung uninvolved tissue samples (19.1%), whereas CD8⁺ T cells isolated from NSCL tumors show less levels of perforin-1 (2.3%), reflecting a more anergic phenotype. Accordingly, the proportion of granzyme B⁺ CD8⁺ T-lymphocytes appears to be increased in uninvolved tissues (27.3%), with only 6.3% of CD8⁺ T lymphocytes expressing Granzyme B in tumor samples (**Figure 4C**).

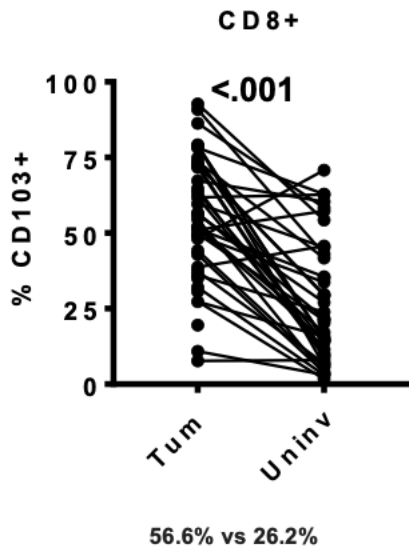


Figure 5 - CD8+ TIL fraction of lung tumors is significantly enriched in CD103+ CD8+ Tissue Resident Memory Cells as compared to uninvolved lung tissues (56.6% vs 26.2%). Results have been originated by evaluating NSCLC fresh samples and their matched uninvolved tissues by multiparametric flow cytometry on a subgroup of patients (N=53) from the ongoing ICON study.

CD103+ cytotoxic T cells are typically referred to as tissue-resident memory T cells. The presence of cytotoxic CD8+ T lymphocytes expressing CD103 in NSCLC infiltrates has been shown to be associated with improved prognoses [51, 52].

The present part of this study aimed to analyse the presence of CD103+ CD8+ T lymphocytes in freshly-resected lung tumor samples and in their matched uninvolved tissue samples. As shown in **Figure 5**, the amount of CD103+ CD8+ tissue-resident memory cells is significantly augmented in lung tumors (56.6%) as compared with their uninvolved counterpart; of note, the presence of CD103+ CD8+ tissue-resident memory cells is more than two times higher in the tumor than in the uninvolved component.

Task 2: immunosignatures detection

Introduction

The present task describes the results obtained by integrating data generated by flow cytometry with clinical parameters of patients enrolled in the ongoing ICON study.

The generation of the described results has been possible thanks to a multi-team effort.

The information obtained by multiparametric flow cytometry on fresh NSCLC/uninvolved lung samples have been compared and matched with clinicopathological features of patients (N=53). As a result, a hierarchical clustering has been obtained, revealing several key features of immune infiltrates which result to be grouped into distinct phenotypes.

Materials and methods

Unsupervised hierarchical clustering

Unsupervised hierarchical clustering was performed using an open-source clustering software (Cluster 3, [53]). Briefly, the table of biomarker abundances (different biomarkers as columns and different samples as rows) were log₂-transformed, centered and normalized using median values of the biomarker and sum of the squares of the values. The data pre-processing resulted in all row-wise and column-wise median values to be equal to zero and magnitudes of the abundances in rows and columns to be equal to 1. The Pearson correlation coefficient has been further used to measure similarities; centroid linkage has been defined as the selected technique to cluster samples and biomarkers. The produced table of normalized abundances and hierarchies (samples and immune markers) were visualized by Java TreeView 3.0 [54].

Results

The first results of the present unsupervised clustering analysis have been generated by flow cytometry data from a total of 53 patients and can be summarized as follows:

- It is possible to notice two distinct groups of NSCLC according to the proportion of CD8⁺ T cells that are found within tumor infiltrates (**Figure 6**, red and blue dashed lines on top).
- NSCLC- infiltrating T lymphocytes can be divided into two distinct phenotypic clusters according to the differential expression levels of PD-1 (**Figure 6**, light orange and purple boxes).

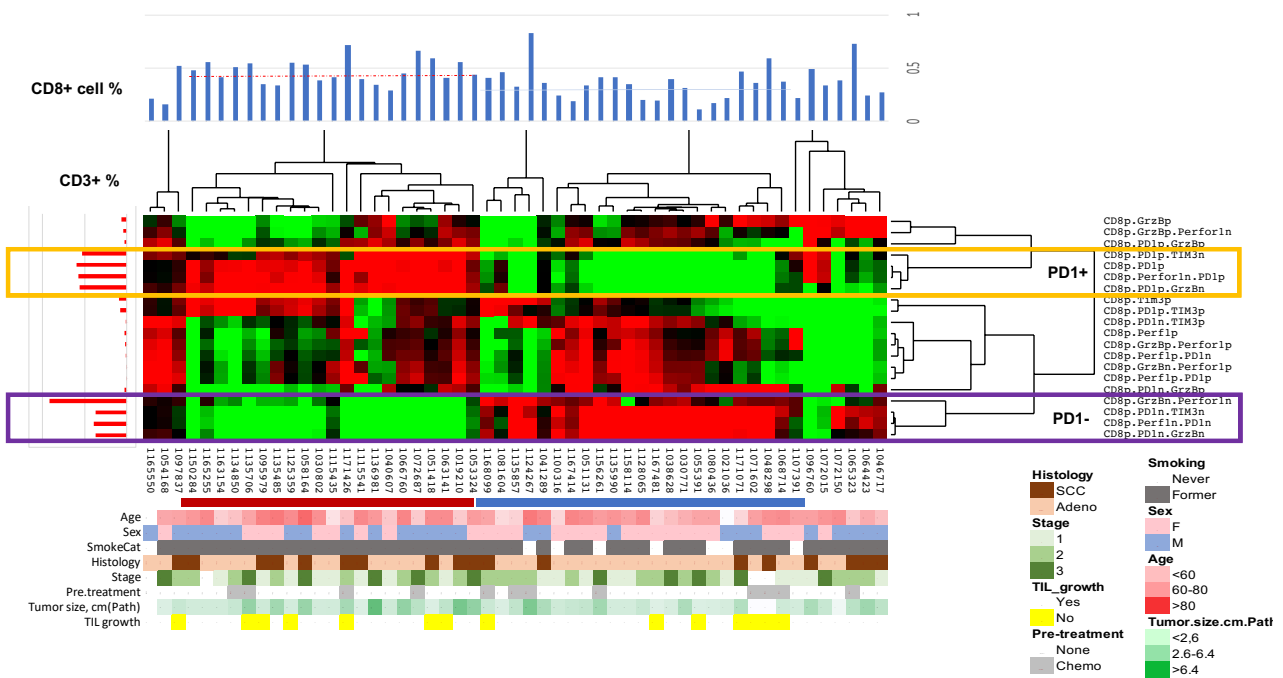


Figure 6 - Unsupervised clustering analysis of multiparameter flow cytometry data revealed that NSCLC tumors cluster in two main groups according to the percentage of CD8⁺ T cells present within the T cell infiltrate (red and blue dashed lines on top indicate the average % of CD8⁺ T cell infiltration observed in each cluster) and the percentage CD8⁺ T cells expressing PD-1 (light orange and purple boxes). Red bars on the left indicate the average % of live CD3⁺ cells measured within the lymphocyte population (N=53).

The second part of the present task was similarly performed on a subpopulation (N=22) of the initial pool of samples, and aimed to analyse a different selection of immunological markers (LAG3, TIM3, Ki67 and ICOS). The differential expression levels of these markers revealed a second phenotypic cluster represented by LAG3, TIM3, Ki67 and ICOS-expressing cells in both CD4⁺ and CD8⁺ non-resident (CD103⁻) T cell fractions (**Figure 7**).

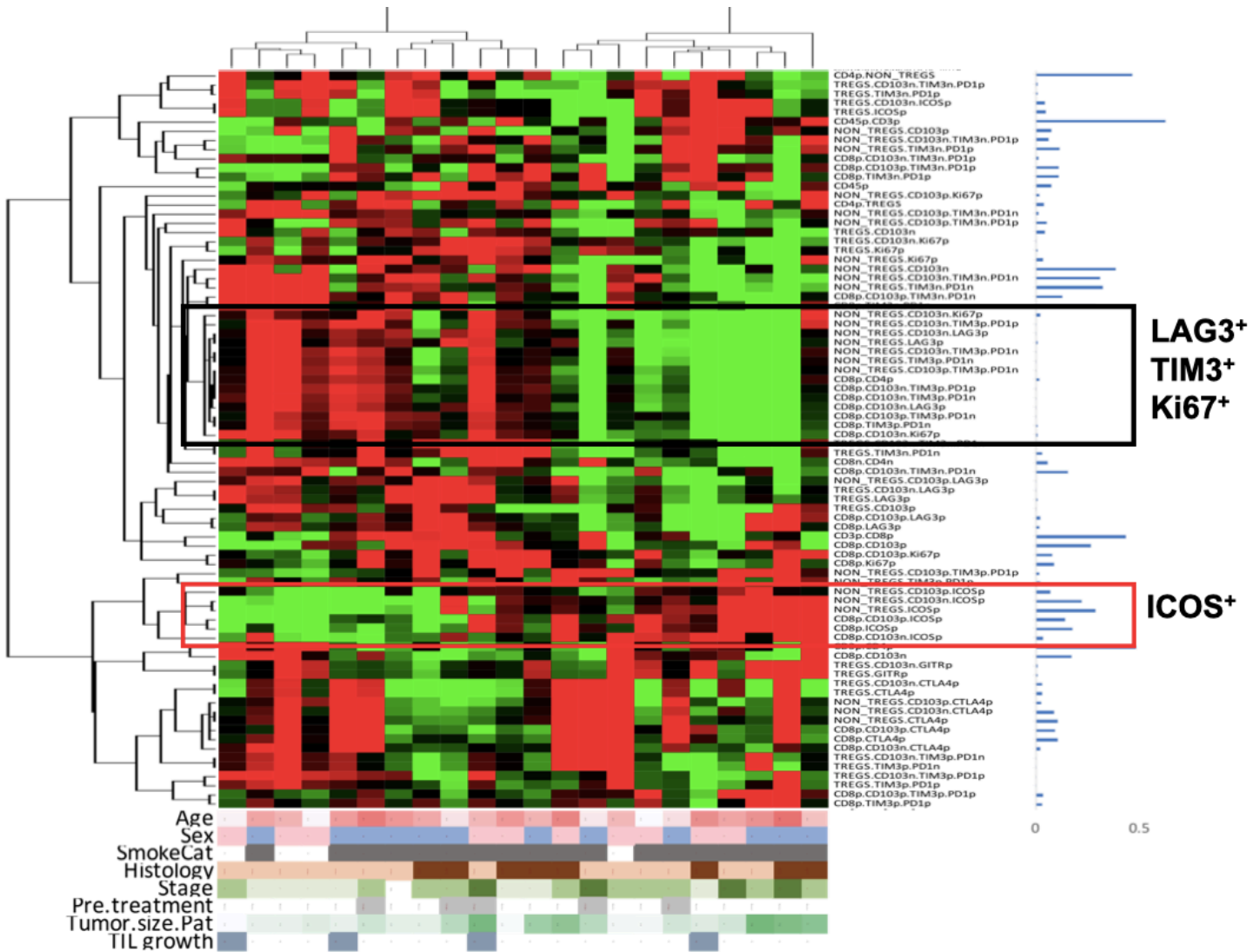


Figure 7 - Unsupervised clustering analysis of multiparameter flow cytometry data on a different selection of immunological markers done on N=22 patients revealed a second clustering pattern primarily driven by differential enrichment in LAG3, TIM3, Ki67 (black box), and ICOS (red box) in both the non-Tregs CD4⁺ and non-resident (CD103⁻) CD8⁺ T cell compartments.

Task 3: isolation and expansion of TIL from NSCLC

Introduction

The following part of the present study is intended to evaluate whether TIL can be isolated and expanded *ex vivo* from freshly-resected NSCLC samples and from their matched uninvolved lung counterparts. The data hereby presented are representative of the first phase of TIL expansion (referred to as pre-REP, Rapid Expansion Protocol).

Materials and methods

Isolation and expansion of TIL *ex vivo*

The expansion process of TIL *ex vivo* comprised the initial expansion of TIL from the tumor fragments over a period of up to 35-days in appropriate culture medium and in presence of IL-2 [55]. Freshly-resected tumor samples are initially cut into smaller fragments (1-3 mm²) in sterile conditions; in parallel, a flow-cytometry-based characterization of the immune infiltrate is performed to retrieve information regarding the baseline status of TIL of the patient. Fragments are then placed in TIL culture media [TIL- CM: RPMI-1640 with GlutaMax (Gibco/Invitrogen), 1 x Pen–Strep (Gibco/Invitrogen), 50 µmol/L 2-mercaptoethanol (Gibco/Invitrogen), 20 µg/mL Gentamicin (Gibco/Invitrogen), and 1 mmol/L pyruvate (Gibco/Invitrogen)] with 6000 IU/ml IL-2 in 24-well plates. Tumor fragments are left in culture for a period of time of up to 30-35 days (4 or 5 weeks); during this interval, cultures are kept under careful observation, with medium changes and fresh addition of IL-2 being performed regularly in order to maintain optimal culture conditions. This first stage results in the obtainment of “pre-REP” TIL, that is an initially-expanded TIL culture which is then used to generate a final TIL infusion product following a “rapid expansion protocol” (REP) [55-57].

Results

Overall, the process of isolation and expansion of TIL ex vivo from NSCLC resulted to be a feasible approach. In order to be claimed as a successful expansion, a minimum threshold of 12×10^6 TIL at the time of freezing was required, within a maximum culturing time of 35 days [58].

Of the total 141 cultured samples – considering both tumor and uninvolved tissue fragments, we documented a 68% rate of success. The histological type of the tumor did not influence the ability to grow TIL.

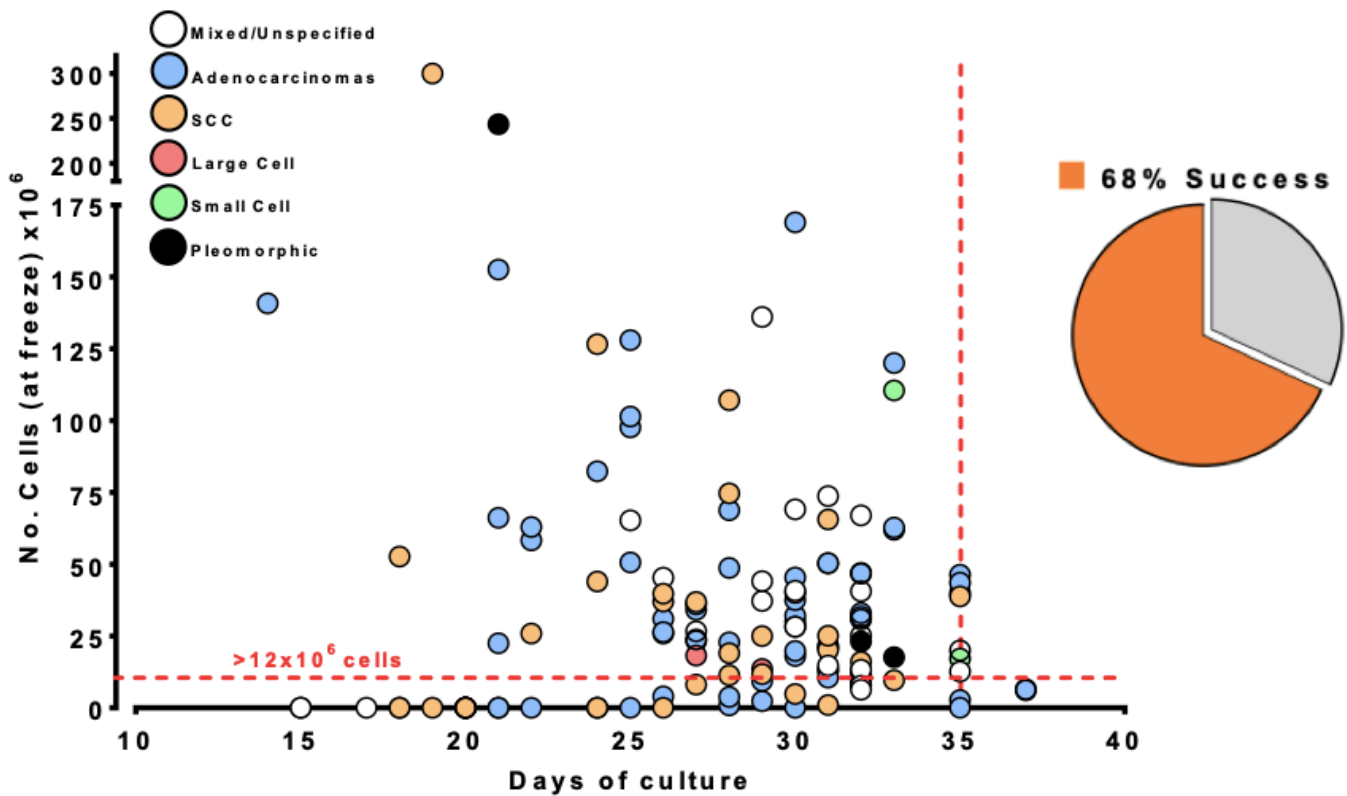


Figure 8 - TIL expansion success (68%, N=141). Successful expansion is defined according to the criteria followed for the MDACC Melanoma TIL clinical trial according to which a successfully expanded TIL product must be composed of at least 12×10^6 cells (horizontal red dotted line) and obtained within 35 days of cell culture (vertical red dotted line) from 6 fragments of resected tissue. [58]

Considering only TIL expanded from uninvolved lung tissue samples, a 66.7 rate of success has been reached; intriguingly, TIL expansion from NSCLC has been feasible at the exact same rate of success, highlighting a possible correlation between the two counterparts (Figure 9).

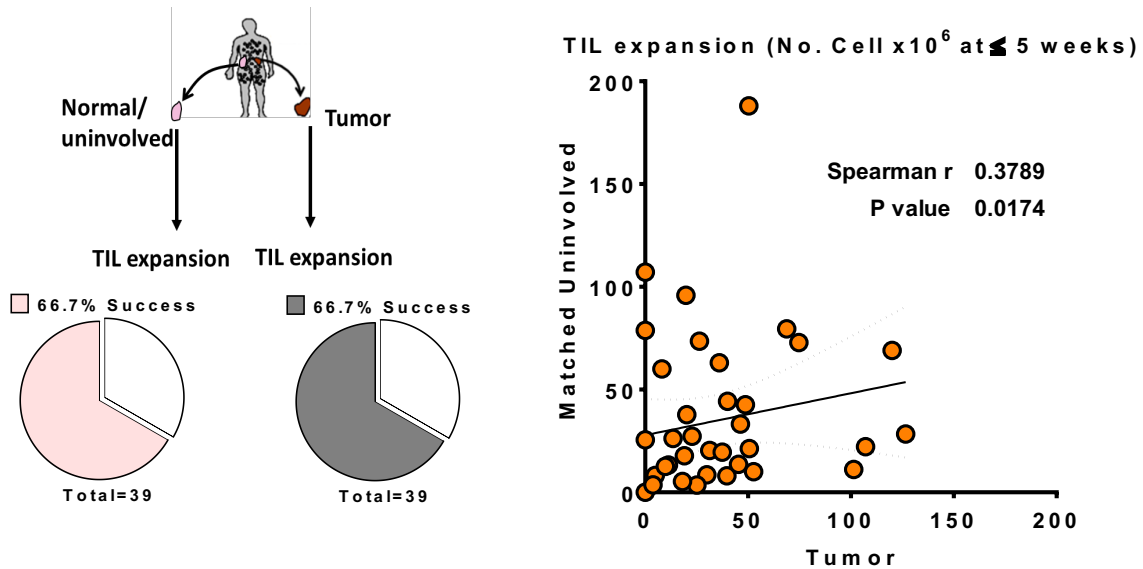


Figure 9 – Expansion of TIL from NSCLC and matched unininvolved tissue and success rates. A significant correlation between the two expansion rates can be highlighted.

When the expansion success is compared with prior chemotherapy-based treatments, it emerges that TIL are more likely to be expanded from patients who are chemotherapy-naïve. In this case, the percentage of success has been calculated as 72.5%, whereas patients who underwent chemotherapy-based treatments prior to sample collection were characterized by a reduced rate of success (56.25%)

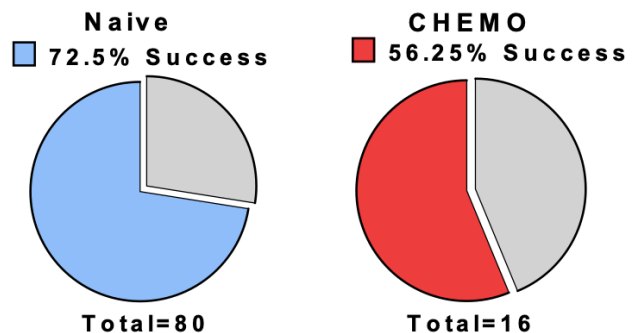


Figure 10 – Comparison between TIL expansion success rates with regards to chemotherapy-naïve patients (left) and patients who received previous chemotherapy (right). The comparison highlights an increased rate of success for the chemotherapy-naïve group of patients.

Chapter 6

As suggested in recent studies, the expansion of TIL *ex vivo* can be improved pharmacologically both in terms of total number of TIL and in terms of TIL product composition [59]. In addition to IL-2, two compounds have been administered in order to increase the number of CD8+ TIL obtained from the pre-REP phase, as well as to reduce the time required to reach the selected success threshold (12×10^6 cells).

- Urelumab, a CD137/4-1BB agonist. CD137/4-1BB represents a co-stimulatory immune checkpoint and is commonly expressed on CD8+ T cells, as well as on CD4+ T cells in minor proportion.

The pharmacological stimulation of CD137/4-1BB has been documented to boost T cell proliferation, survival, and activation, also increasing IL-2 production [59].

- OKT3, an anti-CD3 monoclonal antibody able to trigger T cell proliferation [59].

As shown in **Figure 11**, the pharmacological stimulation of OKT3 and 4-1BB led to the obtainment of pre-REP TIL products in a significantly shorter time as compared with the classical method, which involves the administration of IL-2 only. To note, the utilization of this new method, referred to as TIL 3.0, resulted in the obtainment of TIL products containing a significantly higher number of lymphocytes.

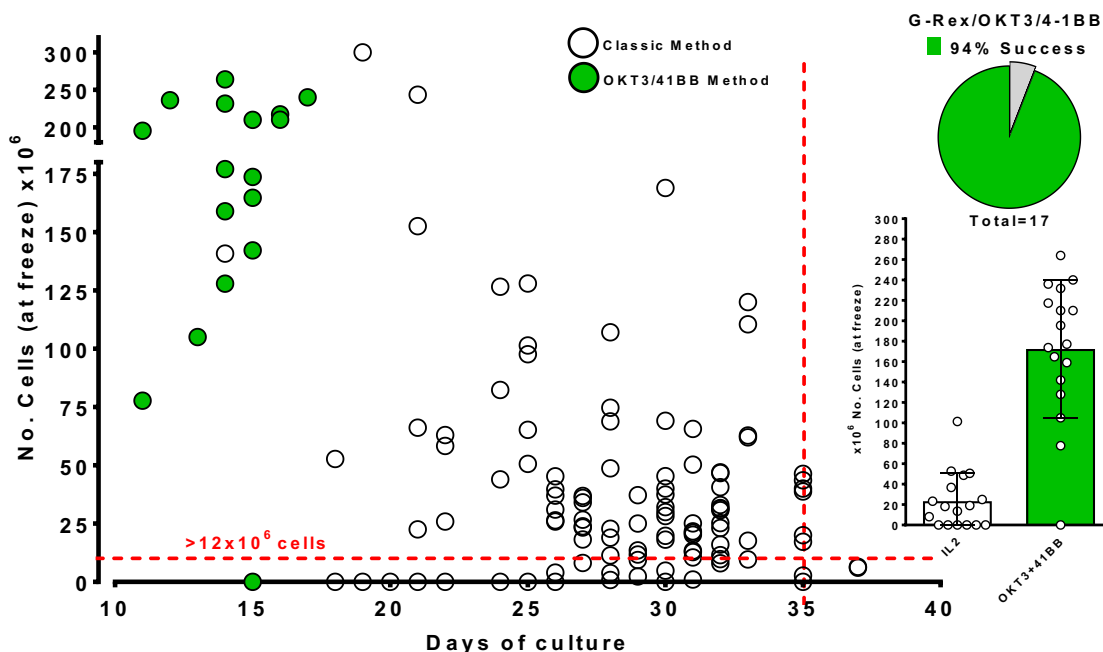


Figure 11 – Comparison between two diverse expansion methods: OKT3/4-1BB stimulation versus classical method (IL-2 only). The results show that the new approach, referred to as TIL 3.0, can lead to the obtainment of TIL products containing a more elevated number of lymphocytes and in a shorter period of time.

Task 4: autologous neoantigen recognition

Introduction

As evidenced in literature, defective antigen presentation by HLA class I has been documented as an important mechanism of cancer immune escape [60]. The TCR recognizes foreign peptides in concert with MHC/HLA class I molecules on the surface of the infected cells. MHC class I molecules preferably bind and present nine amino acid long peptides, which mainly originates from proteins expressed in the cytosol of the presenting cell. In most vertebrates, MHCs exist in a number of different allelic variants that each binds a specific and very limited set of peptides.

Recent studies indicate that TIL are able to recognize neoantigens as a result of cancer-specific mutations within the tumor lesion [41-44]. Moreover, data published in the last 5 years indicate that the clinically-observed tumor regressions might be due to an extended presence of neoantigen-reactive TIL within the infused TIL product [41, 44].

These findings can explain the observed low rate of autoimmune-based toxicities and suggest that tumors presenting high rates of mutational loads can be potentially perfect candidates for TIL therapy. Among highly-mutated malignancies, melanoma represented a major clinical success due to the high amount of mutations also in reflection to UV-radiation exposure. Accordingly, lung cancer, due to an etiopathogenesis involving tobacco smoking amongst other causes, has been proposed as an highly-mutated type of tumor and therefore as a potential candidate for neoantigen recognition from TIL. The same assumption can be extended also to other types of solid tumors showing microsatellite instability or sharing a viral etiopathogenesis [61].

Materials and methods

In silico prediction and peptide synthesis

In silico prediction algorithms have been developed to calculate either the sequence of potentially immunogenic peptides as well as their affinity for a specific HLA allelic variant [62-65]. In the first-in-human clinical trials experimenting personalized neoantigen based vaccines, HLA binding affinity was shown to be fundamental for driving the selection of candidates [66, 67].

This task of the present study has been possible by making use of the whole exome sequencing data from the tumor tissue identifying the mutations for each patient and thanks to an *in silico* prediction of the peptides covering these mutations susceptible to bind to the patient's HLA molecules. The affinities of peptides for HLA allelic variants was predicted by using publically available NetMHC algorithm.

TIL cultures from a total of 4 patients were tested for neoantigen reactivity, who were previously selected on the base of whole exome sequencing data and matched autologous tumor-derived cell lines availability (**Table 4**).

	<i>Tissue ID</i>	<i>Number of synthesized peptides</i>
<i>Patient 1</i>	971183	87 peptides
<i>Patient 2</i>	972244	58 peptides
<i>Patient 3</i>	973138	116 peptides
<i>Patient 4</i>	973796	45 peptides

Table 4 – Number of synthesized peptides for each patient and tissue IDs.

Chapter 6

Peptides predicted to be immunogenic were synthesized. Solid-phase peptide synthesis has been performed by utilizing an Intavis-AG MultiPep peptide synthesizer. During the synthesis, reagents were let to continuously circulate while performing an optimization of reaction parameters like deprotection, coupling times, and washing steps.

Quality control has been performed by confirming the identities of the peptides by mass spectrometry. Then, peptides have been dissolved in Dimethyl Sulfoxide (DMSO) to reach a stock concentration of 10 mg/ml. Peptides solutions have been further diluted to obtain the final working concentration of 5 µg/ml. However, an initial titration between three different doses (1µg/ml, 5µg/ml, and 10µg/ml) has been performed in order to select the best working concentration of peptides allowing for detection with ELISPOT plates.

Evaluation of autologous reactivity

Autologous reactivity was detected through enzyme-linked immunospot (ELISPOT) assay. This methodology allows for the quantification of antigen-specific T cells by the enumerating T cells secreting interferon gamma (IFN-γ) in each well. Briefly, rapidly-expanded TIL from each of the selected patients were thawed and placed in culture for 24 hours in presence of IL-2. Then, IL-2 was removed and TIL were allowed to rest for a period of 6 hours and a half. Subsequently, TIL were cultured overnight (15-17 hours) in presence of their matched peptides which were previously grouped into pools composed by 4 to 5 units. Peptide pools were generated by grouping units with similar affinity prediction values in order to maximize HLA-binding competition. After several washing cycles, autologous reactivity was detected by measuring the release of IFN-γ on ELISPOT plates.

In order to corroborate our data, a pool of control peptides from sequences of viruses that the human population is frequently exposed to (flu, CMV, EBV) or not (HIV) was selected and included in each experiment (**Table 5**).

Type of control	Domain	Sequence	HLA restriction
<i>Positive</i>	Influenza A PB1	VSDGGPNLY	A1
<i>Positive</i>	Influenza A Matrix 1	GILGFVFTL	A2
<i>Positive</i>	EBV EBNA3A	RLRAEAQVK	A3
<i>Positive</i>	EBV EBNA3B	IVTDFSVIK	A11
<i>Positive</i>	EBV BRLF1	DYCNVLNKEF	A24
<i>Positive</i>	HCMV pp65	TPRVTGGGAM	B7
<i>Negative</i>	HIV rev	ILKEPVHGV	A2
<i>Negative</i>	HIV gag	SLYNTVATL	A0201

Table 5 – Control peptides used to corroborate autologous reactivity data in ELISPOT assays.

Additionally, the conditions shown in **Table 6** were selected to provide additional controls.

Condition	Type of control
<i>TIL medium</i>	Negative
<i>TIL alone (in TIL medium)</i>	Negative
<i>DMSO (dissolved in TIL medium)</i>	Negative
<i>PMA/ionomycin</i>	Positive

Table 6 – Additional control conditions selected for ELISPOT testing.

In order to corroborate the results obtained from Patient 3, a flow cytometry assay has been performed in parallel to ELISPOT assay aiming to measure the expression levels of 4-1BB on TIL from the same patient. Briefly, TIL were placed in 96-well plates and cultured for 17 hours in presence of those peptides for which autologous reactivity was detected. Subsequently, TIL were stained for surface expression of 4-1BB and gated to select CD8+ T cells. The detection of increased expression levels of 4-1BB on CD8+ T lymphocytes was used to assess T cell activation subsequent to autologous recognition of neoantigens.

Results

The recognition of mutated peptides/neoantigens has been detected for two patients out of four.

TIL expanded from Patient 3 (patient's sample ID: 973138) show a strong release of IFN- γ in conjunction to the autologous recognition of two peptides (peptide #2, peptide #3). Compared with negative controls, TIL autologous reactivity towards these peptides is strongly augmented as shown by the number of spots revealed with ELISPOT assay (**Figure 12**).

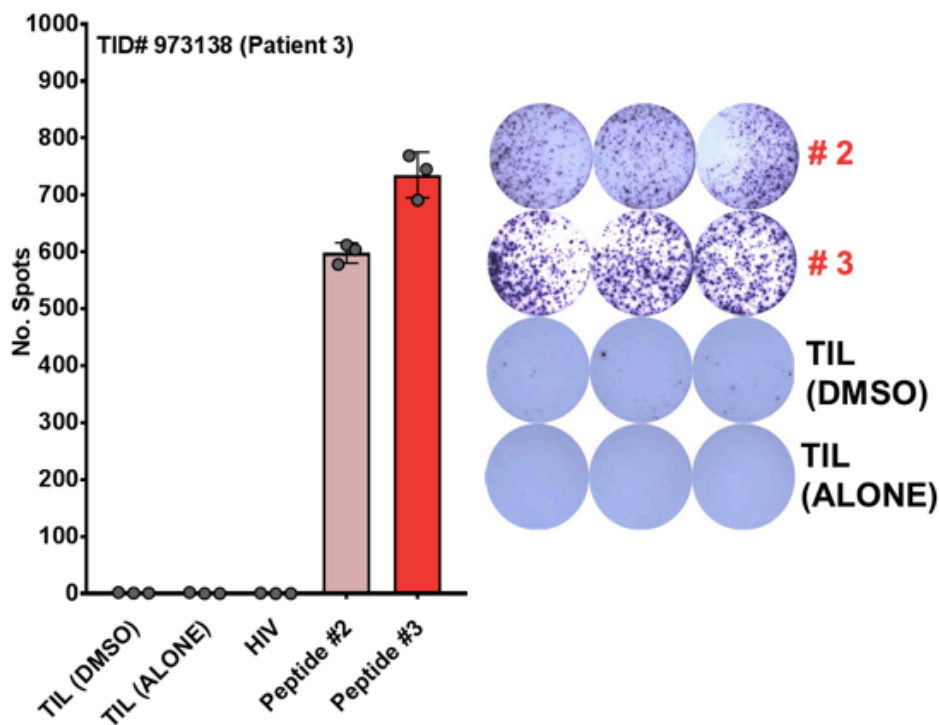


Figure 12 - Mutant peptide recognition was detected in TIL expanded from 2 of 4 patients tested. Quantification and representative images of ELISPOT results are shown for Patient 3.

When the expression levels of 4-1BB of the same TIL after a 17 hours incubation with the same peptides were measured, it emerges that both peptide #2 and peptide #3 are able to trigger activation of CD8⁺ T cells (**Figure 13**).

Chapter 6

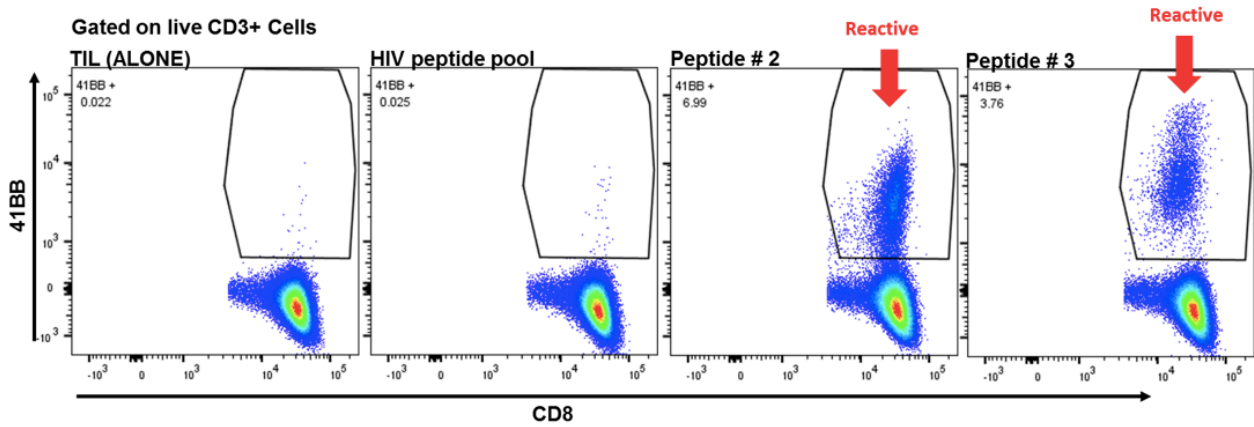


Figure 13 - TIL from patient 3 were co-incubated for 24 hours with autologous mutant peptides and stained with anti-4-1BB antibody for assessment of T cell activation by flow cytometry. The results highlight T cell activation due to neoantigen recognition by TIL.

Autologous reactivity has been detected also on patient 2 (972244) with regards to two peptides. In this case, the number of detected spots resulted to be less intense as compared with Patient 4. However, the comparison with negative controls highlights a clear release of IFN- γ in the ELISPOT plate (**Figure 14**).

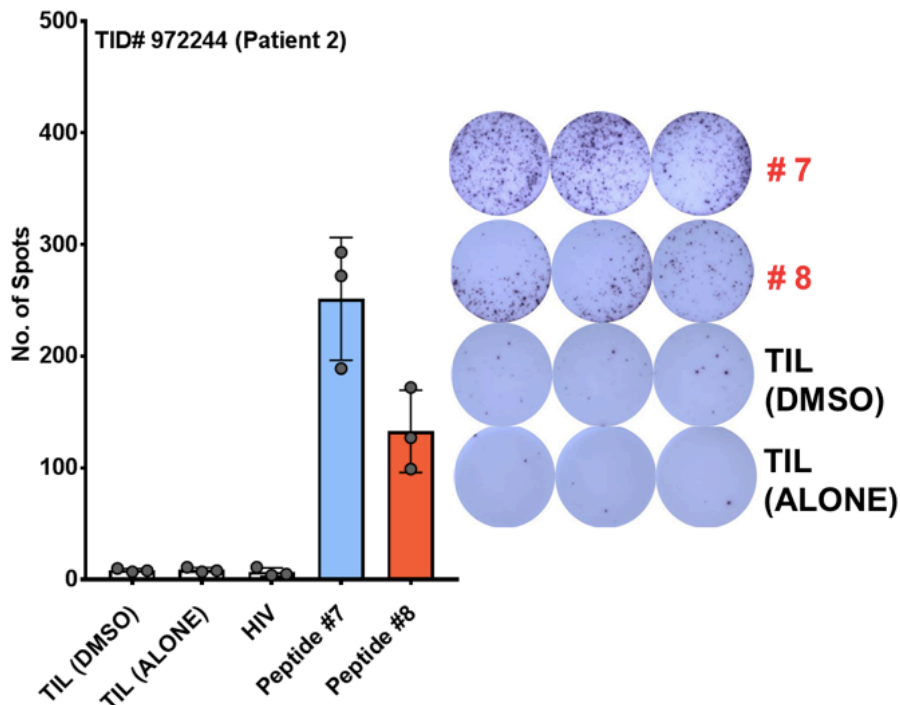


Figure 14 - Neoantigen peptide recognition was detected in TIL expanded from 2 of 4 patients tested. Quantification and representative images of ELISPOT results are shown for Patient 2.

Chapter 6

The evaluation of autologous reactivity of TIL from the remaining patients (Patient 1 and Patient 4) did not highlight any release of IFN- γ with experimental peptides (**Figure 15A-B**, respectively). However, these patients were seen to respond to FLU M1-58 peptides, which have been selected as positive controls.

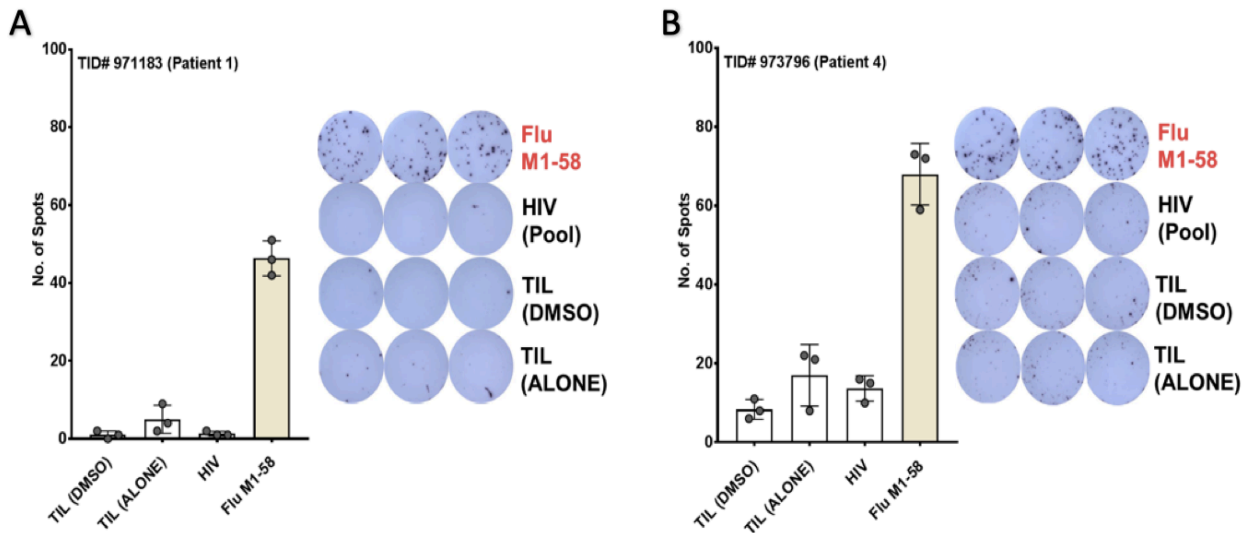


Figure 2 - Neoantigen peptide recognition was detected in TIL expanded from 2 of 4 patients tested. Quantification and representative images of ELISPOT results are shown for Patient 1 and Patient 4.

In summary, two patients out of four exhibited autologous reactivity toward predicted neoantigens. In **Table 7** and **Table 8**, additional information about patients and about reactive peptides are provided, respectively.

	Tissue ID	Reactivity toward:		Patient HLA allele
		Mutated peptide	Viral peptide	
Patient 1	971183	None	Flu M1-58	A*02.01, B*07.02, B*15.03, C*02.10, C*07.02
Patient 2	972244	#7, #8	None	A*30.01, A*02.01, B*15.01, B*40.01, C*03.03, C*03.04
Patient 3	973138	#2, #3	None	A*30.02, A*02.01, B*44.03, B*18.01, C*05.01, C*04.01
Patient 4	973796	None	Flu M1-58	A*02.01, A*11.01, B*35.01, B*51.01, C*14.02, C*04.01

Table 7 – Additional information about patients for whom autologous reactivity was evaluated.

#	Sequence	Length (AA)	AA substitution	Mutation	Gene ID	Predicted Mutant Peptide Affinity for selected HLA alleles			
						HLA.A.02.01	HLA.A.30.01	HLA.B.15.01	HLA.B.40.01
#2	AELGIYPAVY	10	D399Y	c.G1195T	ATP5B	33999.03	1084.73	81.57	21.54
#3	ALWMQACFL	9	G724W	c.G2170T	OAS3	23.96	4594.58	31518.35	25585.6
#7	SEVTAF AAL	9	V244A	c.T731C	ADK	15085.97	23249.29	1453.36	7.12
#8	TESEVTAF AAL	11	V244A	c.T731C	ADK	15996.02	31878.01	5981.51	7.21

Table 8 – Additional information about peptides for which autologous reactivity with TIL has been recorded.

Conclusion

The results described in the present Chapter demonstrate that the expansion of TIL from NSCLC is a feasible procedure, supported by a 68% of success. Lung tumor tissues are well infiltrated with T cells; in this context, CD3+ immune cells isolated from NSCLC are present in higher proportions within the tumor component as compared with the uninvolved lung tissue. The immune monitoring of infiltrates from freshly-resected NSCLC samples and from their matched uninvolved counterparts also points out the existence of a highly immunosuppressive microenvironment: NSCLC immune infiltrates result to have lower CD8+ T-cell content and are mostly enriched for Tregs as compared to the surrounding uninvolved tissue.

Within CD8+ T cell population, it appears that the immunosuppressive microenvironment exerts a detrimental effect of the activation of infiltrating CD8+ T cells, with high expression of suppressive molecules related to chronic antigen stimulation such as PD-1, TIM-3 and LAG-3. Tumor-infiltrating CD8+ T cells are enriched for proliferative (Ki67+) and activated (ICOS+) cells but lack the cytotoxic potential (low perforin and granzyme B expression). NSCLC TIL thus appear dysfunctional in comparison to T cells infiltrating the non-involved lung tissue which are highly cytotoxic and have low levels of immune regulatory checkpoint molecules (PD-1, TIM-3, LAG-3).

The results of the present study also highlight autologous neoantigen recognition mediated by TIL expanded *ex vivo* from NSCLC. This finding, in addition to further confirm the feasibility of TIL therapy in NSCLC, highlights important mechanisms of immune escape. The fact that TIL are able to recognize a mutation in the patient's tumor after expansion *ex vivo* implies that patient's tumor cells were expressing the same mutated peptide and should have been targeted. However, either through direct suppressive mechanisms on T cells or through a down-regulation of the antigenic presentation by dysregulation of the antigen processing and presentation machinery, the tumor was still allowed to grow, suggesting that immune resistance mechanisms are at play.

Acknowledgements

The author of this thesis wishes to thank Prof. Chantale Bernatchez and the whole TIL lab team for all the support provided during the time spent abroad. Special thanks to Dr. Lorenzo Federico for the friendly, generous efforts demonstrated and for his unstoppable scientific dedication to the project.

The present research has been possible thanks to nurses Mary Ann Gianan and Craig DeGraaf, blood team Patrice Lawson, Heather Napoleon, Mayra Vasquez and Eric Prado, all thoracic OR nurses and anesthesiologists at MD Anderson Cancer Center, and Heidi Wagner, Elena Bogatenkova and the Institutional Tissue Bank team. This work was supported by contributions to The University of Texas MD Anderson Cancer Center Lung Cancer Moon Shots Program and by the NIH/NCI under award number P30CA016672 and used the Tissue Biospecimen and Pathology Resource, Research Histopathology Facility, Bioinformatics Shared Resource, and Biostatistics Resource Group).

Special thanks to the patients and their families.

Ethics Approval: The study was approved by MD Anderson's IRB (LAB90-020, PA13-0589 and PA15-1112).

References

1. Kargl, J., et al., *Neutrophils dominate the immune cell composition in non-small cell lung cancer*. Nat Commun, 2017. **8**: p. 14381.
2. Lavin, Y., et al., *Innate Immune Landscape in Early Lung Adenocarcinoma by Paired Single-Cell Analyses*. Cell, 2017. **169**(4): p. 750-765 e17.
3. Lizotte, P.H., et al., *Multiparametric profiling of non-small-cell lung cancers reveals distinct immunophenotypes*. JCI Insight, 2016. **1**(14): p. e89014.
4. Torre, L.A., R.L. Siegel, and A. Jemal, *Lung Cancer Statistics*. Adv Exp Med Biol, 2016. **893**: p. 1-19.
5. Boloker, G., C. Wang, and J. Zhang, *Updated statistics of lung and bronchus cancer in United States (2018)*. J Thorac Dis, 2018. **10**(3): p. 1158-1161.
6. Siegel, R.L., K.D. Miller, and A. Jemal, *Cancer statistics, 2018*. CA Cancer J Clin, 2018. **68**(1): p. 7-30.
7. Hecht, S.S., *Lung carcinogenesis by tobacco smoke*. Int J Cancer, 2012. **131**(12): p. 2724-32.
8. Gorlova, O.Y., et al., *Aggregation of cancer among relatives of never-smoking lung cancer patients*. Int J Cancer, 2007. **121**(1): p. 111-8.
9. Tirmarche, M., et al., *Risk of lung cancer from radon exposure: contribution of recently published studies of uranium miners*. Ann ICRP, 2012. **41**(3-4): p. 368-77.
10. Wei, S., et al., *Genome-wide gene-environment interaction analysis for asbestos exposure in lung cancer susceptibility*. Carcinogenesis, 2012. **33**(8): p. 1531-7.
11. Zappa, C. and S.A. Mousa, *Non-small cell lung cancer: current treatment and future advances*. Transl Lung Cancer Res, 2016. **5**(3): p. 288-300.
12. Jemal, A., et al., *Increasing lung cancer death rates among young women in southern and midwestern States*. J Clin Oncol, 2012. **30**(22): p. 2739-44.
13. Hecht, S.S., *Tobacco smoke carcinogens and lung cancer*. J Natl Cancer Inst, 1999. **91**(14): p. 1194-210.
14. Whitrow, M.J., et al., *Environmental exposure to carcinogens causing lung cancer: epidemiological evidence from the medical literature*. Respirology, 2003. **8**(4): p. 513-21.
15. Krewski, D., et al., *Residential radon and risk of lung cancer: a combined analysis of 7 North American case-control studies*. Epidemiology, 2005. **16**(2): p. 137-45.
16. Berman, D.W. and K.S. Crump, *A meta-analysis of asbestos-related cancer risk that addresses fiber size and mineral type*. Crit Rev Toxicol, 2008. **38** **Suppl 1**: p. 49-73.
17. Vineis, P. and K. Husgafvel-Pursiainen, *Air pollution and cancer: biomarker studies in human populations*. Carcinogenesis, 2005. **26**(11): p. 1846-55.
18. Hwang, S.J., et al., *Lung cancer risk in germline p53 mutation carriers: association between an inherited cancer predisposition, cigarette smoking, and cancer risk*. Hum Genet, 2003. **113**(3): p. 238-43.
19. Ramalingam, S. and C. Belani, *Systemic chemotherapy for advanced non-small cell lung cancer: recent advances and future directions*. Oncologist, 2008. **13** **Suppl 1**: p. 5-13.
20. Metro, G., *EGFR targeted therapy for lung cancer: are we almost there?* Transl Lung Cancer Res, 2018. **7**(Suppl 2): p. S142-S145.
21. Mok, T.S., et al., *Osimertinib or Platinum-Pemetrexed in EGFR T790M-Positive Lung Cancer*. N Engl J Med, 2017. **376**(7): p. 629-640.
22. Riely, G.J., et al., *Frequency and distinctive spectrum of KRAS mutations in never smokers with lung adenocarcinoma*. Clin Cancer Res, 2008. **14**(18): p. 5731-4.

Chapter 6

23. Ostrem, J.M., et al., *K-Ras(G12C) inhibitors allosterically control GTP affinity and effector interactions*. *Nature*, 2013. **503**(7477): p. 548-51.
24. Koivunen, J.P., et al., *EML4-ALK fusion gene and efficacy of an ALK kinase inhibitor in lung cancer*. *Clin Cancer Res*, 2008. **14**(13): p. 4275-83.
25. Solomon, B.J., et al., *First-line crizotinib versus chemotherapy in ALK-positive lung cancer*. *N Engl J Med*, 2014. **371**(23): p. 2167-77.
26. Planchard, D., et al., *Dabrafenib in patients with BRAF(V600E)-positive advanced non-small-cell lung cancer: a single-arm, multicentre, open-label, phase 2 trial*. *Lancet Oncol*, 2016. **17**(5): p. 642-50.
27. Faehling, M., et al., *Oncogenic driver mutations, treatment, and EGFR-TKI resistance in a Caucasian population with non-small cell lung cancer: survival in clinical practice*. *Oncotarget*, 2017. **8**(44): p. 77897-77914.
28. Gautschi, O., et al., *Targeted Therapy for Patients with BRAF-Mutant Lung Cancer: Results from the European EURAF Cohort*. *J Thorac Oncol*, 2015. **10**(10): p. 1451-7.
29. Anguera, G. and M. Majem, *BRAF inhibitors in metastatic non-small cell lung cancer*. *J Thorac Dis*, 2018. **10**(2): p. 589-592.
30. Reck, M., et al., *Pembrolizumab versus Chemotherapy for PD-L1-Positive Non-Small-Cell Lung Cancer*. *N Engl J Med*, 2016. **375**(19): p. 1823-1833.
31. Kowanetz, M., et al., *Differential regulation of PD-L1 expression by immune and tumor cells in NSCLC and the response to treatment with atezolizumab (anti-PD-L1)*. *Proc Natl Acad Sci U S A*, 2018.
32. Antonia, S.J., et al., *Durvalumab after Chemoradiotherapy in Stage III Non-Small-Cell Lung Cancer*. *N Engl J Med*, 2017. **377**(20): p. 1919-1929.
33. McDermott, D.F. and M.B. Atkins, *Interleukin-2 therapy of metastatic renal cell carcinoma--predictors of response*. *Semin Oncol*, 2006. **33**(5): p. 583-7.
34. Stevanovic, S., et al., *Complete regression of metastatic cervical cancer after treatment with human papillomavirus-targeted tumor-infiltrating T cells*. *J Clin Oncol*, 2015. **33**(14): p. 1543-50.
35. Wu, R., et al., *Adoptive T-cell therapy using autologous tumor-infiltrating lymphocytes for metastatic melanoma: current status and future outlook*. *Cancer J*, 2012. **18**(2): p. 160-75.
36. Besser, M.J., et al., *Clinical responses in a phase II study using adoptive transfer of short-term cultured tumor infiltration lymphocytes in metastatic melanoma patients*. *Clin Cancer Res*, 2010. **16**(9): p. 2646-55.
37. Radvanyi, L.G., et al., *Specific lymphocyte subsets predict response to adoptive cell therapy using expanded autologous tumor-infiltrating lymphocytes in metastatic melanoma patients*. *Clin Cancer Res*, 2012. **18**(24): p. 6758-70.
38. Inozume, T., et al., *Selection of CD8+PD-1+ lymphocytes in fresh human melanomas enriches for tumor-reactive T cells*. *J Immunother*, 2010. **33**(9): p. 956-64.
39. Gros, A., et al., *PD-1 identifies the patient-specific CD8(+) tumor-reactive repertoire infiltrating human tumors*. *J Clin Invest*, 2014. **124**(5): p. 2246-59.
40. Yu, X. and X. Wang, *Tumor immunity landscape in non-small cell lung cancer*. *PeerJ*, 2018. **6**: p. e4546.
41. Lu, Y.C., et al., *Mutated PPP1R3B is recognized by T cells used to treat a melanoma patient who experienced a durable complete tumor regression*. *J Immunol*, 2013. **190**(12): p. 6034-42.
42. Robbins, P.F., et al., *Mining exomic sequencing data to identify mutated antigens recognized by adoptively transferred tumor-reactive T cells*. *Nat Med*, 2013. **19**(6): p. 747-52.

Chapter 6

43. Tran, E., et al., *Cancer immunotherapy based on mutation-specific CD4+ T cells in a patient with epithelial cancer*. *Science*, 2014. **344**(6184): p. 641-5.
44. Assadipour, Y., et al., *Characterization of an Immunogenic Mutation in a Patient with Metastatic Triple-Negative Breast Cancer*. *Clin Cancer Res*, 2017. **23**(15): p. 4347-4353.
45. Geng, Y., et al., *Prognostic Role of Tumor-Infiltrating Lymphocytes in Lung Cancer: a Meta-Analysis*. *Cell Physiol Biochem*, 2015. **37**(4): p. 1560-71.
46. Reynders, K. and D. De Ruyscher, *Tumor infiltrating lymphocytes in lung cancer: a new prognostic parameter*. *J Thorac Dis*, 2016. **8**(8): p. E833-5.
47. Zeng, D.Q., et al., *Prognostic and predictive value of tumor-infiltrating lymphocytes for clinical therapeutic research in patients with non-small cell lung cancer*. *Oncotarget*, 2016. **7**(12): p. 13765-81.
48. Ameratunga, M., et al., *PD-L1 and Tumor Infiltrating Lymphocytes as Prognostic Markers in Resected NSCLC*. *PLOS ONE*, 2016. **11**(4): p. e0153954.
49. Anderson, A.C., N. Joller, and V.K. Kuchroo, *Lag-3, Tim-3, and TIGIT: Co-inhibitory Receptors with Specialized Functions in Immune Regulation*. *Immunity*, 2016. **44**(5): p. 989-1004.
50. Wei, S.C., C.R. Duffy, and J.P. Allison, *Fundamental Mechanisms of Immune Checkpoint Blockade Therapy*. *Cancer Discov*, 2018. **8**(9): p. 1069-1086.
51. Djenidi, F., et al., *CD8+CD103+ tumor-infiltrating lymphocytes are tumor-specific tissue-resident memory T cells and a prognostic factor for survival in lung cancer patients*. *J Immunol*, 2015. **194**(7): p. 3475-86.
52. Ganesan, A.P., et al., *Tissue-resident memory features are linked to the magnitude of cytotoxic T cell responses in human lung cancer*. *Nat Immunol*, 2017. **18**(8): p. 940-950.
53. de Hoon, M.J., et al., *Open source clustering software*. *Bioinformatics*, 2004. **20**(9): p. 1453-4.
54. Saldanha, A.J., *Java Treeview--extensible visualization of microarray data*. *Bioinformatics*, 2004. **20**(17): p. 3246-8.
55. Dudley, M.E., et al., *Generation of tumor-infiltrating lymphocyte cultures for use in adoptive transfer therapy for melanoma patients*. *J Immunother*, 2003. **26**(4): p. 332-42.
56. Dudley, M.E. and S.A. Rosenberg, *Adoptive-cell-transfer therapy for the treatment of patients with cancer*. *Nat Rev Cancer*, 2003. **3**(9): p. 666-75.
57. Dudley, M.E. and S.A. Rosenberg, *Adoptive cell transfer therapy*. *Semin Oncol*, 2007. **34**(6): p. 524-31.
58. Forget, M.A., et al., *A Novel Method to Generate and Expand Clinical-Grade, Genetically Modified, Tumor-Infiltrating Lymphocytes*. *Front Immunol*, 2017. **8**: p. 908.
59. Tavera, R.J., et al., *Utilizing T-cell Activation Signals 1, 2, and 3 for Tumor-infiltrating Lymphocytes (TIL) Expansion: The Advantage Over the Sole Use of Interleukin-2 in Cutaneous and Uveal Melanoma*. *J Immunother*, 2018. **41**(9): p. 399-405.
60. Rodriguez, J.A., *HLA-mediated tumor escape mechanisms that may impair immunotherapy clinical outcomes via T-cell activation*. *Oncol Lett*, 2017. **14**(4): p. 4415-4427.
61. Fernandez-Poma, S.M., et al., *Expansion of Tumor-Infiltrating CD8(+) T cells Expressing PD-1 Improves the Efficacy of Adoptive T-cell Therapy*. *Cancer Res*, 2017. **77**(13): p. 3672-3684.
62. Lundegaard, C., et al., *NetMHC-3.0: accurate web accessible predictions of human, mouse and monkey MHC class I affinities for peptides of length 8-11*. *Nucleic Acids Res*, 2008. **36**(Web Server issue): p. W509-12.
63. Teku, G.N. and M. Vihinen, *Pan-cancer analysis of neoepitopes*. *Sci Rep*, 2018. **8**(1): p. 12735.
64. Lundegaard, C., O. Lund, and M. Nielsen, *Prediction of epitopes using neural network based methods*. *J Immunol Methods*, 2011. **374**(1-2): p. 26-34.

Chapter 6

65. Moreau, V., et al., *PEPOP: computational design of immunogenic peptides*. BMC Bioinformatics, 2008. **9**: p. 71.
66. Ott, P.A., et al., *An immunogenic personal neoantigen vaccine for patients with melanoma*. Nature, 2017. **547**(7662): p. 217-221.
67. Sahin, U., et al., *Personalized RNA mutanome vaccines mobilize poly-specific therapeutic immunity against cancer*. Nature, 2017. **547**(7662): p. 222-226.